Late Devonian-Carboniferous faulting
in NW Finnmark and controlling fabrics

Jean-Baptiste P. Koehl[1,2], Steffen G. Bergh[1,2], Per-Terje Osmundsen[3,4,5], Thomas F. Redfield[3], Kjetil Indrevær[2,5], Halldis Lea[1], Espen Bergø[1]

1) Department of Geosciences, University of Tromsø, N-9037 Tromsø, Norway.

2) Research Centre for Arctic Petroleum Exploration (ARCEx), University of Tromsø, N-9037 Tromsø, Norway.

3) Geological Survey of Norway (NGU), Leiv Erikssons vei 39, 7491 Trondheim, Norway.

4) University Center in Svalbard, 9171 Longyearbyen, Norway.

5) Department of Geosciences, University of Oslo, P.O. Box 1047 Blindern, NO-0316 Oslo, Norway.

Abstract. A Late Devonian (?) - Carboniferous episode of regional extension related to the collapse of the Caledonides triggered the formation of major basin-bounding faults, e.g. Troms-Finnmark Fault Complex, and offshore basins in the SW Barents Sea, such as the Nordkapp Basin and smaller triangular to sigma-shaped (half-) graben basins on the Finnmark Platform. New high-resolution aeromagnetic and bathymetry data from the shallow shelf (strandflat) show that analog fault systems are present in coastal and onshore areas of NW Finnmark. We investigate the Langfjord-Vargsund fault, a NW-dipping, zigzag-shaped, onshore-nearshore, coast-parallel, extensional brittle fault complex, trending parallel to the Vestfjorden-Vanna fault complex in Lofoten-Vesterålen and Western Troms. This fault complex consists of alternating NNE-SSW and ENE-WSW striking normal fault segments that merge into triangular basins on the Finnmark Platform. Nearshore coastal fjords show several triangular, sigma-shaped mini-basins, e.g. the Ryggefjorden trough, bounded by zigzag-shaped fault segments of the Langfjord-Vargsund fault, and they may represent analogs to shallow and deep offshore, Devonian-Carboniferous basins such as the Nordkapp Basin prior to the deposition of late Paleozoic evaporites and subsequent diapirism. Moreover, the Langfjord-Vargsund fault accommodated hundreds of meters to a few kilometers of down-to-the-NW normal movement during post-Caledonian extension. In northern Finnmark, the Langfjord-Vargsund fault is offset ca. 28 km right-laterally by steep, WNW-ESE trending, strike-slip fault segments of the Trollfjorden-Komagelva Fault Zone, a reactivated Neoproterozoic, margin-orthogonal transfer fault zone that segmented onshore and nearshore areas of NW Finnmark from the offshore Finnmark Platform east. The island of Magerøya is potentially located within the fault-tip process zone of the Trollfjorden-Komagelva Fault Zone and the fault most likely dies out to the west. Similarly, a ca. 2 km left-lateral offset of the Langfjord-Vargsund fault in Revsbotn is linked to sinistral strike-slip movement along the Akkarfjord fault, a steep, WNW-ESE to ENE-WSW trending brittle fault forming steep escarpments in nearshore fjords and in northeast Sørøya. We propose that the Akkarfjord fault may have initiated as part of an oblique, conjugate fault set to the Trollfjorden-

Komagelva Fault Zone in Timanian (?) times and was reactivated synchronously with the Langfjord-Vargsund fault. Steeply dipping fault segments of the Langfjord-Vargsund formed as extensional splay-faults along inverted, Caledonian, brittle-ductile thrusts, such as the Talvik and the Kvenklubben (thrust) faults, which they eventually truncated and decapitated. Other controlling fabrics include favourably oriented, (folded) Precambrian fabrics and units depicted by new aeromagnetic data, e.g. steeply NW-plunging, upright and gently NE-plunging, inclined folds, which may have provided preferential zones of weakness for Caledonian thrust faults and post-Caledonian normal faults to form along steeply dipping fold limbs and define major bends over fold hinges. In addition, large-scale, NW-SE trending belts of granite-gneiss and macrofolded volcano-sedimentary rocks delineated by matching aeromagnetic anomalies are possibly downthrown to the northwest by the Langfjorden-Vargsund fault. A Late Devonian-Carboniferous age for the Langfjord-Vargsund fault is supported by radiometric dating of dolerite dykes and fault gouge, and by seismic interpretation of syn-tectonic sedimentary wedges along the possible offshore extension of the Langfjord-Vargsund fault.

1. Introduction

The North Atlantic passive margin off northern Norway and the Barents Sea evolved through multiple events of extension from the late Paleozoic to the early Cenozoic that ended with the breakup of the North Atlantic Ocean and the development of a transform plate margin off the west coast of Spitsbergen (Faleide et al., 1993, 2008; Dore et al., 1999; Cianfarra & Salvini, 2015). The margin offshore Western Troms and NW Finnmark (Figure) comprises the Finnmark Platform, a platform area adjacent to the onshore regions, and major NE-SW trending, fault-bounded deep offshore basins such as the Hammerfest and Nordkapp basins. These basins are bounded by major extensional faults like the Troms-Finnmark Fault Complex (TFFC; Gabrielsen et al., 1990; Indrevær et al., 2013). A possible onshore analog to the TFFC is the SE-dipping Vestfjord-Vanna fault complex (VVFC), bounding the Lofoten ridge and West Troms Basement Complex horst to the southeast (Olesen et al., 1997; Bergh et al., 2010; Indrevær et al., 2013; Figure). Another coast-parallel major fault is the Langfjord-Vargsund fault (LVF; Zwaan & Roberts, 1978; Worthing, 1984; Olesen et al., 1990; Roberts & Lippard, 2005), a poorly studied fault that strikes overall NE-SW, dominantly dips to the NW and displays a zigzag-shaped pattern of alternating NNE-SSW and ENE-WSW striking faults in map view, similar to that of the TFFC and VVFC (Figure). We explore the possible northeastward continuation and linkage of the latter with the LVF. Furthermore, the SW Barents Sea margin is segmented by NW-SE trending transfer fault zones, the Senja Shear Zone and Fugløya transfer zone (Indrevær et al., 2013), which strike sub-parallel to the onshore Neoproterozoic Trollfjorden-Komagelva Fault Zone (TKFZ) in eastern Finnmark (Siedlecki, 1980; Herrevold et al., 2009) and to the Kokelv Fault on the Porsanger Peninsula (Gayer et al., 1985; Lippard & Roberts, 1987; Rice, 2013). The TKFZ is believed to continue farther west, off the coast where it is thought to interact with and merge into the WNW-ESE trending fault segment of the

TFFC (Gabrielsen, 1984; Vorren et al., 1986; Gabrielsen & Færseth, 1989; Gabrielsen et al., 1990; Roberts et al., 2011; Bergø, 2016; Lea, 2016).

The present study aim at providing a better correlation between brittle fault segments of the LVF and TKFZ in nearshore areas of NW Finnmark, and their possible link to late Paleozoic faults and (half-) grabens structures on the Finnmark Platform and within coastal fjords of NW Finnmark, e.g. in Ryggefjorden (Figure), using field observations, fjord bathymetry and aeromagnetic data (Gernigon et al., 2014; Nasuti et al., 2015). The main goal is to characterize the onshore fault-fracture geometry and kinematics, and discuss their formation and interaction in space and time as analogs for offshore fault systems. We specifically study two dominant fault complexes in NW Finnmark, the NE-SW trending LVF and the WNW-ESE trending TKFZ and how they link and interact to produce zigzag/rhombic-shaped basins in nearshore fjords of NW Finnmark. Further, we discuss the architecture of the TKFZ, possible similarities with adjacent WNW-ESE trending faults, e.g. the Kokelv Fault on the Porsanger Peninsula (Figure), and its potential continuation offshore, to the northwest. We also discuss tentative factors that controlled the location of these major faults in basement and Caledonian host rocks. We compare our results with offshore faults and basins on the Finnmark Platform and briefly discuss the geometry and potential linkage of the TKFZ with the TFFC and related offshore basin-bounding faults (Gabrielsen & Færseth, 1989; Roberts et al., 2011; Bergø, 2016; Lea, 2016). Finally, we present an alternative model for the geometry of the speculated western extension of the TKFZ off the coast of Finnmark in which the TKFZ dies out southeast of the TFFC and WNW-ESE trending faults exposed onshore the island of Magerøya are part of the TKFZ fault-tip process zone.

2. Geological setting

Coastal areas in Western Troms and Finnmark along the SW Barents Sea margin (Figure) consist of Neoarchean to Paleoproterozoic basement rocks (e.g. Zwaan, 1995; Bergh & Torske, 1988; Bergh et al., 2010), partly preserved autochthonous Neoproterozoic rocks (Kirkland et al., 2008a, b) and a succession of Caledonian nappes (Andersen, 1981, 1984; Ramsay et al., 1985; Figure). Basement rocks in NW Finnmark are exposed within tectonic windows as horsts and ridges, e.g. the Alta-Kvænangen (Bøe & Gautier, 1978; Zwaan & Gautier, 1980), Altenes and Repparfjord-Komagfjord tectonic windows (Pharaoh et al., 1982, 1983; Bergh & Torske, 1988; Jensen, 1996; Torgersen & Viola, 2014). Neoproterozoic and Caledonian metasedimentary and meta-igneous rocks dominate on the shallow shelf and onshore areas (Indrevær & Bergh, 2014; Figure). These rocks belong to the Kalak Nappe Complex, the Magerøy Nappe and the Seiland Igneous Province (Ramsey et al., 1979, 1985; Andersen, 1981, 1984; Kirkland et al., 2005; Corfu et al., 2006). On the Finnmark Platform, successions of late Paleozoic to Cenozoic sedimentary basins and highs formed during the collapse of the Caledonides and subsequent rifting of the NE Atlantic Ocean.

2.1. Precambrian and Caledonian geology

In the study area, Paleoproterozoic rocks crop out in the Altenes, Repparfjord-Komagfjord (Pharaoh et al., 1982, 1983; Bergh & Torske, 1988; Jensen, 1996) and Alta-Kvænangen (Bøe & Gautier, 1978; Zwaan & Gautier, 1980; Gautier et al., 1987) tectonic windows. The basement suite of the Altenes and Alta-Kvænangen tectonic windows consist of low-grade metavolcanics and metasedimentary rocks of the Raipas Group formed in NW-SE trending Archean- (?) Paleoproterozoic rift basins (Bergh & Torske, 1986, 1988) or as part of a foreland basin during the Svekokarelian Orogeny (Torske & Bergh, 2004). These basement rocks are deformed by steep, km-scale, NW-plunging folds (Zwaan & Gautier, 1980; Gautier et al., 1987), which show similar trend and wavelength as Precambrian fold structures in the West Troms Basement Complex (Bergh et al., 2010). Paleoproterozoic basement rocks of the Repparfjord-Komagfjord tectonic window display slightly higher metamorphic grades and are deformed by km-scale, gently NE-plunging Svecofennian folds (Reitan, 1963; Pharaoh et al., 1982, 1983; Torgersen & Viola, 2014).

In eastern Finnmark, thin Neoproterozoic to Cambrian (para-) autochtonous metasedimentary rocks overly basement rocks overly Paleoproterozoic basement rocks and also occur within the Lower Allochthon (Corfu et al., 2014). Neoproterozoic sedimentary strata of the Barents Sea Group (Siedlecki, 1980) crop out on the Varanger Peninsula mostly north of the TKFZ (Figure). These rocks were deposited in foreland basins related to the Timanian Orogeny (Roberts & Siedlecka, 2002; Andresen et al., 2014), and were affected by large-scale, NW-SE trending folds and by the formation of the WNW-ESE trending TKFZ (Jonhson et al., 1978; Roberts & Siedlecka, 2002; Siedlecka et al., 2004; Herrevold et al., 2009). On the eastern part of the Varanger Peninsula, the TKFZ is characterized by a single, major fault segment (Siedlecka & Siedlecki, 1967; Siedlecka & Roberts, 1992; Herrevold et al., 2009) that extends in the fjord to the southeast (Roberts et al., 2011; Figure) and links up with the Sredni-Rybachi Fault Zone onshore the Kola Peninsula farther southeast (Roberts et al., 1997). In the western part of the Varanger Peninsula, the TKFZ splays into several subsidiary fault segments showing duplex-like geometries (Siedecka & Siedlecki, 1967; Siedlecka, 1975). Maximum lateral displacement along the TKFZ was constrained to 250 km dextral strike-slip movement (Bylund, 1994) using paleomagnetic data while a more recent restoration model indicates a maximum lateral displacement of 207 km (Rice, 2013).

Caledonian rocks make up most of the coastal region of NW Finnmark. On the Porsanger Peninsula, the Kalak Nappe Complex consists of amphibolite facies metapsammites, paragneisses and schists with a well-developed foliation and low-angle thrusts that strike NE-SW and dip gently to the northwest (Ramsey et al., 1979, 1985; Corfu et al., 2014). The allochthonous thrust sheets of the Kalak Nappe Complex include Proterozoic basement rocks, clastic metasedimentary rocks, and plutons of the Seiland Igneous Province (Corfu et al., 2014). Nappe internal fabrics include a prominent gently NW-

dipping foliation, east-verging, NNE-SSW trending, recumbent folds, a major low-angle basal thrust zone and subsidiary thrusts that accommodated top-to-the-ESE contractional motion (Ramsey et al., 1985; Kirkland et al., 2005). This nappe complex was interpreted as an exotic terrane from the Iapetus Ocean and Laurentian shield that was accreted onto Baltica during Caledonian deformation events (Kirkland et al., 2008a). However, paleocurrent and provenance analyses suggest a Baltican affinity for metasedimentary rocks of the Kalak Nappe Complex (Roberts, 2007; Zhang et al., 2016).

The Seiland Igneous Province (580-560 Ma) is made up of mafic-ultramafic plutons related to the rifting of the Iapetus Ocean (Elvevold et al., 1994; Corfu et al., 2014). New geophysical studies show that the Seiland Igneous Province is characterized by two deep-reaching roots below the islands of Seiland and Sørøya, revealing a maximum 10 km thickness for the Kalak Nappe Complex (Pastore et al., 2016). In addition, NW Finnmark coastal areas show ENE-WSW to NNE-SSW trending, Ediacaran metadolerite dykes also linked to the rifting of the Iapetus Ocean (Roberts 1972; Siedlecka et al., 2004; Nasuti et al., 2015).

Late Ordovician to early Silurian greenschist facies schists and meta-volcanic units of the Magerøy Nappe crop out on the island of Magerøya, northeastern Sørøya and on the Porsanger Peninsula (Figure ; Andersen, 1981, 1984; Kirkland et al., 2005, 2007; Corfu et al., 2014) and are intruded by gabbroic – e.g. the Honningsvåg Igneous Complex (Corfu et al., 2006) – and granitic plutons – e.g. the Finnvik Granite (Andersen, 1981). Major structures in the Magerøy Nappe include NNE-SSW trending, east-verging, asymmetric folds and NE-SW trending low-angle Caledonian foliation and ductile thrusts (Andersen, 1981).

2.2. Post-Caledonian brittle faults and margin architecture

2.2.1. Post-Caledonian offshore basins

From the end of the Caledonian Orogeny to the breakup of the NE Atlantic, the SW Barents Sea experienced multiple pulses of extension that began during extensional collapse of the Caledonides in the Devonian-Carboniferous. This collapse phase may have lasted until the early/mid Permian leading to exhumation of core complexes both onshore and offshore northern Norway, e.g. in mid-Norway (Osmundsen et al., 2005) and Lofoten-Vesterålen (Klein & Steltenpohl, 1999; Klein et al., 1999; Steltenpohl et al., 2004; Steltenpohl et al., 2011), and development of large basins such as the Ottar, Nordkapp and Hammerfest basins (Dengo & Røssland, 1992; Breivik et al., 1995; Gudlaugsson et al., 1998). Exhumation of core complex in Lofoten-Vesterålen is thought to have occurred along inverted Caledonian shear zones (Steltenpohl et al., 2011), which may represent onshore analogs to the newly recorded Sørøya-Ingøya shear zone in the SW Barents Sea (Koehl et al., 2018). This large-scale shear zone defines a large spoon-shaped trough that may have controlled formation of major triangular to sigma-shaped offshore basins such as the Nordkapp, Hammerfest and Ottar basins (Breivik et al., 1995;

Gudlaugsson et al., 1998; Indrevær et al., 2013) and minor (half-) grabens on the Finnmark Platform (Samuelsberg et al., 2003; Rafaelsen et al., 2008; Koehl et al., 2018; Figure). This shear zone also likely controlled the deposition of Devonian-Carboniferous clastic sediments on the Finnmark Platform and in the southwesternmost Nordkapp basin (Koehl et al., 2018; Figure). These sediments and the underlying Sørøya-Ingøya shear zone detachment are potential analogs to Middle Devonian sedimentary basins in western- (Séranne et al., 1989; Chauvet & Séranne, 1994; Wilks & Cuthbert, 1994; Osmundsen & Andersen, 2001) and mid-Norway (Braathen et al., 2000).

2.2.2. Post-Caledonian faults and fractures

Devonian-Carboniferous basins are typically bounded by zigzag-shaped fault complexes composed of steep, ENE-WSW to NNE-SSW trending, arcuate normal faults (Lippard & Roberts, 1987; Gabrielsen et al., 1990; Doré et al., 1999; Roberts & Lippard, 2005; Faleide et al., 2008; Indrevær et al., 2013). A classic example is the overall NW-dipping TFFC that runs along the coasts of Troms and Finnmark and terminates as a NNE-dipping fault that separates the Finnmark Platform west from the southwesternmost Nordkapp basin (Figure ; Gabrielsen et al., 1990; Koehl et al., 2018). Another example is the Måsøy Fault Complex (Figure ; Gabrielsen et al., 1990) that bounds the southwesternmost Nordkapp basin and the Nordkapp Basin to the southeast. The main fault segment of this fault complex possibly formed as a brittle splay-fault during partial inversion of the Sørøya-Ingøya shear zone in the Mid/Late Devonian-early Carboniferous (Koehl et al., 2018).

In onshore areas, post-Caledonian faults are present in Lofoten-Vesterålen (Bergh et al., 2007; Eig, 2008; Eig & Bergh, 2011; Hansen & Bergh, 2012; Hansen et al., 2012), Western Troms (Indrevær et al., 2013; Davids et al., 2013) and NW Finnmark (Roberts, 1971; Worthing, 1984; Lippard & Roberts, 1987; Townsend, 1987a; Rykkelid, 1992; Lippard & Prestvik, 1997; Roberts & Lippard, 2005). These faults trend NNE-SSW, ENE-WSW and NW-SE and partly controlled the rhombic geometry of adjacent offshore basins (Bergh et al., 2007; Eig, 2008; Eig & Bergh, 2011; Hansen et al., 2012; Hansen & Bergh, 2012; Indrevær et al., 2013). A characteristic example is the onshore-nearshore, zigzag-shaped, NNE-SSW and ENE-WSW trending VVFC that can be traced northward to Western Troms as the contact between Precambrian basement rocks in the northwest and downdropped Caledonian Nappes in the southeast (Figure ; Indrevær et al., 2013).

In NW Finnmark, Zwaan & Roberts (1978) proposed the existence of a zigzag-shaped, NNE-SSW and ENE-WSW striking, NW-dipping fault complex, the LVF, to explain the abrupt transition from Paleoproterozoic rocks of the Repparfjord-Komagfjord, Altenes and Alta-Kvænangen tectonic windows in the southeast to rocks of the Kalak Nappe Complex and Seiland Igneous Province in the northwest across Langfjorden and Vargsundet (Figure). The geometry, kinematics, timing of formation and linkage of this fault complex is, however, poorly studied and remain uncertain. Recent studies show that two major brittle-ductile, NW-dipping faults in the footwall of the LVF, the Kvenklubben and

Porsavannet faults, acted as thrust faults during the Caledonian Orogeny, were reactivated as post-Caledonian brittle normal faults and potentially merge with the LVF at depth (Torgersen & Viola, 2014; Torgersen et al., 2014).

Northwestwards, in the hanging-wall of the LVF, brittle normal faults and synchronous fracture sets trending ENE-WSW and NW-SE were reported by Worthing (1984) in the island of Seiland while Roberts (1971) described ENE-WSW to NE-SW trending, NW-dipping brittle faults (e.g. Kjøtvika and Skarvdalen faults; Figure 2) and WNW-ESE trending fractures in northeastern Sørøya (Figure). Slickenside lineations on the Skarvdalen fault and other ENE-WSW to NE-SW trending faults indicate normal-dextral, oblique-slip sense of shear whereas WNW-ESE trending faults typically show sinistral strike-slip movement (Roberts, 1971). Based on observed fracture trends and kinematics, Worthing (1984) and Roberts (1971) proposed that ENE-WSW to NE-SW and WNW-ESE trending brittle faults and fractures in NW Finnmark formed as conjugate, dominantly strike-slip fracture sets due to WNW-ESE directed maximum stress and vertical intermediate stress. On the Porsanger Peninsula (Figure), Townsend (1987a) described post-Caledonian brittle faults including the Snøfjorden-Slatten fault (Passe, 1978), the Njoal Neset fault and the Selvika-Eiterfjorden fault (Hayes, 1980; Figure 2). Adjacent to the island of Magerøya in northernmost Finnmark, Andersen (1981) suggested the presence of an ENE-WSW to WNW-ESE trending, north-dipping, arcuate normal fault, the Magerøysundet fault, in the fjord that separates the island of Magerøya from the Porsanger Peninsula (Figure & Figure 2). Post-Caledonian, down-to-the-NE, normal motion was inferred along this fault, which appears to have juxtaposed rocks of the Kalak Nappe Complex on the Porsanger Peninsula in the south against rocks of the Magerøya Nappe onshore Magerøya in the north.

2.2.3. Post-Caledonian transfer fault zones

The Lofoten-Vesterålen and SW Barents Sea margins are segmented by large NNW-SSE to WNW-ESE trending transfer fault zones that strike oblique to the margin (Gabrielsen, 1984; Gabrielsen & Færseth, 1989; Faleide et al., 2008; Eig & Bergh, 2011; Indrevær et al., 2013; Gernigon et al., 2014). The largest of these is the offshore De Geer Zone (Faleide et al., 2008; Cianfarra & Salvini, 2015) separating the SW Barents Sea margin from the Lofoten-Vesterålen margin. This transfer zone merges southwards into the Senja Fracture Zone along basement-seated weakness zones, e.g. the Senja Shear Belt and Bothnian-Senja Fault Complex (Zwaan, 1995). These basement weakness zones account for switches of polarity of major normal faults, e.g. along the VVFC (Figure ; Olesen et al., 1993, 1997). Farther north, Indrevær et al. (2013) described attitude changes along the VVFC across the NNW-SSE trending Fugløya transfer zone (Figure), and argued that the VVFC connects with the Måsøy and Nysleppen fault complexes offshore, to the northeast (Figure). Northeastwards, the Tiddlybanken Basin (Mattingsdal et al., 2015) developed along WNW-ESE trending faults that segmented the Nordkapp Basin (Figure).

In NW Finnmark, a potential candidate to represent a transfer zone is the Neoproterozoic, margin-oblique, WNW-ESE trending TKFZ (Siedlecki, 1980; Herrevold et al., 2009), which can be traced eastwards onto the Kola Peninsula in Russia where it was mapped as a narrow, single-segment fault (Roberts et al., 1997, 2011). On the Varanger Peninsula, the TKFZ splays into several sub-parallel fault segments that bound duplex structures (Siedecka & Siedlecki, 1967; Siedlecki et al., 1974). In the west, the TKFZ is thought to proceed offshore where it appears to correlate with a large escarpment north of Magerøya, and into the Barents Sea where it supposedly merges with the WNW-ESE trending fault segment of the TFFC to form triangular-shaped mini-basins (Gabrielsen, 1984; Vorren et al., 1986; Townsend, 1987a; Gabrielsen & Færseth, 1989; Gabrielsen et al., 1990; Roberts et al., 2011; Bergø, 2016; Lea, 2016). This paper explores an alternative model where the TKFZ progressively widens westwards, possibly offsets the LVF and dies out offshore west of Magerøya (Figure). Other subsidiary potential transfer fault zones in NW Finnmark include the Kokelv Fault, a NNE-dipping inferred from abrupt changes in metamorphic grades (Gayer et al., 1985; Lippard & Roberts, 1987), the WNW-ESE to ENE-WSW trending Akkarfjord fault in northeastern Sørøya, a subvertical, sinistral strike-slip fault (Figure ; Roberts, 1971) that possibly offsets the NE-SW trending LVF in a left-lateral fashion in Revsbotn (Figure ; this study), and the Markopp fault in Repparfjorden (Figure), a NE-dipping, low-angle extensional brittle fault located near the contact between Precambrian rocks of the Repparfjord-Komagfjord tectonic window in the southwest and Caledonian rocks of the Kalak Nappe Complex in the northeast (Figure & Figure 2; Torgersen et al., 2014).

2.2.4. Absolute dating of post-Caledonian faults

Absolute ages of post-Caledonian faulting in NW Finnmark are provided by a few radiochronological studies (Lippard & Prestvik, 1997; Davids et al., 2013; Torgersen et al., 2014; Koehl et al., submitted). First, recent K/Ar analyses of brittle fault gouge of the Kvenklubben fault in the Repparfjord-Komagfjord tectonic window, in the footwall of the LVF yielded Carboniferous to early Permian ages and a subsidiary Early Cretaceous age (Torgersen et al., 2014). Second, the majority of K/Ar radiometric dating of fault gouge in NW Finnmark indicate that normal faulting came to a halt in mid Permian times (Koehl et al., submitted). By comparison, K/Ar dating of illite clay minerals found along the VVFC and related brittle normal faults in adjacent areas of Western Troms and Lofoten-Vesterålen yielded Late Devonian-early Carboniferous ages (Davids et al., 2013). Third, ^{40}Ar/^{39}Ar dating of dolerite dykes that intruded along WNW-ESE trending brittle faults onshore Magerøya yielded Visean ages (early Carboniferous; Roberts et al., 1991; Lippard & Prestvik, 1997). These dolerite dykes produce narrow, positive aeromagnetic anomalies on high-resolution aeromagnetic data (Nasuti et al., 2015) that will be used to infer the presence of brittle faults in NW Finnmark. Dolerite dykes are also present in the eastern part of the Varanger Peninsula (Guise & Roberts, 2002) and on the Kola Peninsula in Russia (Roberts & Onstott, 1995), where ^{40}Ar/^{39}Ar dating yielded Late Devonian ages.

3. Methods and databases

3.1. Structural field study

Brittle faults were mapped and characterized at outcrop scale with main purpose to collect orientation data for brittle faults and hostrock ductile fabrics, unravel fault-fracture geometries, and study kinematic indicators in order to infer displacement magnitude along brittle faults in NW Finnmark. In addition, the research team gathered information about relative timing relationships between different fault sets where available. Structural data are plotted in lower-hemisphere equal-area stereonets as poles or great circles of planar fabrics, and as slip-linars of linear features (Goldstein & Marshak, 1988).

3.2. Satellite images and Digital Elevation Model (DEM) data

Digital 2D and 3D satellite imaging was used to infer the presence of brittle faults in the study area using surface intersections and tectonically controlled topographic lineaments. The interpretation of brittle faults and fractures on this dataset is based on the assumption that a large part of the observed lineaments in Norway are directly linked to the tectonic history and structural regime that affected northwestern Finnmark and northeastern Troms. Previous regional interpretations of similar datasets seem to confirm this assumption (Gabrielsen et al., 2002). The present satellite image dataset is from www.norgei3d.no. Brittle faults interpreted on satellite images were compared and correlated with fieldwork, aeromagnetic, topography and bathymetry data, as well as with published bedrock maps (Roberts, 1973, 1987, 1998; Gautier et al., 1987; Zwaan et al., 1987; Robins, 1990a, b).

3.3. Bathymetry and topography data

Nearshore bathymetry data were provided by the sea-mapping division of Norwegian mapping authorities (Kartverket Sjødivisjonen), and cover the strandflat area off the coasts and parts of the fjord network of NW Finnmark and northeastern Troms (Figure 4). However, areas closer to the shore and narrow fjords, are not covered by the bathymetry dataset. The bathymetry data were acquired with a maximum resolution of 25 x 25 m horizontally and 10 m vertically. Onshore topography data have a lateral resolution of 10x10 m and a vertical resolution of 10 m. The interpretation of bathymetry data aims at studying the trend, length and dip of submarine escarpments, troughs and ridges observed on the strandflat, where glacial sediments are supposedly absent. Similar studies of the submarine relief on the strandflat off the coasts of Western Troms (Indrevær & Bergh, 2014) enabled to identify both Precambrian basement ductile fabrics, Caledonian thrust nappes and post-Caledonian brittle faults. In NW Finnmark, however, glacial sediments cover parts of the strandflat and fjords, and abundant glacial features such as ploughmarks, glacial troughs (e.g. Djuprenna trough), moraines (Ottesen et al., 2008; Barbolla et al., in prep.) and large glacial sediment fans (Vorren et al., 1986; Figure 4) complicate the

interpretation of brittle faults because of the tendency of glacial drainage systems to use pre-existing troughs and zones of weakness in the bedrock (e.g. brittle faults, bedrock ductile fabrics). We therefore apply bathymetry data to correlate lineaments on the strandflat in NW Finnmark with onshore geology and lineaments mapped in the field, on satellite photographs, topography data and from previous studies (Gabrielsen, 1984; Vorren et al., 1986; Lippard & Roberts, 1987; Townsend, 1987a; Roberts et al., 2011). Glacial features are not described and ductile fabrics are exclusively discussed when potentially controlling the formation of brittle faults.

3.4. Aeromagnetic anomaly data

We applied supplementary onshore-nearshore aeromagnetic data from the Geological Survey of Norway including aeromagnetic data (Figure 5a) and a tilt derivative function data (Figure 5b) to identify abrupt changes in the bedrocks that may localize brittle faults, and to delineate possible magmatic intrusions (e.g. dolerite dykes) emplaced along brittle faults (cf. Nasuti et al., 2015). Importantly, significantly different rocks may yield very similar magnetic responses. A crucial example in northern Finnmark is the similar narrow, positive aeromagnetic anomalies produced both by dolerite dykes emplaced along brittle faults (cf. dotted white lines in Figure 5a & b; Roberts et al., 1991; Nasuti et al., 2015) and by folded metasedimentary beds (cf. dotted yellow lines in Figure 5b; Roberts & Siedlecka, 2012; Roberts & Williams, 2013). We will therefore use aeromagnetic data as a confirmation tool to infer the presence of potential brittle faults in NW Finnmark. The aeromagnetic data are compiled from surveys acquired with different flight-line spacing and flying altitude: 500 and 200 m.a.s.l. respectively in western Finnmark, 1000 and 200 m in northern Troms, and 200 and 60 m in eastern and southern Finnmark (Olesen, pers. comm; Nasuti et al., 2015).

4. Results

Three major fault trends were identified among which margin-parallel (1) ENE-WSW and (2) NNE-SSW trending faults (e.g. LVF) dominate the southwestern part of Finnmark from Sørkjosen to Revsbotn (Figure , Figure 2 & Figure 3), while margin-oblique (3) WNW-ESE trending faults (e.g. TKFZ) are more abundant in the northeast on the Porsanger Peninsula and Magerøya (Figure 2 & Figure 3). We describe the onshore-nearshore geometry and kinematic characters and, where possible, relative timing constraints of map-scale faults belonging to these three major trends (Figure 2 & Figure 3) and link fault traces using bathymetry data from adjacent fjords (Figure 4) and aeromagnetic data (Figure 5). We specifically emphasize the influence of the geometry of ENE-WSW and NNE-SSW trending faults on shaping the LVF and their interaction with margin-oblique WNW-ESE trending faults like the TKFZ to form rhombic-shaped (half-) graben basins (Figure & Figure 2).

4.1. ENE-WSW and NNE-SSW trending faults

Faults in Sørkjosen-Langfjorden-Altafjorden

In Sørkjosen, a major NNW-dipping fault, the Sørkjosen fault, and associated minor faults-fractures are exposed in a ca. one km-long, NNW-SSE trending roadcut in granodioritic Kalak Nappe Complex gneisses with a sub-horizontal foliation (Figure 6a). On satellite images, this fault coincides with a major ENE-WSW trending lineament that can be traced across the fjord, to the northeast, as a series of pronounced, sub-parallel, NE-SW to NNE-SSW trending lineaments (Figure 6b) but quickly dies out to the west (Figure 2). In addition, E-W to WNW-ESE trending lineaments, potentially representing older brittle faults, appear to curve into the Sørkjosen fault (cf. dashed red lines in Figure 6a). At outcrop scale, the Sørkjosen fault core comprises meter-thick lenses of cataclastic fault-rocks crosscut by a dense network of microfaults and veins partly filled up with calcite cement (Figure 6c). Slickenside lineations along clay-rich fault surfaces in the fault core indicate normal dip-slip to normal oblique-slip, down-to-the-NNW movement, which is also supported by a gradual clockwise rotation of foliation surfaces in granodioritic gneiss toward the fault core (Figure 6c). The amount of normal offset along the Sørkjosen fault is difficult to resolve because of the lack of geological markers that can be correlated across the fault. However, the apparent offset of a ca. 30 cm-thick amphibolite unit between footwall and hanging-wall suggests vertical throw of a minimum of ca. 10 meters (Figure 6a), while a maximum estimate of 500 m is based on the thickness of the granodioritic unit of the Kalak Nappe Complex (Zwaan et al., 1987).

Further, in the hanging-wall of the Søkjosen fault, we observed minor antithetic, SSE-dipping brittle faults characterized by vertically splaying, listric geometries defining half-graben structures (Figure 6d). Normal offsets of a sub-horizontal granodioritic gneiss felsic band shows that displacement along these faults is in the order of a few decimeters. In the footwall, we observed a succession of dominantly NNW- to NW-dipping brittle faults showing various amount of down-to-the-NW normal offset. Near the Sørkjosen fault core, a NNW-dipping fault displays ca. 10-15 m vertical offset of a ca. 30 cm thick amphibolite unit (Figure 6a). Southwards, minor subparallel faults show decreasing amount of vertical offset of geological markers from a few meters down to a few centimeters (Figure 6a). In the southernmost part of the roadcut, most minor brittle faults are planar in cross-section and occasionally form meter-wide horst-graben structures showing cm-scale normal offsets of felsic gneiss bands (Figure 6e).

In Straumfjordbotn, ca. 20 km east of Sørkjosen (Figure 2), a large ESE- to SE-dipping fault, the Straumfjordbotn fault crops out and correlates with a minor NNE-SSW trending lineament on satellite images and strikes subparallel to a nearby major NE-SW trending escarpment (Figure 6f). The Straumfjordbotn fault exhibits slickengrooves that indicate down-to-the ESE/SE normal movement (Figure 6g) of uncertain magnitude due to a lack of convincing correlation markers on both sides of the

fault. The fault core is about 0.5 m-wide and shares similar characteristics with that of the Sørkjosen fault. For example, both fault cores are constituted of clay-rich cataclastic fault-rocks with abundant calcite cement. Considering the proximity, fault-core similarities and opposite dip of the Straumfjordbotn and Sørkjosen faults, we interpret the Straumfjordbotn fault as a subsidiary, antithetic splay fault of the Sørkjosen fault.

Langfjorden is a 50 km-long, narrow linear fjord in western Finnmark that trends ENE-WSW (Figure & Figure 2). Slickensided brittle faults with similar strike, NNW to NW dips and normal dip-slip to normal-dextral oblique-slip movement indicators (Figure 7a) occur in gabbroic rocks of the Seiland Igneous Province on the northern shore of the fjord (Figure 7a). The faults show centimeter-thick lenses of calcite-cemented cataclastic fault-rock and locally incorporate decimeter/meter-scale lenses of granitic augen gneiss (Figure 7a) that typically dominates Caledonian lithology on the southern shore of Langfjorden (Roberts, 1973). We consider these faults to represent synthetic splay-faults of the LVF, which is believed to lie at the bottom of the fjord (Zwaan & Roberts, 1978; Lippard & Roberts, 1987; Roberts & Lippard, 2005), and the lenses of granitic gneiss as fault lenses downfaulted to the north-northwest due to extensional movement along the LVF and associated splay-faults.

In the Øksfjorden peninsula, north of Langfjorden, NNE-SSW and ENE-WSW trending linear escarpments are visible on satellite images, some of which align into and correlate with high-angle, NNW- to WNW-dipping brittle faults, e.g. the Øksfjorden fault, which trends oblique to the gently west-dipping Caledonian hostrock fabric (Figure 7b). In map view, the Øksfjorden fault shows an arcuate geometry, trending ENE-WSW in Øksfjorden and curving anticlockwise into NE-SW strike to the northeast (Figure 7b), comparable to that of the LVF (Figure 2). At outcrop-scale, slickensided surfaces along the Øksfjorden fault suggest normal dip-slip extensional movement and dominant fault-rock found along the fault include fault gouge and calcite-filled cataclasite of amphibolitic hostrock (Figure 7b). The Øksfjorden fault coincides with a smooth, arcuate lineament in the nearby fjord that may represent the western prolongation of the fault (Figure 7c), which truncates the southeastern extension of a presumably older NE-dipping brittle fault on the northern shore of Øksfjorden (Figure 7b). Although partly truncated by a circular trough filled with glacial sediments, the Øksfjorden fault continues onshore to the west where it gradually curves into a WNW-ESE trend, parallel with a similarly trending topographic depression (Figure 2, Figure 4 & Figure 7c). In this area, the Øksfjorden fault shows a ca. 200-250 m right-lateral offset of a large lens of garnet-bearing gneiss within the Seiland Igneous Province (Roberts, 1973) suggesting that the Øksfjorden fault partly accommodated dextral strike-slip movement along strike. This differs from the normal dip-slip sense of shear inferred from onshore slickenside data in Øksfjorden (see Figure 7b). Nonetheless, the trend, arcuate geometry, similarity of fault-rock composition despite the change in hostrocks, and consistent extensional (dip-slip to oblique-slip) kinematic indicators suggest that the Øksfjorden fault is part of the same fault system as the Langfjorden, Sørkjosen and Straumfjordbotn faults, i.e. the LVF.

New road cuts along the western shore of Altafjorden unveiled multiple ENE-WSW to NE-SW trending, dominantly NW-dipping brittle faults, e.g. the Altafjorden fault 1 (Figure 7d), arranged in half-graben structures (Figure 2 & Figure 7d & e). These faults offset foliated Caledonian meta-arkose of the Kalak Nappe Complex and meta-psammitic schists and Paleoproterozoic meta-arkose of the Alta-Kvænangen tectonic window. Most major fault surfaces display slickengrooves that indicate normal dip-slip to normal-dextral oblique-slip sense of shear (Figure 7d & e). Normal motion along brittle faults in this area is also supported by apparent upwards bending (drag-folding) of flat-lying hostrock foliation into high-angle brittle faults (Figure 7d). Fault cores include multiple slip-surfaces that display faulting-related clay minerals (gouge) and cataclastic lenses of hostrock. Other, NW- to north-dipping brittle faults such as the Talvik fault (cf. Figure 2 & Figure 7e) show evidence of both normal brittle and ductile reverse motion, indicating that brittle faults in Altafjorden may have experienced several movement episodes. Ductile kinematic indicators along the Talvik fault include sheared quartz σ-clasts and a distributed viscous fabric within the fault core (Figure 7e) similar to that of the Kvenklubben fault in Vargundet (Torgersen & Viola, 2014), indicating top-to-the-SE thrusting. The analysis of crosscutting relationships between ductile and brittle fault fabrics show that ductile fabrics are consistently truncated by brittle fabrics (Figure 7e), thus indicating that ductile thrusting occurred first and was later overprinted by brittle cataclasis. Since the inferred top-to-the-SE transport direction matches those proposed by Townsend (1987b) and Marti (2013) for the Kalak Nappe Complex south of Langfjorden, the contractional kinematic indicators likely evidence a phase of Caledonian ductile thrusting. We therefore propose that normal faults observed on the western shore of Altafjorden, e.g. the Talvik fault (Figure 7e), formed as Caledonian ductile thrusts that accommodated top-to-the-SE movement and were reactivated as normal faults during post-Caledonian extension, as proposed along the analog Kvenklubben fault in Vargsundet (Torgersen & Viola, 2014).

In Storekorsnes, on the eastern shore of Altafjorden, near the southwestern tip of Vargsundet (Figure & Figure 2), the dominant fault trend switches to a NNE-SSW trend (Figure 7f) that is slightly oblique to the ENE-WSW/NE-SW trend that dominates in Langfjorden, Øksfjorden and along the western shore of Altafjorden (cf. Figure 7a, b, c & d). In this area, brittle faults commonly display meter-scale normal offsets of geological markers (e.g. shallow-dipping mafic dykes; cf. Figure 7f) and ductile hostrock gneissic fabric and define meso-scale horst and graben structures (Figure 7f). Slickensided fault surfaces indicate normal dip-slip movement (e.g. Figure 7f). Near the western tip of the Storekorsnes peninsula we observed a steep, ca. 5 m-wide, ESE-dipping (i.e. opposite to that of the LVF) fault, termed the Storekorsnes fault, characterized by a wide fault corridor and cataclastic fault-rock. This large fault crosscuts a 50 cm-thick mafic dyke that was not observed in the hanging-wall and this suggests that the fault accommodated movement > 10 m, although vertical throw could not be estimated with accuracy at outcrop scale. Because of the proximity of the Storekorsnes fault to the LVF

in Vargsundet, and by analogy to the opposite dips of the Straumfjordbotn fault and adjacent Sørkjosen fault, we interpret the ESE-dipping Storekorsnes fault as an antithetic, minor splay-fault of the LVF.

In Langfjorden, Altafjorden and Vargsundet (Figure), the trace of the LVF correlates with steep ENE-WSW to NNE-SSW trending submarine escarpments observed on bathymetry data (Figure 7g). Notably in the outermost part of Altafjorden, a wide glacial trough overlaps two escarpments trending ENE-WSW to NE-SW and NE-SW to NNE-SSW respectively located at the northeastern end of Langfjorden and at the southwestern tip of Varsundet (Figure 7g). These escarpments align and possibly merge, mimicking the map-view geometry of the LVF, i.e. striking ENE-WSW in Langfjorden and NNE-SSW in Vargsundet (Figure 7g). A similar glacial trough defines a topographic depression in the sound between Sørøya and Stjernøya (Figure 2 & Figure 7h). This trough, herein termed the Sørøy sub-basin, is bounded by two escarpments that trend ENE-WSW and NNE-SSW parallel to the coastlines of the islands of Stjernøya and Seiland (Figure 7h). These escarpments exemplify the zigzag geometry of the LVF in Altafjorden (Figure 7g) and, thus, may correspond to brittle faults analogous to fault segments of the LVF.

Aeromagnetic data illustrate well the bed rock architecture of western Troms and Finnmark, with broad zones (ca. 10-80 km) of NW-SE to NNW-SSE trending, alternating negative and positive anomalies that reflect the lithology of Precambrian rocks in the West Troms Basement Complex (Bergh et al., 2010) and Alta-Kvænangen tectonic window (e.g. Melezhik et al., 2015; Henderson et al., 2015). In addition, large pods of positive anomalies north of Langfjorden correspond to ultramafic rocks of the Seiland Igneous Province located within a ca. 80 km-wide, negative anomaly of felsic metamorphic assemblages (cf. Roberts, 1973; Pastore et al., 2016). In Sørkjosen, Langfjorden, Altafjorden and Vargsundet, the trace of the LVF is outlined by multiple abrupt contrasts in aeromagnetic signals (Figure 5a). Most prominent, Precambrian, NW-SE to NNW-SSE trending, ca. 70-80 km-wide, negative anomalies northwest of Sørkjosen (e.g. below the islands of Ringvassøya and Vannøya, and below the Seiland Igneous Province) abruptly narrow across the LVF to ca. 10-30 km (Figure 5a). Similarly but conversely, a 30 km-wide NW-SE to NNW-SSE trending, positive anomaly north of Sørkjosen abruptly widens to ca. 80 km across the LVF, southeast of Sørkjosen (Figure 5a). We propose that these NW-SE to NNW-SSE trending, alternating positive and negative aeromagnetic anomalies correspond to belts of macrofolded Precambrian basement granites and gneisses and volcano-sedimentary rocks downfaulted to the northwest by the LVF (Figure 5a).

In outermost areas of Altafjorden, pronounced, narrow, NNW-SSE trending, positive anomalies coincide with folded, steeply west-dipping Precambrian meta-volcanic units in the Alta-Kvænangen (Figure 8a & b; Roberts, 1973; Zwaan & Gautier, 1980; Bergh & Torske, 1988). Northwards, this anomaly abruptly curves into E-W to ENE-WSW trend and extends below the eastern shore of Altafjorden where it merges with a north-dipping meta-volcanic unit of the Altenes tectonic window (Figure 8a & b; Roberts, 1973) of analog composition and metamorphic grade (Jensen, 1996). We

propose that meta-volcanic units of the Alta-Kvænangen and Altenes tectonic windows link up in Altafjorden and define a steeply NW-plunging, antiformal fold structure (Figure 8a & b). This Precambrian fold is located just south of a major bend of the LVF, which NNW-dipping fault segment in Langfjorden parallels the NNW-dipping northern limb of the Precambrian antiform, suggesting that changing Precambrian bedrock fabrics may have controlled the geometry of the LVF and related brittle faults in Altafjorden (cf. Figure 7d and later discussion).

Between Sørøya and Stjernøya (Figure), aeromagnetic data depict large pods of high positive aeromagnetic anomalies ascribed to rocks of the Seiland Igneous Province (Pastore et al., 2016). These pods are truncated by narrow, irregular, E-W and NE-SW trending, negative aeromagnetic anomalies, some of which coincide with the southeastern boundary of the Sørøy sub-basin (Figure 8c). The zigzag pattern defined by these anomalies matches a similar pattern of NW-dipping subsurface escarpments in the fjord off the northern coast of Stjernøya and Seiland, interpreted as brittle faults (Figure 7h). Despite a weak mismatch in trend and location of the anomalies and bathymetry scarps, we interpret these negative anomalies to reflect the extention of the Sørøy sub-basin boundary-faults at depth (Figure 8c).

Faults on the Porsanger Peninsula

Northeast of Vargsundet and Repparfjorden (Figure & Figure 2), a large NNE-SSW trending escarpment, appearing as a ca. 10 m-deep river gully in the field, correlates with multiple N-S to NE-SW trending, dominantly WNW-dipping brittle faults (Figure 9a). Slickensided fault surfaces in the river gully indicate normal dip-slip to sinistral-normal oblique-slip sense of shear (Figure 9a) and incorporated cm-thick lenses of quartz-filled cataclastic fault-rock. This major escarpment and similarly trending, outcrop-scale faults align with the LVF in Vargsundet and are therefore interpreted as the continuation of the LVF (Figure 2), most likely representing minor, syntethic splay faults of the LVF (Figure 9a). This is supported by a narrow, zigzagging, ENE-WSW to NNE-SSW trending, positive aeromagnetic anomaly that stretches from the northeastern part of Vargsundet to the river gully north of Repparfjorden (Figure 9b), where it parallels outcrop brittle faults (cf. Figure 9a), and gradually dies out towards Revsbotn.

West of Kvaløya, bathymetry data show a network of steep, interconnected NW-SE to WNW-ESE trending and E-W to ENE-WSW trending escarpments, in conjunction with pervasive, smooth, NE-SW trending corrugations at the bottom of the fjord (Figure 9c). These corrugations correspond in geometry, frequency and orientation with the strike of a main foliation fabric of the bedrock gneisses onshore Kvaløya, displaying a prominent and consistent NE-SW trend and moderate to gentle NW dip (Roberts, 1973). The presence of partly overlapping ENE-WSW, and oblique E-W trending brittle faults is inferred from the relative steep character of ENE-WSW to E-W trending escarpments and from a ca. 400 m wide, left-lateral offset of a NW-SE trending lineament in the fjord (Figure 9c), potentially indicating sinistral strike-slip movement along E-W to ENE-WSW trending brittle faults there.

15

The Porsanger Peninsula consists of Caledonian meta-psammites, schists and banded gneisses with a dominantly flat-lying foliation, deeply incised by a series of interconnected fjords and brittle faults and fractures trending NW-SE to WNW-ESE (cf. next section), ENE-WSW, and subsidiarilly NNE-SSW (cf. Figure 2, Figure 3 & Figure 9d). The orientation of major fjords consistently matches the strike of the predominant, local fault trend. For example, most faults and fractures in Eiterfjorden strike NNE-SSW, e.g. Selvika-Eiterfjorden fault (Figure 2 & Figure 9d; Townsend, 1987a), though NNE-SSW are subsidiary on the Porsanger Peninsula, and this possibly suggests that glaciers preferentially eroded along existing brittle faults. ENE-WSW and NNE-SSW trending faults, e.g. the Snøfjorden-Slatten fault (Townsend, 1987a), correlate with a suite of similarly trending lineaments on satellite photographs (cf. Figure 9e). This major fault can be traced from Revsbotn to the southwestern tip of Ryggefjorden in the northeast (Figure & Figure 2) where it displays listric and splaying attitudes that form large duplex-like and relay-ramp structures between overlapping faults in map view (cf. Figure 9f). At outcrop scale, minor fractures flatten and sole into prominent fault surfaces producing listric and splaying geometries generating half-graben and graben structures in cross-section.

Slickensided, ENE-WSW trending fault surfaces on the Porsanger Peninsula mostly reveal normal dextral/sinistral oblique-slip motion, whereas movement along subsidiary NNE-SSW trending faults dominantly is normal dip-slip (Figure 3). Such fault character is supported by rotation of ductile hostrock fabric across brittle faults. In outcrops, the fault-core of the SE-dipping Snøfjorden-Slatten fault defines several meter-wide zones of shattered hostrock composed of clay-rich fault gouge and cataclastic fault-rock lenses (Figure 9g). Overall, the geometric and kinematic character of ENE-WSW and NNE-SSW trending brittle faults on the Porsanger Peninsula suggest they are genetically related to the LVF. More specifically, the Snøfjorden-Slatten fault (Figure 9g) may represent the onshore continuation of the LVF on the Porsanger Peninsula or corresponds to an antithetic splay-fault of the LVF. This is also supported by the apparent alignment of the Snøfjorden-Slatten fault (Figure 9e & g) with a major NE-SW to NNE-SSW trending escarpment observed northeast of Repparfjorden (Figure 2 & Figure 9a).

Bathymetry data in Revsbotn (Figure) show steep, south-dipping escarpments that merge with major onshore lineaments of comparable E-W to ENE-WSW trend on the Porsanger Peninsula. Westwards, the submarine escarpments link up with E-W to WNW-ESE trending lineaments that correlate with brittle faults, some of which potentially offsetting the Kjøtvika fault from the Skarvdalen fault in Northeast Sørøya, e.g. the Akkarfjord fault (Figure 9h; Roberts, 1971). These escarpments trend oblique to NE-SW to NNE-SSW trending ridges associated with ductile bedrock fabrics onshore Kvaløya (Figure 9c & h) and to glacial ploughmarks in Revsbotn, and, thus, we interpreted them as brittle faults (Figure 9h). This dominant E-W fault trend is oblique to the WNW-ESE to NW-SE trending Kokelv Fault that terminates at the southeastern end of Revsbotn (Figure 2 & Figure 9h), suggesting that the Kokelv Fault is truncated and offset by E-W trending faults in Revsbotn. Furthermore,

16

topographic data on the northeastern shore of Revsbotn, and bathymetry data in Snøfjorden, display steep, NNE-SSW trending escarpments (Figure 9h & i) that overlap with series of brittle faults crosscutting the sub-horizontal Caledonian at high-angle. We interpret these NNE-SSW trending escarpments as the continuation of the LVF across Revsbotn (Figure 9h).

A dense network of interconnected, steep, NNE-SSW and ENE-WSW trending lineaments forming a ca. 2 km-wide depression, the Ryggefjorden trough, is observed on bathymetry data (Figure 10a-d). In map view, the Ryggefjorden trough has an asymmetric sigma shape essentially resulting from the arcuate geometry of a large WNW-dipping escarpment that bounds the trough to the southeast and that abruptly curves into a N-S trend at the northeastern end of Ryggefjorden (Figure 10a-d). The sigma shape of the trough is controlled by a few major, steeply dipping, NNE-SSW trending escarpments and subsidiary ENE-WSW trending escarpments (Figure 10a-d). Major scarps dip to the east-southeastwards in the northwestern part and west-northwestwards in the southeastern part of the trough (Figure 10c-e), and accommodate significant drops of in relief within the trough, separating a series of gently dipping, rugged terraces that deepen towards the center of Ryggefjorden (Figure 10e). Since the bedrock foliation in the area is largely sub-horizontal (Figure 10e; Roberts, 1998), we interpret the steep escarpments in the Ryggefjorden trough as brittle normal faults and the gently dipping, rugged terraces as eroded, tilted, domino-like fault-blocks. The main NNE-SSW trending, southeast boundary-fault of the Ryggefjorden trough merges with NE-SW trending lineaments representing the northeastern extension of the Snøfjorden-Slatten fault, a possible fault segment/splay of the LVF, on the Porsanger Peninsula (cf. Figure 9e), and may therefore correspond to the northeastern continuation of the LVF. In the northeastern part of the trough, the southeast boundary-fault displays an undulating geometry in map-view and is clearly crosscut by trough-internal, ENE-WSW trending escarpments that die out to the northeast (see Figure 10a-d). We ascribe the switch from linear to undulating geometry of the southeast boundary-fault of the trough to minor movement along ENE-WSW trending faults (Figure 10a-d), suggesting faulting along ENE-WSW trending faults subsequently to the formation of NNE-SSW trending faults.

Detailed interpretation of bathymetry data further show that NNE-SSW trending faults in Ryggefjorden consistently curve anticlockwise into N-S trend to the northeast (Figure 10a & c) and extend northwards as arcuate, NNW-SSE to NNE-SSW trending escarpments bounding a series of arcuate, left-stepping, NNE-SSW trending, sigma-shaped troughs that can be traced to the apex of a large glacial fan (Vorren et al., 1986) near the shelf-break, west of Magerøya (Figure 11a). We propose these arcuate-shaped, NNE-SSW to NNW-SSE trending escarpments bounding left-stepping, NNE-SSW trending, sigma-shaped troughs represent analogs to faults bounding the Ryggefjorden trough and, thus, may represent the northern prolongation of the LVF (Figure 11a).

Faults on Magerøya

Metasedimentary and mafic plutonic rocks of the Magerøy Nappe are truncated by a series of prominent WNW-ESE trending lineaments (see next section) and subsidiary ENE-WSW trending lineaments (Figure 11b). For example, the NNE-dipping Magerøysundet fault (Figure & Figure 2) mapped during construction of the subsea tunnel between Magerøya and the Porsanger Peninsula (Rykkelid, 1992). Notably, across this fault the Magerøy Nappe and a major granite body (Finnvik Granite; Andersen 1981), disappear to the southwest, thus suggesting significant downfaulting to the northeast along the Magerøysundet fault (Andersen et al., 1982). On satellite images, however, the westward continuation of the Magerøysundet fault correlates with a steep E-W trending escarpment that crosscuts rocks of the Kalak Nappe Complex (Figure 11c), indicating that the fault can be traced westwards onto the Porsanger Peninsula. Field studies indicate two prominent sets of steeply dipping fractures trending ENE-WSW and WNW-ESE, while NNE-SSW faults are scarce (Figure 2, Figure 3 & Figure 11b). Exceptions occur, e.g. in a quarry within the Honningsvåg Igneous Complex where ENE-WSW and NNE-SSW trending fractures are abundant (Figure 11d). Kinematic analysis of slickensided, ENE-WSW trending fault surfaces reveal dominant sinistral- to dextral-normal oblique-slip movements, notably including a prominent strike-slip component (Figure 3), while a few NNE-SSW trending faults yield normal dip-slip sense of shear. In Helnes, in the northeastern part of Magerøya, ENE-WSW trending faults and lineaments are truncated by presumed younger, laterally continuous WNW-ESE trending faults (Figure 11e). However, opposite crosscutting relationships were also observed, e.g. in a quarry on Magerøya (Figure 11d), advocating synchronous formation of the ENE-WSW and WNW-ESE trending brittle faults.

In the southern part of Magerøya, the presumed downfaulting to the northeast of the Finnvik Granite along the Magerøysundet fault is not verified by aeromagnetic data (Figure 11f). The negative anomaly of the Finnvik Granite can be traced into the Magerøysundet fjord in the southwest but the anomaly is nowhere offset (Figure 11f). We therefore believe that the NNW-dipping Magerøysundet fault observed in the tunnel to Magerøya (Rykkelid, 1992) rather extends west-southwestwards onto the Porsanger Peninsula, as interpreted from satellite images (Figure 11c) rather than into the Magerøysundet fjord.

4.2. WNW-ESE trending faults

Faults on Magerøya

WNW-ESE trending lineaments are most abundant on the island of Magerøya and the Porsanger Peninsula, i.e. near the trace of the TKFZ (cf. Figure , Figure 2 & Figure 3). Satellite images show that the topography on Magerøya is controlled by large-scale, steep, WNW-ESE (and subsidiary ENE-WSW) trending lineaments arranged in rhombic-shaped, duplex-like geometries (Figure 11b & Figure 12a). At outcrop scale, WNW-ESE trending escarpments correlate with dense networks of subparallel,

(sub)vertical brittle faults and fractures (Figure 12a & b) often appearing as large fault corridors and joint swarms (Gabrielsen & Koestler, 1987), e.g. in Helnes (Figure 11e) and along the southern shore of Tufjorden in the west (Figure 12a), sometimes intruded by dolerite dykes (Roberts et al., 1991) and occasionally forming half-graben structures (Figure 12c). . Swarms of WNW-ESE trending fault (Figure 12b) generally show limited displacement in the order of a few centimeters, with up to 0.5 m-thick, lenses of calcite-cemented cataclasite fault-cores (Figure 12c). Slickensides along fault surfaces indicate dominant sinistral strike-slip and subordinate oblique-normal sense of shear (Figure 3). The dominance of sinistral strike-slip kinematics is supported by tens of meter left-lateral offsets of a felsic intrusion in the Magerøy Nappe and by the offset of the contact between the Magerøy Nappe and the Kalak Nappe Complex along WNW-ESE trending brittle faults in western Magerøya (Andersen, 1981). Supplementary, S-shaped rhombic, duplex-like structures formed by the interaction of WNW-ESE and ENE-WSW trending lineaments (Figure 11b) confirm sinistral strike-slip extensional (transtentional) movement along WNW-ESE trending faults.The observed merging of the two fault sets, combined with contrasting dextral and sinistral strike-slip motion on some ENE-WSW and WNW-ESE trending faults suggest a synchronous, conjugate formation of the two fault trends. Moreover, the similar duplex-like geometries formed by these conjugate fault sets onshore Magerøya suggest a genetic relationship with analog, fault-bounded, duplex structures along the TKFZ on the Varanger Peninsula (Siedlecki, 1980).

Detailed geometric studies of brittle faults in a quarry within the Honningsvåg Igneous Complex show SW-dipping, low-angle listric faults merging into each other downwards (Figure 11d & Figure 12d). These faults incorporate thin lenses of cataclastic fault-rock superimposed onto SW-dipping, ductile shear zones in foliated amphibolite schists. The ductile shear zones comprise tight, partly offset, asymmetric Z-shaped folds (Figure 12d) and minor shear bands. The asymmetric Z-shaped folds are interpreted as drag folds formed by top-to-the-NE thrusting (cf. orange marker and upper-right frame in Figure 12d), i.e. oblique to Caledonian nappe transport directions in general. Low-angle, SW-dipping brittle faults that truncate these Caledonian-oblique thrusts comprise slickenside lineations that indicate oblique normal-dextral, down-to-the-SW sense of shear (Figure 11d & Figure 12d), supporting low-angle, extensional reactivation of the ductile thrusts and the formation of overlying, subparallel normal faults as extensional splay-faults.

Analysis of bathymetry data west of Magerøya reveals pervasive, ENE-WSW trending corrugations (Figure 11a). Across Tufjorden (Figure), these ENE-WSW trending corrugations curve into a NNE-SSW trend (Figure 11a) that laterally coincides with a similar switch in trend of the dominant Caledonian bedrock fabrics onshore Magerøya, i.e. from ENE-WSW in western Magerøya to NNE-SSW trend in northern Magerøya (Andersen, 1981). On the strandflat west of Magerøya, these presumed Caledonian fabric corrugations are crosscut by laterally continuous, WNW-ESE trending gullies that correlate with major WNW-ESE trending faults and lineaments seen onshore Magerøya (Figure 11a). The largest WNW-ESE trending gullies occur in Tufjorden (Figure 11a), parallel to the

coastline of the fjord, and is bounded to the south by a steep NNE-dipping escarpment that accommodates a major drop in topography (Figure 11a). This escarpment coincides with a large, WNW-ESE trending lineament on satellite photographs onshore Magerøya, interpreted as a major brittle fault (Figure 12a), thus supporting the presence of steep, WNW-ESE trending faults west of Magerøya and in Tufjorden. Notably, the presumed major fault along Tufjorden offsets the Caledonian nappe contact between the Magerøya Nappe in the east and the Kalak Nappe Complex in the west by ca. 2-3 km left-laterally, as seen from a significant step to the northwest across Tufjorden (Figure 11a; Andersen, 1981; Robins, 1990a). On tilt-derivative aeromagnetic data, the nappe contact is outlined by a narrow, NNE-SSW trending system of positive and negative anomalies (Figure 11f) that extend across Tufjorden to the north and are offset ca. 3-4 km left-laterally below the nappe contact (Figure 11f). The offset of aeromagnetic anomalies and of the nappe contact on bathymetry data are comparable in magnitude and geometry (left-lateral) and are ascribed to a steep, WNW-ESE trending escarpment interpreted as a major brittle fault in Tufjorden (Figure 11a). Left-lateral strike-slip movement and/or down-to-the-NE, oblique-normal motion is thus inferred for the WNW-ESE trending fault in Tufjorden, which is supported by the analysis of (dominantly sinistral strike-slip) slickenside lineations along WNW-ESE trending faults onshore Magerøya (Figure 3**Figure 2**). Left-lateral strike-slip movement is further supported by left-stepping geometry of NNE-SSW trending, sigma-shaped troughs and related bounding faults on the strandflat west of Magerøya, which seem to step by > 1 km to the northwest across WNW-ESE trending submarine escarpments (Figure 11a). The mismatch between the location of the main WNW-ESE trending fault in Tufjorden and the actual step/offset of the aeromagnetic anomalies may be caused the northeastwards dip of the main fault in Tufjorden combined with aeromagnetic imaging of deeper segment of the fault (Figure 11f).

Aeromagnetic data in this area also show a ca. 15 km-wide, NNE-SSW trending, positive anomaly below the Ryggefjorden trough and the tentative extension of the trough to the south onto the Porsanger Peninsula (Figure 12e). Along-strike northwards, this 15 km-wide, positive anomaly defines a several kilometer left-step similar to the succession of left-stepping, NNE-SSW trending, sigma-shaped troughs observed on bathymetry data west of Magerøya (Figure 11a). The left-step of the positive aeromagnetic anomaly (Figure 12e) coincides with a large escarpment observed on bathymetry data that merges into brittle fault-related lineaments onshore Magerøya to the east (Figure 11a & b), thus suggesting sinistral strike-slip offset along a major WNW-ESE trending brittle fault (Figure 12e) in accordance with dominant kinematic indicators along WNW-ESE trending faults onshore Magerøya (Figure 3).

Offshore bathymetry data in Helnes, east of Magerøya, show NNE-SSW to NE-SW trending escarpments arranged subparallel to gently ESE-dipping bedrock foliation onshore Magerøya (Figure 12f; Andersen, 1981). These Caledonian fabrics coincide with similarly trending, positive anomalies on aeromagnetic data (Figure 11f) and are cut by a network of WNW-ESE trending submarine escarpments

interacting with a set of subsidiary NNW-SSE trending escarpments to create a Z-like, rhomboid-shaped trough (Figure 12f) aligned parallel to the dominant brittle fault sets observed onshore Magerøya. The Z-shaped, rhombic geometry of the trough off the coast at Helnes is similar to the shape of typical strike-slip duplex features formed by brittle faults onshore Magerøya (Figure 11a & b) and on the Varanger Peninsula (e.g. TKFZ; Siedlecki, 1980), and, therefore, suggests that WNW-ESE trending brittle faults in Helnes accommodated oblique-normal movement, which is comparable to the results from analysis of slickensides on WNW-ESE trending faults onshore Magerøya (cf. Figure 3). In terms of a brittle transtensive setting, we propose the offshore sigma-shaped trough in Helnes developed as a small-scale pull-apart basin along WNW-ESE trending, initially sinistral strike-slip faults that were reactivated as dextral strike-slip faults. Their analog geometries and location close to the TKFZ suggests these faults represent brittle fault segments of the TKFZ. An additional argument to link WNW-ESE trending faults onshore-nearshore Magerøya to the TKFZ is the occurrence of multiple, narrow, WNW-ESE trending, positive aeromagnetic anomalies running from the Varanger Peninsula (key locality of the TKFZ) to Magerøya (Figure 5a & b and Figure 11f) and representing dolerite dykes intruded along WNW-ESE trending brittle faults (Roberts et al., 1991; Nasuti et al., 2015). These anomalies truncate NNE-SSW to NE-SW trending submarine escarpments and subparallel, positive aeromagnetic anomalies representing Caledonian fabrics (Figure 11f; Roberts & Siedlecka, 2012), and extend onto Helnes where they correlate with large WNW-ESE trending fault corridors (Figure 11e & Figure 12f), thus suggesting that fault segments of the TKFZ intruded by dolerite dykes continue westwards onto Magerøya (Figure 4, Figure 5a & b and Figure 11f).

Faults on the Porsanger Peninsula

The Porsanger Peninsula is incised by several large ENE-WSW and WNW-ESE to NW-SE trending fjords that truncate the gently dipping bedrock foliation of the Kalak Nappe Complex. The dominant surface lineaments trending WNW-ESE and ENE-WSW largely overlap with exposed/inferred onshore brittle faults (Figure 2 & Figure 9d). For example, the NNE-dipping Kokelv Fault defines a series of NW-SE to WNW-ESE escarpments in the southern part of the Porsanger Peninsula (Figure 9d). This fault trends subparallel to the TKFZ and downthrows rocks of the Kalak Nappe Complex to the northeast (Gayer et al., 1985; Lippard & Roberts, 1987). Outcrops near the trace of Kokelv Fault and on the western coastline of the Porsanger Peninsula support the existence of pervasive, subvertical, NW-SE trending fractures similar to those observed on Magerøya. These fractures display limited amount of lateral offset, generally < 2 m. Slickensided fault surfaces suggest that NW-SE trending faults accommodated dominant sinistral strike-slip and subsidiary dextral strike-slip movement (Figure 3) and, locally, cataclastic fault-rocks were found along faults exhibiting low-angle, listric geometries, and these were characterized by highly fractured lenses of hostrock and fault-related clay/gouge material.

Bathymetry data west of the Porsanger Peninsula (Figure), show large WNW-ESE to NW-SE trending escarpments in Snøfjorden (Figure 9i) that coincide with onshore and nearshore troughs. In Snøfjorden, large ENE-WSW trending escarpments interpreted as brittle faults merge into WNW-ESE to NW-SE trending escarpments, curving clockwise in map-view (Figure 9i). We propose that WNW-ESE to NW-SE trending escarpments correspond to brittle faults that accommodated dextral strike-slip movement and conceivably drag-folded, presumably older, ENE-WSW trending faults. Dextral motion is supported by observed kinematic indicators on similarly trending faults onshore the Porsanger Peninsula (Figure 3).

Bathymetry data farther west, between the island of Kvaløya and Sørøya (Figure), show several NW-SE to WNW-ESE and E-W to ENE-WSW trending escarpments interpreted as brittle faults laterally offsetting each other (Figure 9c). The former may be traced east-southeastwards onshore Kvaløya where they line up with WNW-ESE trending linear valleys and lineaments (Figure 9c). These linear features are interpreted as brittle faults since they are mostly arranged oblique to the dominant NE-SW striking bedrock foliation on Kvaløya (Jansen et al., 2012), which is also seen as large number of corrugations on the adjacent seafloor (Figure 9c). West of Kvaløya, a 170 m-wide right-lateral offset of an ENE-WSW to NE-SW trending fault suggest dextral strike-slip motion along WNW-ESE trending faults. Thus, WNW-ESE and ENE-WSW striking faults laterally offset each other (see white arrows in Figure 9c), suggesting they formed synchronously.

Faults in Langfjorden-Altafjorden

Farther southwest, at the intersection of Langfjorden and Altafjorden (Figure), the LVF makes a major bend in map-view from average ENE-WSW trend in Langfjorden to NNE-SSW trend towards Vargsundet (Figure & Figure 2). At the easternmost tip of Langfjorden, a low-angle, SW-dipping brittle fault, the Storhaugen fault (Marti, 2013), is exposed near the shoreline (Figure 2 & Figure 12g). The fault trends orthogonal to the LVF and, hence, sub-parallel to the TKFZ and Kokelv Fault (Figure 2), and crosscuts felsic and mafic metasedimentary units of the Kalak Nappe Complex (Figure 12g). Slickenfibers and asperities found along the main fault surface indicate a normal-sinistral oblique-slip sense of shear (Figure 12g). Moreover, the hostrock fabrics in the footwall of the fault curve and merge into the brittle fault fabric, interpreted as drag folds due to normal sense of shear along the Storhaugen fault. This interpretation is consistent with cm- to dm-scale normal offsets of foliation surfaces across minor brittle fault splays in the footwall of the Storhaugen fault (Figure 12g).

The Storhaugen fault can be traced into the fjord as one of several, steep, NNW-SSE trending escarpments (Figure 7g). In the south, these escarpments correlate with the onshore, steeply SW-dipping ductile foliation of macro-folded, Proterozoic, volcano-sedimentary rocks of the Alta-Kvænangen tectonic window (Figure 7g; Roberts, 1973; Zwaan & Gautier, 1980). We tentatively ascribe the Storhaugen fault, which crosscuts at high angle the fabric of the Kalak Nappe Complex (Figure 12g), to

have formed along favorably oriented limbs of Proterozoic folds at depth, and to have propagated upwards into the overlying Kalak Nappe Complex. This inference is supported by aeromagnetic data in Altafjorden showing that the Storhaugen fault and related WSW-dipping submarine escarpments line up with a NNW-SSE trending, positive aeromagnetic anomaly (Figure 8a & b). We interpret this anomaly to represent steeply WSW-dipping meta-volcanic unit in the Alta-Kvænangen tectonic window, which we previously correlated to an analog unit on the eastern shore of the fjord in the Altenes tectonic window (Figure 8a & b). This unit clearly appears to form a steep, NW-plunging, antiform fold structure in Altafjorden, which western limb may have provided a suitably oriented zone of weakness at depth for the Storhaugen fault to form (Figure 8a & b).

Bathymetry data between Altafjorden and the Sørøy sub-basin show a prominent WNW-ESE trending escarpment that bounds the Sørøy sub-basin to the southwest and extends eastwards into Altafjorden, coinciding with a major counterclockwise bend in trend of the LVF (Figure & Figure 7h). This major escarpment trends parallel to the TKFZ and we interpret it as a large WNW-ESE trending brittle fault. On tilt-derivative aeromagnetic data, this major lineament coincides with a negative anomaly, which supports an interpretation as a brittle fault (Figure 8b & c).

5. Discussion

In the discussion below we address and argue for the extent and linkage of segments of the two major fault trends LVF and TKFZ in NW Finnmark and their relationship to zigzag/rhombic-shaped nearshore basins, interaction of the two fault trends, controlling basement factors, absolute timing constraints, and implications for correlation with offshore faults.

5.1. Architecture and extent of the Langfjord-Vargsund Fault

We have mapped and argued for multiple zigzag-shaped, NNE-SSW and ENE-WSW trending fault strands of the LVF in NW Finnmark that follow the coast-parallel trend of the onshore-nearshore VVFC and offshore TFFC (Figure). These major fault complexes bound onshore basement horsts, the Lofoten ridge and West Troms Basement Complex, in which the VVFC down-drops Caledonian rocks to the east (Figure ; Olesen et al., 1997; Indrevær et al., 2013). The studied LVF segments may arguably, represent the northeastwards extension of the VVFC as a joint system of margin-parallel faults, or alternatively define a separate fault complex.

Considering strong similarities in fault architecture (zigzag shape and listric fault geometries), kinematics (normal dip- to oblique-slip), and inferred magnitude of displacement along the LVF and VVFC (i.e. a few hundreds of meters to a few kilometers; Indrevær et al., 2013), we favor they belong to the same fault system. An argument against the VVFC and LVF belonging to the same fault complex

23

is that the LVF mainly dips to the NW whereas the VVFC dips to the SE. This contrast in dip direction, however, may be explained by linkage of alternating syntethic and antitethic fault strands (Figure 6, Figure 7, Figure 9 & Figure 10), and/or a switch in polarity across tentative transfer fault zones (cf. Olesen et al., 1997; Bergh et al., 2007). For instance, Indrevær et al. (2013) argued that the VVFC extends offshore and merges with the Måsøy and Nysleppen fault complexes (Figure), and that a shift in polarity between the SE-dipping VVFC and NW-dipping Måsøy Fault Complex is due to transfer movements along the Fugløya transfer zone. Nevertheless, the Sørkjosen portion of the LVF extends to the southwest, across the Fugløya transfer zone, as observed in the field (Figure 6) and on aeromagnetic data (Figure 5 & Figure 8b), and possible correlation across Lyngenfjord (Figure 4) suggests it links up with the Laksvatn fault, a major, NW-dipping, inverted Caledonian thrust fault (Figure ; Davids et al., 2013) that separates the Lyngen and Nordmannvik nappes (Slagstad, 1995; Kvassnes et al., 2004) and may have accommodated down-to-the-WNW extension during the collapse of the Caledonides (Schiffer, 2017). Thus, we reject the possibility of the VVFC and LVF representing fault strands of the same fault complex and, instead, argue that they represent antithetic fault complexes of a single, coast-parallel fault system.

Farther northeast, the LVF is expressed as major faults (in Sørkjosen) and multiple minor splay faults with planar to listric geometries (in Straumsfjorden, Langfjorden, Øksfjorden and Altafjorden), striking ENE-WSW (and subsidiarilly NNE-SSW) and mostly dipping to the northwest (Figure 14). SE-dipping faults (e.g. the Straumfjordbotn and Storekorsnes faults; Figure 2 and Figure 6f & g) are interpreted as antithetic to the LVF and, when combined with the LVF, form horst-graben structures (Figure 6a & e and Figure 7f). Fault cores with calcite-cemented cataclasites and gouge are present along most observed faults (Figure 7a & b). We interpret subsidiary synthetic faults (e.g. Øksfjorden fault; Figure 6b) as dip-slip normal or dextral-oblique normal splays and fault segments (Figure 2 & Figure 3) that may connect with larger fault strands of the LVF, e.g. Langfjorden (Figure 7a), through bends and steps transition zones. The presence of a major NW-dipping normal fault in Langfjorden is supported by submarine escarpments on bathymetry data (Figure 4 & Figure 7g) and by narrow, zigzag-shaped, negative anomalies on tilt-derivative data (Figure 8b), indicating an abrupt lithological transition below the fjord (Fairhead et al., 2008). Moreover, further arguments include the juxtaposition of rocks of the Seiland Igneous Province against rocks of the Kalak Nappe Complex across Langfjorden (Figure ; Roberts, 1973; Zwaan & Roberts, 1978), and geophysical data indicating a very deep root for the Seiland Igneous Complex (Pastore et al., 2016), which may have been down-dropped to the northwest by several kilometers.

Near the mouth of Altafjorden, the LVF abruptly curves into a NNE-SSW trend (Figure 2 & Figure 7g) before bending into ENE-WSW trend again in Vargsundet-Repparfjorden (Figure 9a & d). This bend is well constrained by a linear fjord-bottom escarpment in Langfjorden and Vargsundet (Figure 4 & Figure 7g) and supported onshore by numerous fault splays with similar shifts in orientation

and comparable normal dip- to oblique-slip kinematic characters (e.g. the Øksfjorden and Storekorsnes faults; Figure 2, Figure 3, Figure 6c-g, Figure 7 & Figure 9a). In addition, the arcuate-shaped Øksfjorden fault (Figure 7b & c) and the zigzag shape of the southeast-boundary fault of the Sørøy sub-basin (Figure 7h & Figure 8c) support the bending attitude of brittle faults in this area and further extension of the LVF from Langfjorden to Vargsundet (Figure 7g).

The extension of the LVF from Sørkjosen to Vargsundet is further supported by abrupt width changes of major, NNW-SSE trending aeromagnetic anomalies interpreted as Precambrian, granite-gneiss and macrofolded volcano-sedimentary belts (Zwaan & Gautier, 1980; Gautier et al., 1987; Bergh et al., 2010; Henderson et al., 2015) across the presumed fault trace (Figure 5a). Abrupt changes in the width of these anomalies across the LVF may be caused by km-scale, down-to-the-NW, normal offsets of e.g. basement, NW-SE trending (macrofolded?) belts, where antiforms become narrower and synforms broaden to the northwest, across the LVF (Figure 5a). Furthermore, the bend of the LVF in Altafjorden coincides with a major change in Proterozoic fabrics, from WSW-dipping in the Alta-Kvænangen tectonic window in the west (Roberts, 1973; Zwaan & Gautier, 1980; Gautier et al., 1987) and basement gneisses south of the Caledonides (Henderson et al., 2015) to NW-dipping in the Altenes (Jensen, 1996) and Repparfjord tectonic windows in the northeast (Reitan, 1963; Pharaoh et al., 1982, 1983).

Fault-bend acommodated linkage of the LVF from Vargsundet to Repparfjorden and Revsbotn (Figure), which is confirmed by a narrow, positive aeromagnetic anomaly (Figure 5a & Figure 9b) aligned parallel to a prominent NNE-SSW trending surface escarpment and further supported by field observations such as normal dip-slip to oblique-slip fault kinematics (Figure 9a). This escarpment was mapped as a large brittle fault separating two tectonic units of the Kalak Nappe Complex and accommodated down-to-the-NW displacement in the order of a few hundreds of meters (Gayer et al., 1985), i.e. comparable to the inferred offset along the LVF in Vargsundet (Zwaan & Roberts, 1978).

On the Porsanger Peninsula, we interpret the SE-dipping Snøfjorden-Slatten fault and related minor faults between Revsbotn and Snøfjorden (Figure 9d, g & h; Passe, 1978; Rice, 1982; Townsend, 1987a) as part of a dip-slip to oblique-slip normal splay-fault formed antithetic to the LVF. East of the Snøfjorden-Slatten fault, the LVF may continue as a suite of interconnected, zigzag-shaped, NNE-SSW to ENE-WSW trending fault-related lineaments that possibly merge with the NW-dipping, southeastern boundary-fault of the trough (Figure 9d & e), thus suggesting a genetic relationship between the LVF and the Ryggefjorden trough.

Bathymetry data suggest that the Ryggefjorden trough (Figure 10) continues as a series of km-scale, left-stepping, NNE-SSW trending, sigma-shaped troughs (Figure 11a). We argue that the several-km width of these troughs and the arcuate geometry of their boundary faults mimic the overall zigzag architecture of the LVF (Figure 2). Consequently, the Ryggefjorden trough and associated left-stepping, NNE-SSW trending, sigma-shaped troughs correspond to graben structures that developed along and

are bounded by the northeastern portion of the LVF (Figure 11a). Offshore seismic studies (Koehl et al., 2018) show that the LVF extends northwards onto the Finnmark Platform east, where it appears as a similar, zigzag-shaped, NW-dipping fault bounding a triangular- to rhomboid-shaped, Carboniferous graben (Figure).

5.2. Linking segments of the Trollfjorden-Komagelva Fault Zone

The TKFZ is best expressed onshore the Varanger peninsula in eastern Finnmark (Figure ; Siedlecki, 1980), but can be traced westward onto Magerøya and the Porsanger Peninsula as steeply dipping, WNW-ESE trending faults and fractures (Figure 11a, b, e & f and Figure 12a-f). Satellite images of Magerøya and bathymetry data from adjacent fjords have revealed close overlap of linear topographic features (fjords, sounds, scarps, depressions, ridges) and brittle faults, and typically the TKFZ forms duplex-like structures in map view (Figure 9f, Figure 11b & e, Figure 11a & Figure 12f). Our field studies show abundance of steep, WNW-ESE trending faults and fracture swarms (Figure 12b) occasionally arranged in graben structures in cross-section (Figure 12c), and that most faults displayed sinistral strike-slip movement (Figure 3). Larger-scale evidences include 3-4 km left-lateral offset of the contact between the Kalak Nappe Complex and the Magerøy Nappe visible on bathymetry and tilt-derivative aeromagnetic anomaly data in Tufjorden (Figure 11a & f), > 10 m offsets of a Caledonian granitic intrusion in western Magerøya (Andersen, 1981), km-scale left-lateral offsets of the Ryggefjorden trough and related troughs (Figure 11a) and a several km, left-lateral offset of a ca. 15 km-wide aeromagnetic anomaly (Figure 12e).

Notably, the Ryggefjorden trough and trough-internal NNE-SSW trending faults (scarps on bathymetry) west of Magerøya are offset several km left-laterally and bent counterclockwise into fault segments of the TKFZ giving the troughs their sigma-shaped geometry in map view (Figure 11a). If this map-view pattern is a product of drag-related bending into WNW-ESE trending fault segments of the TKFZ, the left-steps and sigma-shaped geometries of the troughs confirm sinistral strike-slip movements along fault segments of the TKFZ (Figure 11a), which is consistent with interpreted onshore kinematic data (Figure 3). Duplex-like geometries of WNW-ESE trending faults and sigma-shaped geometry of offset troughs in nearshore-onshore areas in northern Finnmark (Figure 9e & f, Figure 11a, b & e, Figure 12b, c & f) resemble the map-view pattern observed onshore Varanger peninsula (Jonhson et al., 1978; Herrevold et al., 2009; Rice, 2013). By contrast, the offshore prolongation of the LVF on the Finnmark Platform east is offset right-laterally by ca. 28 km (Koehl et al., 2018). This correlation is based on zigzaging map-view geometries, comparable magnitude of normal movement (a few hundred meter to a few km), and synchronous faulting ages obtained from K/Ar dating of onshore fault-gouge (Davids et al., 2013; Torgersen et al., 2014; Koehl et al., submitted) and syn-tectonic sedimentary wedges offshore (Koehl et al., 2018). Dextral strike-slip movement is also supported by the Z-shaped,

duplex-like trough observed on bathymetry data northeast of Magerøya (Figure 12f), which may have formed as a mini pull-apart basin along an initially sinistral strike-slip (transpressional) fault reactivated as a dextral strike-slip (transtensional) fault segment during post-Caledonian extension. Importantly, the LVF in Ryggefjorden aligns along a NE-SW axis with its potential continuation on the Finnmark Platform (cf. dotted red line in Figure 13a), suggesting that left- and right-lateral offsets along margin-oblique segments of the TKFZ nullify/counter-balance one another, and that the TKFZ had a limited impact on the structuring of the margin.

East of Magerøya, linear WNW-ESE trending fractures are abundant both onshore and on bathymetry data (Figure 11a, b & c and Figure 12a, b & c). These linear features correspond well with narrow, anastomosing, positive aeromagnetic anomalies, some of which correlate with dolerite dyke swarms (Figure 5a & b, Figure 11f & Figure 12e; Nasuti et al., 2015) related to early Carboniferous extension along WNW-ESE to E-W trending, reactivated fault segments of the TKFZ (cf. Roberts et al., 1991; Lippard & Prestvik, 1997).

Narrow, WNW-ESE trending, positive aeromagnetic anomalies (Figure 5b) similar to those reflecting dolerite dykes and fault segments of the TKFZ in Magerøya characterize areas of eastern Finnmark (Nasuti et al., 2015). On the Varanger Peninsula, the TKFZ and positive aeromagnetic anomalies define a narrow, ca. 12 km-wide belt (Figure 5b & Figure 13a; Siedlecka & Siedlecki, 1967; Siedlecki, 1980; Nasuti et al., 2015) that extends offshore bounding potential Late Devonian (?) - Carboniferous grabens (Figure ; Roberts et al., 2011). These anomalies diverge/splay into multiple, sub-parallel segments westward onto the Nordkinn Peninsula and Magerøya, defining a much broader, ca. 25 km-wide area (same width as Magerøya). West of Magerøya the anomalies weaken and die out (Figure 5a & b), and are not found on the Finnmark Platform (Gernigon et al., 2014). This suggests dolerite dykes and, potentially, subsidiary fault segments of the TKFZ, die out to the west as the TKFZ "fault-tip process zone" (Figure 13b; Shipton & Cowie, 2003; Braathen et al., 2013), thus not supporting a genetic relationship of the TKFZ and adjacent WNW-ESE trending fault segment of the Troms-Finnmark Fault Complex (Figure). Another argument is the counter-balancing/nullifying effect of sinistral (Figure 11a; Andersen, 1981) and dextral (Figure 12f) movements along brittle fault segments of the TKFZ, showing that the LVF remains aligned along a NE-SW trending axis although the fault is locally offset by multiple segments of the TKFZ (cf. dotted red line in Figure 13a).

5.3. Interaction of the Langfjord-Vargsundet fault and Trollfjorden-Komagelva Fault Zone

On Magerøya and the Porsanger peninsula, in the area of junction of the LVF and TKFZ (Fig. 1), the two studied fault complexes strongly interact in shaping the landscape, defining steep and narrow fjords, sounds and bedrock lineaments (Figure 9d & Figure 11b). The lineaments commonly merge to form duplex-like structures (Figure 9e & f and Figure 11a, b & e). Analysis of crosscutting relationships

27

between the two fault trends shows that they most probably formed and evolved synchronously, as they both crosscut and/or offset each other (Figure 9c & i and Figure 11d & e). Notably, on Magerøya and the Porsanger Peninsula, WNW-ESE and ENE-WSW trending faults are more abundant than margin-parallel NNE-SSW trending faults (Figure 2 & Figure 3), and both sets display dominant strike-slip sense of shear, significantly contrasting with normal dip-slip NNE-SSW trending fault segments of the LVF (cf. Figure 3). This suggests that the two (ENE-WSW and WNW-ESE trending) fault sets formed synchronously as a joint set of e.g. conjugate strike-slip dominated faults, possibly along favorable, inherited basement grains (see next section).

Our field studies on Magerøya, show a much lower density of WNW-ESE trending faults in Silurian rocks of the Honningsvåg Igneous Complex (Figure 11d; Corfu et al., 2006) while meta-sedimentary rocks of the Magerøy Nappe display a substancially higher frequency of such faults (Figure 2, Figure 3, Figure 11a, b & e, Figure 12b, g & f). This suggests that inferred, WNW-ESE directed, post-Caledonian extension (Bergh et al., 2007; Hansen et al., 2012; Indrevær et al., 2013), which is responsible for vertical movements in the order of a few hundreds of meter to a few km along margin-parallel fault complexes (e.g. LVF and VVFC), had only a minor impact on the margin-orthogonal TKFZ with localized reactivation of individual fault segments (cf. Figure 11a & f, Figure 12e & Figure 13a). Such localized fault reactivation occurs as large-magnitude, km-scale left-lateral offsets of zigzag-shaped fault-segments of the LVF that bound a series of NNE-SSW trending sigma-shaped troughs west of Magerøya (Figure 11a & f and Figure 12e) supported by abrupt drag-related left-bends of the troughs boundary-faults when approaching WNW-ESE trending, fault-related lineaments (cf. Figure 10a & c and Figure 11a). By contrast, a ca. 28 km, right-lateral offset of the LVF is inferred across a northern fault segment of the TKFZ on the Finnmark Platform east, just northeast of Magerøya (Koehl et al., 2018), clearly suggesting that strike-slip reactivation of TKFZ during post-Caledonian extension post-dated or occurred synchronously with the formation of the LVF and related (half-) grabens (Figure 13a).

5.4. Basement fabric control on post-Caledonian brittle faulting

Influence of Precambrian fabrics

NW-SE to NNW-SSE trending Archean and Proterozoic fabrics of western Troms and Finnmark are well displayed on aeromagnetic data as successive, negative and positive anomalies (Figure 5a). Of importance is the location of the major bend of the LVF in Altafjorden (Figure 8a & b). This bend imitates the changing attitude (trend and dip) of limbs of NW-plunging (refolded) antiform-synform folds in metavolcanic rocks (Figure 8a & b), which dip steeply WSW in the Alta-Kvænangen tectonic window in the west (Roberts, 1973; Bergh & Torske, 1988) and NNW in the Altenes tectonic window in the east (Jensen, 1996), therefore suggesting changes in Precambrian bedrock trends affected the initiation of the LVF. Westwards, highly magnetic metavolcanic units delineating the NW-plunging

antiform in Altafjorden define a second, NW/WNW-plunging, antiform-like structure (Figure 8a & b), which coincides with the field occurrence of a similarly trending antiform south of Langfjorden (Zwaan & Gautier, 1980; Gautier et al., 1987). Importantly, the northern, NNW-dipping limb of this antiform parallels the adjacent, Langfjorden segment of the LVF and related NNW-dipping faults on the eastern side of Altafjorden (e.g. Altafjorden fault 1; Figure 7d & e), while the WSW-dipping, western limb of the antiform in Altafjorden matches the orientation of the SW-dipping Storhaugen fault (Figure 12g), suggesting these faults initiated along steeply dipping Precambrian units (Figure 8a). Farther northeast, in Vargsundet, the LVF trends parallel to the northwestern limb of a major NE-plunging, antiform fold in the Repparfjord-Komagfjord tectonic window (Reitan, 1963; Pharaoh et al., 1982, 1983) and defines another map-view bend (zigzag pattern) above the prolongation of the fold hinge at the junction of Vargsundet and Repparfjorden (Figure 9b), thus supporting substantial influence/control of Precambrian ductile fabrics on the architecture of post-Caledonian brittle faults in NW Finnmark (Figure 5, Figure 8a & b and Figure 9b).

In Revsbotn, the LVF makes a ca. 2 km left step interpreted as an effect of left-lateral strike-slip movement on the WNW-ESE to ENE-WSW trending Akkarfjord fault (Roberts, 1971; Figure 2 & Figure 9h), which is supported by dominant sinistral strike-slip to oblique-normal movement on WNW-ESE and ENE-WSW trending faults on the Porsanger Peninsula (Figure 3) and on northeastern Sørøya (Roberts, 1971), suggesting that the Akkarfjord fault acted as a strike-slip transfer fault during post-Caledonian extension. The lack of WNW-ESE trending fabrics and lineaments in Revsbotn suggests that the Akkarfjord fault truncated the NNE-dipping Kokelv Fault (Figure 2, Figure 9d & h; Gayer et al., 1985; Lippard & Roberts, 1987). West of Magerøya, the LVF and associated NNE-SSW trending troughs in Ryggefjorden and northwards are laterally bent and offset along WNW-ESE trending brittle fault segments of the TKFZ (Figure 10 & Figure 11a) that also seem to control atypical, top-to-the-NE transport direction along Caledonian thrust observed in the Honningsvåg Igneous Complex on Magerøya (Figure 12d), thus confirming the impact of inherited, Precambrian, WNW-ESE fault trend on the LVF and related margin-parallel fault complexes.

By contrast, dip- to oblique-slip, WNW-ESE to NW-SE trending faults such as the Storhaugen fault in Altafjorden (Figure 7g & Figure 12g), the Kokelv Fault in Revsbotn (Figure 13a & Figure 14; Gayer et al., 1985) and the Markopp fault in Repparfjorden (Figure 2; Torgersen et al., 2014) do not seem to impact the geometry of the LVF. Furthermore, aeromagnetic data in Sørkjosen and Langfjorden show that the NNW-SSE trending Fugløya transfer zone and its onshore extension, the Bothnian-Kvænangen Fault Complex (Figure), do not appear to affect the LVF (cf. Figure 5a & Figure 8b) despite accommodating switches of polarity between the VVFC and Måsøy Fault Complex (Indrevær et al., 2013).

On the Varanger Peninsula, the TKFZ defines a network of closely interacting WNW-ESE and ENE-WSW trending faults (Siedlecki, 1980; Roberts & Olovyanishnikov, 2004; Kirkland et al., 2008b),

as do similar fault strands onshore-nearshore Magerøya and the Porsanger Peninsula (Figure 7c, Figure 9f, h & i, Figure 11a, b & e and Figure 12f). We interpret these two brittle fault sets to have formed synchronously as conjugate sets, a claim supported by kinematic data, i.e. sinistral (-dextral) strike-slip for WNW-ESE trending and sinistral, oblique-normal for ENE-WSW trending faults (Figure 2) onshore Magerøya and the Porsanger Peninsula (this study), the island of Seiland (Worthing, 1984) and northeastern Sørøya (e.g. along the Akkarfjord fault; Roberts, 1971). Consequently, if the TKFZ initiated in Neoproterozoic times (cf. Johnson et al., 1978; Herrevold et al., 2009; Roberts & Siedlecka, 2012; Rice, 2013), both brittle fault sets may be inherited Timanian (?) structures and e.g. the Akkarfjord fault (Figure 9h) may have formed as a conjugate to the TKFZ.

Influence of Caledonian fabrics

Along the western shore of Altafjorden (Figure), extension utilized existing, ductile mylonitic fabrics along the Talvik fault formed during top-to-the-south Caledonian thrusting (Towsend, 1987b; Marti, 2013) to accommodate down-to-the-north, normal dip-slip movement (Figure 7e). Similar controlling effects of brittle faulting are inferred for the Kvenklubben (thrust) fault in the Repparfjord-Komagfjord tectonic window along the southeastern shore of Vargsundet (Figure ; Torgersen & Viola, 2014; Torgersen et al., 2014). This SE-dipping, low-angle fault acted as a brittle-ductile thrust during the Caledonian Orogeny and was later reactivated as a normal fault that possibly merge with the LVF at depth (cf. figure 2b in Torgersen & Viola, 2014 and Torgersen et al., 2014).

Further, we argue that arcuate, zigzag-shaped faults, e.g. Langfjorden and Vargsundet fault segments of the LVF and Øksfjorden fault (Figure 2 and Figure 7a & b), formed during the early stages (?) of late/post-orogenic collapse of the Caledonides as high-angle splay-faults of inverted, low-angle, Caledonian thrusts (e.g. the Kvenklubben and Talvik faults; Figure 14a & b). Incremental extension may have localized along high-angle splay-faults (e.g. LVF; Figure 14c), which eventually decapitated inactive portions of low-angle Caledonian thrust faults by more than 100 m (Figure 14d). This model is supported by consistent down-to-the-NW, normal movement on high-angle, brittle fault segments of the LVF (Figure 7a, b & e), and by juxtaposition (down-drop?) of rocks of the Seiland Igneous Province against rocks of the Kalak Nappe Complex across Langfjorden (Roberts, 1973) and Precambrian basement rocks across Vargsundet (Zwaan & Roberts, 1978). Further support of a high-angle splay origin for fault-segments of the LVF is the preservation of ca. 6-8 km-wide lenses of Kalak Nappe Complex rocks in the footwall of the LVF in Vargsundet (Torgersen & Viola, 2014; Figure) and hundreds of meter-wide pods of units of the Seiland Igneous Province in the footwall of the LVF in Langfjorden (Marti, 2013), suggesting that rocks of the Seiland Igneous Province and Kalak Nappe Complex were thrusted southeastwards above basement rocks and then down-dropped and preserved to the northwest of Langfjorden and Vargsundet due to km-scale normal movement along the LVF.

A similar origin, i.e. as high-angle, normal splay-faults of inverted, low-angle Caledonian thrusts, was proposed for normal faults that bound Middle Devonian collapse basins in western Norway (Andersen et al., 1994; Wilks & Cuthbert, 1994) and for the formation of the main fault segment of the Måsøy Fault Complex along the Sørøya-Ingøya shear zone offshore, on the Finnmark Platform west (Koehl et al., 2018; Figure). In addition, a seismic study by Phillips et al. (2016) in the North Sea discusses an analog relationship between a large, listric, basin-bounding, post-Caledonian normal fault, the Åsta Fault, and a thick, low-angle, Caledonian mylonitic shear zone that represents the offshore extension of the Karmøy Shear Zone (Fossen & Hurich, 2005; Fossen, 2010; Phillips et al., 2016). We believe the LVF represents an onshore-nearshore analog to the Måsøy Fault Complex (SW Barents Sea) and the Åsta Fault (North Sea).

In igneous rocks of the Magerøy Nappe, gently SW-dipping, mylonitic, shear zones formed by top-to-the-NE thrusting and were reactivated as low-angle, listric, dextral oblique-normal faults with down-to-the-SW movement (Figure 11d & Figure 12d). The thrust faults formed subsequently to the intrusion of the Honningsvåg Igneous Complex, i.e. in Silurian times (Corfu et al., 2006), likely during the Scandian stage of the Caledonian Orogeny. The NE-directed transport direction, however, is almost perpendicular to that of main Caledonian thrusting in Finnmark (top-to-the-SE; Townsend, 1987b; Marti, 2013), indicating the early TKFZ may have acted as an oblique thrust ramp. The truncation of these ductile shear zones by sub-parallel, low-angle, SW-dipping brittle normal faults with down-to-the-SW normal movements suggests the shear zones were inverted as oblique, post-Caledonian, low-angle normal faults that localized the formation of subsequent, high-angle, extensional brittle splay-faults (Figure 12d).

5.5. Timing of brittle faulting and dolerite dykes intrusion

Accurate timing of onshore post-Caledonian brittle faulting along the studied LVF and TKFZ in Finnmark is only partly constrained by absolute datings (Lippard & Prestvik, 1997; Torgersen et al., 2014), but indirect dating of basin-bounding faults from seismic data on the Finnmark Platform provide important clues for onshore/nearshore comparison (e.g. Indrevær et al., 2013; Koehl et al., 2018). Furthermore, dating the emplacement of mafic dolerite dykes along the TKFZ (cf. Figure 5a & b, Figure 11f & Figure 12e) provides an excellent framework to discuss extensional episodes when brittle fault initiation and reactivation may have occurred (cf. Roberts et al., 1991; Nasuti et al., 2015). On the Varanger Peninsula, dolerite dykes intruded along NE-SW and N-S trending brittle faults yielded Late Devonian (ca. 370 Ma) $^{40}Ar/^{39}Ar$ ages (Guise & Roberts, 2002), whereas Carboniferous (Visean) ages (337.3 ±0.4 Ma and 340 ±4 Ma) of similar dykes on Magerøya trending WNW-ESE were obtained by Lippard & Prestvik (1997). Since the dykes on Magerøya are not fractured and/or offset by WNW-ESE trending brittle faults, these intrusions post-dated the early Carboniferous reactivation episode of the

31

TKFZ (Lippard & Prestvik, 1997). It seems reasonable to assume similar ages for most dolerite dykes observed in northern and eastern Finnmark (Figure 5a & b; Nasuti et al., 2015) and nearby Russia (Roberts & Onstott, 1995). Accordingly, the observed strike-slip reactivation of the TKFZ can be constrained to the collapse of the Caledonides in Late Devonian-early Carboniferous times (Figure 14a-c) and that most faults became inactive shortly after the emplacement of dolerite dykes in the Visean (Lippard & Prestvik, 1997; Figure 14d). Farther (south-) west in Finnmark, however, new K/Ar radiometric dating of NW-SE trending faults in the Repparfjord-Komagfjord tectonic window (e.g. the Markopp fault; Figure 2; Torgersen et al., 2014) and of minor WNW-ESE trending fault segments of the TKFZ that are not cemented by dolerite dykes (Koehl et al., submitted) suggest brittle faulting persisted until mid-Permian times.

The LVF can be correlated with nearshore and offshore faults on the Finnmark Platform where seismic analysis indicates extensive faulting activity had ceased by the end of the late Carboniferous, since very few faults truncate Permian sedimentary strata (Koehl et al., 2018). Recent K/Ar dating of brittle fault segments and splays of the LVF in NW-Finnmark, e.g. Talvik and Kvenklubben faults (Torgersen et al., 2014; Koehl et al., submitted), yielded abundant, partly younger, early Carboniferous to mid-Permian ages, thus suggesting extensive and widespread faulting during the collapse of the Caledonides, and subsidiary Mid/Late Jurassic-Early Cretaceous ages indicative of mild reactivation related to the early stages of the rifting of the NE-Atlantic. By comparison, in Western Troms and Lofoten-Vesterålen, K/Ar dating of fault gouge of the VVFC (Davids et al., 2013) similarly showed widespread faulting in the Late Devonian-early Permian and sporadic, minor reactivation of brittle faults from the mid Permian to Early Cretaceous. Notably, a Late Devonian age was obtained for the Laksvatn fault (Davids et al., 2013), which can be directly linked to the Sørkjosen fault segment of the LVF (Figure).

5.6. Comparison with deep offshore basins

Our data and results document the existence of triangular, sigma-shaped grabens and half-grabens bounded by zigzag-shaped, ENE-WSW to NNE-SSW trending normal fault segments of the LVF in nearshore areas of NW Finnmark, e.g. Ryggefjorden trough (Figure 10). These grabens and half-grabens are similar in shape and geometry, though relatively smaller, to late Paleozoic (half-) grabens recorded on seismic data on the Finnmark Platform east (Koehl et al., 2018) and to the southwestern segment of the Nordkapp Basin farther offshore (Figure ; Gudlaugsson et al., 1998). The present, map-view, sigma-shaped geometry of the LVF and related onshore-nearshore brittle faults and (half-) grabens have arguably been shaped by existing Caledonian thrust faults (Torgersen & Viola, 2014) and attitudes of Precambrian belts and folds at depth (cf. Figure 8a & b and Figure 9b; Reitan, 1963; Zwaan & Gautier, 1980; Pharaoh et al., 1982, 1983; Gautier et al., 1987; Bergh & Torske, 1988). Deeper offshore basins

like the Hammerfest and Nordkapp basins, and adjacent coast-parallel faults such as the TFFC and VVFC (Figure 14e), all follow existing basement trends and share the same geometric properties as the LVF (cf. Gernigon et al., 2014). This is particularly true for the Ryggefjoren trough (Figure 10) and the southwestern segment of the Nordkapp Basin (Figure). Assuming that the LVF and related Ryggefjorden trough and southwestern segment of the Nordkapp Basin formed in the Mid/Late Devonian-early Carboniferous (Davids et al., 2013; Koehl et al., 2018), the Ryggefjorden trough may represent an exhumed "window" into contemporaneous faults and sedimentary strata, e.g. below late Carboniferous-early Permian evaporites in the Nordkapp Basin (Jensen & Sørensen, 1992; Koyi et al., 1993; Nilsen et al., 1995).

6. Conclusions

1) A system of large ENE-WSW and NNE-SSW trending normal faults in NW Finnmark line up to form a major zigzag-shaped, margin-parallel, steeply NW-dipping fault complex, the Langfjord-Vargsund fault, which accommodated down-to-the-NW normal displacement in the order of hundreds of meters to a few km. This fault complex is interpreted to have formed as a brittle splay of a low-angle, NW-dipping, Caledonian brittle-ductile thrusts that were partly inverted during late/post-orogenic collapse of the Caledonides. The Langfjord-Vargsund fault represents an onshore-nearshore analog to the offshore Troms-Finnmark and Måsøy fault complexes, which are thought to have formed along the Sørøya-Ingøya shear zone, a presumably inverted Caledonian thrust.

2) The WNW-ESE trending, margin-orthogonal Trollfjorden-Komagelva Fault Zone corresponds to a major, reactivated Neoproterozoic fault that acted as a strike-slip transfer fault, segmenting NW Finnmark from the Finnmark Platform east during post-Caledonian extension and laterally offsetting the Langfjord-Vargsund fault by up to 28 km. Post-Caledonian, km-scale sinistral and dextral offsets by fault segments of the Trollfjorden-Komagelva Fault Zone counter-balance one another and the fault zone dies out west of the island of Magerøya, which represents an exposed portion of the fault-tip process zone.

3) The WNW-ESE to ENE-WSW trending Akkarfjord fault may be part of an inherited Neoproterozoic conjugate fault set to the Trollfjorden-Komagelva Fault Zone and later acted as a strike-slip transfer fault offsetting the Langfjord-Vargsund fault ca. 2 km left-laterally.

4) Gently NW-dipping, brittle-ductile Caledonian thrust faults, and steep NW-plunging and gently NE-plunging Precambrian folds in Paleoproterozoic basement rocks provided favorable weakness zones that controlled the formation of steep, post-Caledonian normal faults as extensional splays of Caledonian thrusts faults and along steep limbs of Precambrian folds.

5) Major faulting events (with km-scale offsets) along WNW-ESE trending fault segments of the Trollfjorden-Komagelva Fault Zone and ENE-WSW and NNE-SSW trending fault segments of the Langfjord-Vargsund fault last occurred in the Late Devonian-Carboniferous. This is supported by radiometric dating of dolerite dykes and fault gouge onshore NW Finnmark, and by seismic interpretation of syn-tectonic sedimentary wedges along the possible offshore extension of the Langfjord-Vargsund fault on the Finnmark Platform east.

6) Half-graben and graben basins were observed on bathymetry data along the Langfjord-Vargsund fault in shallow shelf areas, e.g. the Ryggefjorden trough. This trough is similar in trend and shape (triangular to sigma-shaped) to major offshore sedimentary basins such as the southwestern segment of the Nordkapp Basin, although relatively smaller, and to other Devonian (?) - Carboniferous basins on the Finnmark Platform east. The Ryggefjorden trough might therefore provide with insights in the early basin architecture of the Nordkapp Basin prior to the deposition of thick, late Carboniferous-early Permian evaporites.

References

Andersen, T.B. 1981: The structure of the Magerøy Nappe, Finnmark, North Norway. *Norges Geologiske Undersøkelse 363*, pp. 1-23.

Andersen, T.B. 1984: The stratigraphy of the Magerøy Supergroup, Finnmark, north Norway. *Norges geologiske undersøkelse 395*, pp. 25-37.

Andersen, T.B., Austrheim, H., Sturt, B.A., Pedersen, S. & Kjærsud, K. 1982: Rb-Sr whole rock ages from Magerøy, North Norwegian Caledonides. *Norsk Geologisk Tidsskrift 62*, pp. 79-85.

34

Andersen, T.B., Osmundsen, P.T. & Jolivet, L. 1994. Deep-crustal fabrics and a model for the extensional collapse of the Southwest Norwegian Caledonides. *Journal of Structural Geology 16*, pp. 1191-1203.

Andresen, A., Agyei-Dwarko, N.Y., Kristoffersen, M. & Hanken, N-M. 2014: A Timanian foreland basin setting for the late Neoproterozoic-Early Palaeozoic cover sequences (Dividal Group) of northeastern Baltica. *In* Corfu, F., Gasser, D. & Chew, D.M. (eds.): *New Perspectives on the Caledonides of Scandinavia and Related Areas*. Geological Society, London, Special Publications 390, pp. 157-175.

Bergh, S.G. & Torske, T. 1986: The Proterozoic Skoadduvarri Sandstone Formation, Alta, Northern Norway: A tectonic fan-delta complex. *Sedimentary Geology 47*, pp. 1-25.

Bergh, S.G. & Torske, T. 1988: Palaeovolcanology and tectonic setting of a Proterozoic metatholeiitic sequence near the Baltic Shield Margin, northern Norway. *Precambrian Research 39*, pp. 227-246.

Bergh, S.G., Eig, K., Kløvjan, O.S., Henningsen, T., Olesen, O. & Hansen, J-A. 2007: The Lofoten-Vesterålen continental margin: a multiphase Mesozoic-Palaeogene rifted shelf as shown by offshore-onshore brittle fault-fracture analysis. *Norwegian Journal of Geology 87*, pp. 29-58.

Bergh, S.G., Kullerud, K., Armitage, P.E.B., Zwaan, K.B., Corfu, F., Ravna, E.J.K. & Myhre, P.I. 2010: Neoarchean to Svecofennian tectono-magmatic evolution of the West Troms Basement Complex, North Norway. *Norwegian Journal of Geology 90*, pp. 21-48.

Bergø, E. 2016: Analyses of Paleozoic and mesozoic brittle fractures in West-Finnmark. *Unpublished Master's Thesis, University of Tromsø*, 128 pp.

Braathen, A., Osmundsen, P-T., Nordgulen, Ø., Roberts, D. & Meyer, G.B. 2000: Orogen-parallel extension of the Caledonides in northern Central Norway: an overview. *Norwegian Journal of Geology 82*, pp. 225-241.

Braathen, A., Osmundsen, P.T., Hauso, H., Semshaug, S., Fredman, N. & Buckley, S.J. 2013: Fault-induced deformation in poorly consolidated, siliciclastic growth basin: A study from the Devonian in Norway. *Tectonophysics 586*, pp. 112-129.

Breivik, A.J., Gudlaugsson, S.T. & Faleide, J.I. 1995: Ottar Basin, SW Barents Sea: a major Upper Palaeozoic rift basin containing large volumes of deeply buried salt. *Basin Research 7*, pp. 299-312.

Bylund, G. 1994: Palaeomagnetism of the Late Precambrian Vadsø and Barents Sea Groups, Varanger Peninsula, Norway. *Precambrian Research 69*, pp. 81-93.

Bøe, P. & Gautier, A.M. 1978: Precambrian primary volcanic structures in the Alta-Kvænangen tectonic window, northern Norway. *Norsk Geologisk Tidsskrift 58*, pp. 113-119.

Chauvet, A. & Séranne, M. 1994: Extension-parallel folding in the Scandinavian Caledonides: implications for late-orogenic processes. *Tectonophysics 238*, pp. 31-54.

Cianfarra, P. & Salvini, F. 2015: Lineament Domain of Regional Strike-Slip Corridor: Insight from the Neogene Transtentional De Geer Transform Fault in NW Spitsbergen. *Pure Appl. Geophys. 172*, pp. 1185-1201.

Davids, C., Wemmer, K., Zwingmann, H., Kohlmann, F., Jacobs, J. & Bergh, S.G. 2013: K-Ar illite and apatite fission track constraints on brittle faulting and the evolution of the northern Norwegian passive margin. *Tectonophysics 608*, pp. 196-211.

Dengo, C.A. & Røssland, K.G. 1992: Extensional tectonic history of the western Barents Sea. *In* Larsen, R.M., Brekke, H., Larsen, B.T. & Talleraas, F. (eds.): *Structural and Tectonic Modelling and its Apllication to Petroleum Geology*, NPF Special Publication 1, pp. 91-107.

Eig, K. 2008: Onshore and offshore tectonic evolution of the Lofoten passive margin, North Norway. *PhD thesis, University of Tromsø*, 256 pp.

Eig, K. & Bergh, S.G. 2011: Late Cretaceous-Cenozoic fracturing in Lofoten, North Norway: Tectonic significance, fracture mechanisms and controlling factors. *Tectonophysics 499*, pp. 190-215.

Elvevold, S., Reginiussen, H., Krogh, E.J. & Bjørklund, F. 1994: Reworking of deep-seated gabbros and associated contact metamorphosed paragneisses in the south-eastern part of the Seiland Igneous Province, northern Norway. *Journal of Metamorphic Geology 12*, pp. 539-556.

Fairhead, J.D., Salem, A., Williams, S. & Samson, E. 2008: Magnetic interpretation made easy: The Tilt-Depth-Dip-$\varDelta K$ method. *SEG Technical Program Expanded Abstracts 2008*, pp. 779-783.

Faleide, J.I., Vågnes, E. & Gudlaugsson, S.T. 1993: Late Mesozoic-Cenozoic evolution of the south-western Barents Sea in a regional rift-shear tectonic setting. *Marine and Petroleum Geology 10*, pp. 186-214.

Faleide, J.I., Tsikalas, F., Breivik, A.J., Mjelde, R., Ritzmann, O., Engen, Ø., Wilson, J. & Eldholm, O. 2008: Structure and evolution of the continental margin off Norway and the Barents Sea. *Episodes 31*, pp. 82-91.

Fossen, H. 2010: Extensional tectonics in the North Atlantic Caledonides: a regional view. *In* Law, R.D., Butler, R.W.H., Holdsworth, R.E., Krabbendam, M. & Strachan, R.A. (eds.): *Continental Tectonics and Mountain Building: The Legacy of Peach and Horne*. Geological Society, London, Special Publications 335, pp. 767-793.

Fossen, H. & Hurich, C.A. 2005: The Hardangerfjord Shear Zone in SW Norway and the North Sea: a large-scale low-angle shear zone in the Caledonian crust. *Journal of the Geological Society 162*, pp. 1-13.

Gabrielsen, R.H. 1984: Long-lived fault zones and their influence on the tectonic development of the southwestern Barents Sea. *Journal of the Geological Society, London 141*, pp. 651-662.

Gabrielsen, R.H. & Færseth, R.B. 1989: The inner shelf of North Cape, Norway and its implications for the Barents Shelf-Finnmark Caledonide boundary. A comment. *Norsk Geologisk Tidsskrift 69*, pp. 57-62.

Gabrielsen, R.H. & Koestler, A.G. 1987: Description and structural implications of fractures in late Jurassic sandstones of the Troll Field, northern North Sea. *Norsk Geologisk Tidsskrift 67*, pp. 371-381.

Gabrielsen, R.H., Færseth, R.B., Jensen, L.N., Kalheim, J.E. & Riis, F. 1990: Structural elements of the Norwegian continental shelf, Part I: The Barents Sea Region. *Norwegian Petroleum Directorate Bulletin 6*, 33 pp.

Gabrielsen, R.H., Braathen, A., Dehls, J. & Roberts, D. 2002: Tectonic lineaments of Norway. *Norwegian Journal of Geology 82*, pp. 153-174.

Gautier, A.M., Zwaan, K.B., Bakke, I., Lundahl, I., Ryghaug, P. & Vik, E. 1987: KVÆNANGEN berggrunnskart 1734 1. 1:50 000, foreløpig utgave. *Norges geologiske undersøkelse*.

Gayer, R.A., Hayes, S.J. & Rice, A.H.N. 1985: The structural development of the Kalak Nappe Complex of Eastern and Central Porsangerhalvøya, Finnmark, Norway. *Nor. geol. unders. bull 400*, pp. 67-87.

Gernigon, L., Brönner, M., Roberts, D., Olesen, O., Nasuti, A. & Yamasaki, T. 2014: Crustal and basin evolution of the southwestern Barents Sea: From Caledonian orogeny to continental breakup. *Tectonics 33*, pp. 347-373.

Goldstein, A. & Marshak, S. 1988: Analysis of fracture array geometry. *In* Marshak, S. & Mitra, G. (eds.): *Basic Methods of Structural Geology*. Prentice Hall, Englewood Cliffs, NJ, pp. 249-267.

Gudlaugsson, S.T., Faleide, J.I., Johansen, S.E. & Breivik, A.J. 1998: Late Palaeozoic structural development of the South-western Barents Sea. *Marine and Petroleum Geology 15*, pp. 73-102.

Guise, P.G. & Roberts, D. 2002: Devonian ages from ^{40}Ar/^{39}Ar dating of plagioclase in dolerite dykes, eastern Varanger Peninsula, North Norway. *Norges geologiske undersøkelse 440*, pp. 27-37.

Hansen, J-A. & Bergh, S.G. 2012: Origin and reactivation of fracture systems adjacent to the Mid-Norwegian continental margin on Hamarøya, North Norway: use of digital geological mapping and morphotectonic lineament analysis. *Norwegian Journal of Geology 92*, pp. 391-403.

Hansen, J-A., Bergh, S.G. & Henningsen, T. 2012: Mesozoic rifting and basin evolution on the Lofoten and Vesterålen Margin, North-Norway; time constraints and regional implications. *Norwegian Journal of Geology 91*, pp. 203-228.

Hayes, S.J. 1980: The Caledonian geology of NE Porsangerhalvøya, Finnmark, North Norway. *Unpublished PhD thesis, University of Wales*.

Henderson, I.H.C., Viola, G. & Nasuti, A. 2015: A new tectonic model for the Palaeoproterozoic Kautokeino Greenstone Belt, northern Norway, based on high-resolution airborne magnetic data and field structural analysis and implications for mineral potential. *Norwegian Journal of Geology 95*, pp. 1-26.

Herrevold, T., Gabrielsen, R.H. & Roberts, D. 2009: Structural geology of the southeastern part of the Trollfjorden-Komagelva Fault Zone, Varanger Peninsula, Finnmark, North Norway. *Norwegian Journal of Geology 89*, pp. 305-325.

Indrevær, K. & Bergh, S.G. 2014: Linking onshore-offshore basement rock architecture and brittle faults on the submerged strandflat along the SW Barents Sea margin, using high-resolution (5 x 5 m) bathymetry data. *Norwegian Journal of Geology 94*, pp. 1-34.

Indrevær, K., Bergh, S.G., Koehl, J-B., Hansen, J-A., Schermer, E.R. & Ingebrigtsen, A. 2013: Post-Caledonian brittle fault zones on the hyperextended SW Barents Sea margin: New insights into onshore and offshore margin architecture. *Norwegian Journal of Geology 93*, pp. 167-188.

Jansen, Ø, Akselsen, J. & Roberts, D. 2012: Berggrunnsgeologisk kart HAMMERFEST 1936 III, M 1:50 000, foreløpig utgave. *Norsk geologiske undersøkelse.*

Jensen, L.N. & Sørensen, K. 1992: Tectonic framework and halokinesis of the Nordkapp Basin, Barents Sea. *In* Larsen, R.M., Brekke, H., Larsen, B.T. & Talleraas, E. (eds.): *Structural and Tectonic Modelling and its Application to Petroleum Geology.* Norwegian Petroleum Society (NPF), Special Publications 1, pp. 109-120.

Jensen, P.A. 1996: The Altenes and Repparfjord tectonic windows, Finnmark, northern Norway: Remains of a Palaeopreterozoic Andean-type plate margin at the rim of the Baltic Shield. *Unpublished Ph.D. Thesis, University of Tromsø.*

Johnson, H.D., Levell, B.K. & Siedlecki, S. 1978: Precambrian sedimentary rocks in East Finnmark, north Norway and their relationship to the Trollfjord-Komagelv fault. *Journal of the Geological Society, London 132*, pp. 517-533.

Kirkland, C.L., Daly, J.S. & Whitehouse, M.J. 2005: Early Silurian magmatism and the Scandian evolution of the Kalak Nappe Complex, Finnmark, Arctic Norway. *Journal of the Geological Society, London 162*, pp. 985-1003.

Kirkland, C.L., Daly, J.S. & Whitehouse, M.J. 2007: Provenance and Terrane Evolution of the Kalak Nappe Complex, Norwegian Caledonides: Implications for Neoproterozoic Paleogeography and Tectonics. *The Journal of Geology 115*, pp. 21-41.

Kirkland, C.L., Daly, J.S. & Whitehouse, M.J. 2008a: Basement-cover relationships of the Kalak Nappe Complex, Arctic Norwegian Caledonides and constraints on Neoproterozoic terrane assembly in the North Atlantic region. *Precambrian Research 160*, pp. 245-276.

Kirkland C.J, Daly, J.S., Chew, D.M. & Page, L.M. 2008b: The Finnmarkian Orogeny revisited: An isotopic investigation in eastern Finnmark, Arctic Norway. *Tectonophysics 460*, pp. 158-177.

Klein, A.C. & Steltenpohl, M.G. 1999: Basement-cover relations and late- to post-Caledonian extension in the Leknes group, west-central Vestvågøy, Lofoten, north Norway. *Norsk Geologisk Tidsskrift 79*, pp. 19-31.

Klein, A.C., Steltenpohl, M.G., Hames, W.E. & Andresen, A. 1999: Ductile and brittle extension in the southern Lofoten archipelago, north Norway: implications for differences in tectonic style along an ancient collisional margin. *American Journal of Science 299*, pp. 69-89.

Koehl, J-B.P., Bergh, S.G., Henningsen, T. & Faleide, J.I. 2018. Mid/Late Devonian-Carboniferous collapse basins on the Finnmark Platform and in the southwesternmost Nordkapp basin, SW Barents Sea. *Solid Earth*.

Koehl, J-B.P., Bergh, S.G. & Wemmer, K. Submitted: Neoproterozoic and post-Caledonian exhumation and shallow faulting in NW Finnmark from K/Ar dating and p/T analysis of fault-rocks. *Solid Earth*.

Koyi, H., Talbot, C.J. & Tørudbakken, B.O. 1993: Salt diapirs of the southwest Nordkapp Basin analogue modelling. *Tectonophysics 228*, pp. 167-187.

Kvassnes, A., Strand, A., Moen-Eikeland, H. & Pedersen, R. 2004: The Lyngen Gabbro: the lower crust of an Ordovician Incipient Arc. *Contributions to Mineralogy and Petrology 148*, pp. 358-379.

Lea, H. 2016: Analysis of Late plaeozoic-Mesozoic brittle faults and fractures in West-Finnmark: geometry, kinematics, fault rocks and the relationship to offshore structures on the Finnmark Platform in the SW Barents Sea. *Unpublished Master's Thesis, University of Tromsø*, 129 pp.

Lippard, S.J. & Prestvik, T. 1997: Carboniferous dolerite dykes on Magerøy: new age determination and tectonic significance. *Norsk Geologisk Tidsskrift 77*, pp. 159-163.

Lippard, S.J. & Roberts, D. 1987: Fault systems in Caledonian Finnmark and the southern Barents Sea. *Norges geologiske undersøkelse Bulletin 410*, pp. 55-64.

Marti, S. 2013: The Kalak Nappe Complex in Northern Norway: unraveling the tectonic evolution using quartz fabrics. *Unpublished Master's Thesis, University of Basel*, 135 pp.

Mattingsdal, R., Høy, T., Simonstad, E. & Brekke, H. 2015: An updated map of structural elements in the southern Barents Sea. *Norwegian Petroleum Directorate*.

Melezhik, V.A., Bingen, B., Sandstad, J.S., Pokrovsky, B.G., Solli, A. & Fallick, A. 2015: Sedimentary-volcanic successions of the Alta-Kvænangen Tectonic Window in the northern Norwegian Caledonides: Multiple constraints on deposition and correlation with complexes on the Fennoscandian Shield. *Norwegian Journal of Geology 95*, pp. 245-284.

Nasuti, A., Roberts, D. & Gernigon, L. 2015: Multiphase mafic dykes in the Caledonides of northern Finnmark revealed by a new high-resolution aeromagnetic dataset. *Norwegian Journal of Geology 95*, pp. 251-263.

Nilsen, K.T., Vendeville, B.C. & Johansen, J-T. 1995: Influence of Regional Tectonics on Halokinesis in the Nordkapp Basin, Barents Sea. *In* Jackson, M.P.A., Roberts, D.G. & Snelson, S. (eds.): *Salt tectonics a global perspective*. AAPG Memoir 65, pp. 413-436.

Olesen, O., Roberts, D., Henkel, H., Lile, O.B. & Torsvik, T.H. 1990: Aeromagnetic and gravimetric interpretation of regional structural features in the Caledonides of West Finnmark and North Troms, northern Norway. *Norsk geologiske undersøkelse Bulletin 419*, pp. 1-24.

Olesen, O., Torsvik, T.H., Tveten, E. & Zwaan, K.B. 1993: The Lofoten-Lopphavet Project – an integrated approach to the study of a passive continental margin, Summary report. 54 pp.

Olesen, O., Torsvik, T.H., Tveten, E., Zwaan, K.B., Løseth, H. & Henningsen, T. 1997: Basement structure of the continental margin in the Lofoten-Lopphavet area, northern Norway: constraints from potential field data, on-land structural mapping and palaeomagnetic data. *Norsk Geologisk Tidsskrift 77*, pp. 15-30.

Osmundsen, P-T. & Andersen, T.B. 2001: The middle Devonian basins of western Norway: sedimentary response to large-scale transtensional tectonics. *Tectonophysics 332*, pp. 51-68.

Osmundsen, P.T., Braathen, A., Sommaruga, A., Skilbrei, J.R., Nordgulen, Ø., Roberts, D., Andersen, T.B., Olesen, O. & Mosar, J. 2005: Metamorphic core complexes along the Mid-Norwegian margin: an overview and some current ideas. In Wandaas, B., Gradstein, F. et al. (eds.): Onshore-offshore relations on the Mid-Norwegian margin. *Norwegian Petroleum Society, Special Publications 12*, pp. 29-41.

Passe, C.R. 1978: The structural geology of east Snøfjord, Finnmark, North Norway. *Unpublished PhD thesis, University of Wales*.

Pastore, Z., Fichler, C. & McEnroe, S.A. 2016: The deep crustal structure of the mafic-ultramafic Seiland Igneous Province of Norway from 3-D gravity modelling and geological implications. *Geophys. J. Int. 207*, pp. 1653-1666.

Pharaoh, T.C., Macintyre, R.M. & Ramsay, D.M. 1982: K-Ar age determinations on the Raipas suite in the Komagfjord Window, northern Norway. *Norsk Geologisk Tidsskrift 62*, pp. 51-57.

Pharaoh, T.C., Ramsay, D.M. & Jansen, Ø. 1983: Stratigraphy and Structure of the Northern Part of the Repparfjord-Komagfjord Window, Finnmark, Northern Norway. *Norges geologiske undersøkelse 377*, pp. 1-45.

Phillips, T., Jackson, C.A-L., Bell, R.E., Duffy, O.B. & Fossen, H. 2016: Reactivation of intrabasement structures during rifting: A case study from offshore southern Norway. *Journal of Structural Geology 91*, pp. 54-73.

Rafaelsen, B., Elvebakk, G., Andreassen, K., Stemmerik, L., Colpaert, A. & Samuelsberg, T.J. 2008: From detached to attached carbonate buildup complexes – 3D seismic data from the Upper Palaeozoic, Finnmark Platform, southwestern Barents Sea. *Sedimentary Geology 206*, pp. 17-32.

Ramberg, I.B., Bryhni, I., Nøttvedt, A. & Rangnes, K. 2008: The making of a land. Geology of Norway. *The Norwegian geological Association, Oslo*.

Reitan, P.H. 1963: The geology of the Komagfjord tectonic window of the Raipas suite, Finnmark, Norway. *Norges geologiske undersøkelse 221*, 71 pp.

Rice, A.H.N. 2013: Restoration of the External Caledonides, Finnmark, North Norway. *In* Corfu, F., Gasser, D. & Chew, D.M. (eds.): *New Perspectives on the Caledonides of Scandinavia and Related Areas*. Geological Society, London, Special Publications 390, pp. 271-299.

Roberts, D. 1971: Patterns of folding and fracturing in north-east Sørøy. *Norges geologiske undersøkelse 269*, pp. 89-95.

Roberts, D. 1972: Tectonic deformation in the Barents Sea region of Varanger Peninsula, Finnmark. *Norges geologiske undersøkelse 282*, pp. 1-39.

Roberts, D. 1973: Geologisk kart over Norge, berggrunnskart. Hammerfest 1:250 000. *Norges geologiske undersøkelse*.

Roberts, D. 1987: Honningsvåg berggrunnsgeologisk kart 2136 4 – 1:50000, foreløpig utgave. *Norges geologiske undersøkelse*.

Roberts, D. 1998: Berggrunnskart Honningsvåg - Geologisk kart over Norge, M 1:250 000. *Norges geologiske undersøkelse*.

Roberts, D. 2007: Palaeocurrent data from the Kalak Nappe Complex, northern Norway: a key element in models of terrane affiliation. *Norwegian Journal of Geology 87*, pp. 319-328.

Roberts, D. & Lippard, S.J. 2005: Inferred Mesozoic faulting in Finnmark: current status and offshore links. *Norges geologiske undersøkelse Bulletin 443*, pp. 55-60.

Roberts, D. & Olovyanishnikov, V. 2004: Structural and tectonic development of the Timanides orogeny. *In* Gee, D.G. & Pease, V. (eds.): *The Neoproterozoic Timanide Orogen of Eastern Baltica*. Geological Society, London, Memoirs 30, pp. 47-57.

Roberts, D. & Onstott, T.C. 1995: $^{40}Ar/^{39}Ar$ laser microprobe analyses and geochemistry of dolerite dykes from the Rybachi and Sredni Peninsulas, NW Kola, Russia. *Norges geologiske undersøkelse Special Publication 7*, pp. 307-314.

Roberts, D. & Siedlecka, A. 2002: Timanian orogenic deformation along the northeastern margin of Baltica, Northwest Russia and Northeast Norway, and Avalonian-Cadomian connections. *Tectonophysics 352*, pp. 169-184.

Roberts, D. & Siedlecka, A. 2012: Provenance and sediment routing of Neoproterozoic formations on the Varanger, Nordkinn, Rybachi and Sredni peninsulas, North Norway and Northwest Russia: a review. *Norges geologiske undersøkelse Bulletin 452*, pp. 1-19.

Roberts, D. & Williams, G.D. 2013: Berggrunnskart KJØLLEFJORD 2236-4 M 1:50 000, foreløpig utgave. *Norges geologiske undersøkelse*.

Roberts, D., Mitchell, J.G. & Andersen, T.B. 1991: A post-Caledonian dyke from Magerøy North Norway: age and geochemistry. *Norwegian Journal of Geology 71*, pp. 289-294.

41

Roberts, D., Olesen, O. & Karpuz, M.R. 1997: Seismo- and noetectonics in Finnmark, Kola Peninsula and the southern Barents Sea. Part 1: Geological and neotectonic framework. *Tectonophysics 270*, pp. 1-13.

Roberts, D., Chand, S. & Rise, L. 2011: A half-graben of inferred Late Palaeozoic age in outer Varangerfjorden, Finnmark: evidence from seismic reflection profiles and multibeam bathymetry. *Norwegian Journal of Geology 91*, pp. 191-200.

Robins, B. 1990a: Nordkapp berggrunnskart 2037 2 – 1:50000, foreløpig utgave. *Norges geologiske undersøkelse*.

Robins, B. 1990b: Skarsvåg berggrunnsgeologisk kart 2137 3 – 1:50000, foreløpig utgave. *Norges geologiske undersøkelse*.

Rykkelid, E. 1992: E69 "FATIMA" – Geologisk undersøkelse av tunnel under Magerøysundet. *Veglaboratoriet, Statens Vegvesen*.

Samuelsberg, T.J., Elvebakk, G. & Stemmrik, L. 2003: Late Paleozoic evolution of the Finnmark Platform, southern Norwegian Barents Sea. *Norwegian Journal of Geology 83*, pp. 351-362.

Schiffer, W.J. 2017: Structural and Metamorphic Implications of the Final Emplacement of the Lyngen Nappe. *Unpublished Master's Thesis, University of Tromsø*, 117 pp.

Séranne, M., Chauvet, A., Seguret, M. & Brunel, M. 1989: Tectonics of the Devonian collapse-basins of western Norway. *Bull. Soc. Géol. Fr. 8*, pp. 489-499.

Shipton, Z.K. & Cowie, P.A. 2003: A conceptual model for the origin of fault damage zone structures in high-porosity sandstones. *Journal of Structural Geology 25*, pp. 333-344.

Siedlecka, A. 1975: Late Precambrian Stratigraphy and Structure of the North-Eastern Margin of the Fennoscandian Shield (East Finnmark – Timan Region). *Norges geologiske undersøkelse 316*, pp. 313-348.

Siedlecka, A. & Siedlecki, S. 1967: Some new aspects of the geology of Varanger peninsula (Northern Norway). *Norges geologiske undersøkelse 247*, pp. 288-306.

Siedlecka, A., Roberts, D., Nystuen, J.P. & Olovyanishnikov, V.G. 2004: Northeastern and northwestern margins of Baltica in Neoproterozoic time: evidence from the Timanian and Caledonian Orogens. *Geological Society, London, Memoirs 30*, pp. 169-190.

Siedlecki, S. 1980: Geologisk kart over Norge, berggrunnskart Vadsø – M 1:250 000. *Norges geologiske undersøkelse*.

Slagstad, D. 1995: Lyngen Magmatic Complex Rypdalen Shear Zone: magmatic and structural evolution. *Geonytt 22*, pp. 22-67.

Steltenpohl, M.G., Hames, W.E. & Andresen, A. 2004: The Silurian to Permian history of a metamorphic core complex in Lofoten, northern Scandinavian Caledonides. *Tectonics 23*, pp. 1-23.

Steltenpohl, M.G., Moecher, D., Andresen, A., Ball, J., Mager, S. & Hames, W.E. 2011: The Eidsfjord shear zone, Lofoten-Vesterålen, north Norway: An Early Devonian, paleoseismogenic low-angle normal fault. *Journal of Structural Geology 33*, pp. 1023-1043.

Torgersen, E. & Viola, G. 2014: Structural and temporal evolution of a reactivated brittle-ductile fault – Part I: Fault architecture, strain localization mechanisms and deformation history. *Earth and Planetary Science Letters 407*, pp. 205-220.

Torgersen, E., Viola, G., Zwingmann, H. & Harris, C. 2014: Structural and temporal evolution of a reactivated brittle-ductile fault – Part II: Timing of fault initiation and reactivation by K-Ar dating of synkinematic illite/muscovite. *Earth and Planetary Science Letters 407*, pp. 221-233.

Torske, T. & Bergh, S.G. 2004: The Caravarri Formation of the Kautokaino Greenstone Belt, Finnmark, North Norway; a Palaeoproterozoic foreland basin succession. *Norges geologiske undersøkelse Bulletin 442*, pp. 5-22.

Townsend, C. 1987a: The inner shelf of North Cape, Norway and its implications for the Baretns Shelf-Finnmark Caledonide boundary. *Norsk Geologisk Tidsskrift 67*, pp. 151-153.

Townsend, C. 1987b: Thrust transport directions and thrust sheet restoration in the Caledonides of Finnmark, North Norway. *Journal of Structural Geology 9*, pp. 345-352.

Vorren, T., Kristoffersen, Y. & Andreassen, K. 1986: Geology of the inner shelf west of North Cape, Norway. *Norsk Geologisk Tidsskrift 66*, pp. 99-105.

Wilks, W.J. & Cuthbert, S.J. 1994: The evolution of the Hornelen Basin detachment system western Norway: implications for the style of late orogenic extension in the southern Scandinavian Caledonides. *Tectonophysics 238*, pp. 1-30.

Worthing, M.A. 1984: Fracture patterns on Eastern Seiland, North Norway and their possible Relationship to Regional Faulting. *Nor. Geol. Unders. Bull. 398*, pp. 35-41.

Zhang, W., Roberts, D. & Pease, V. 2016: Provenance of sandstones from Caledonian nappes in Finnmark, Norway: Implications for Neoproterozoic-Cambrian palaeogeography. *Tectonophysics 691*, pp. 198-205.

Zwaan, K.B. 1995: Geology of the West Troms Basement Complex, northern Norway, with emphasis on the Senja Shear Belt: a preliminary account. *Geological Survey of Norway Bulletin 427*, pp. 33-36.

Zwaan, K.B. & Gautier, A.M. 1980: Alta and Gargia. Description of the geological maps (AMS-M711) 1834 1 and 1934 IV 1:50 000. *Norges geologiske undersøkelse 357*, pp. 1-47.

Zwaan, K.B. & Roberts, D. 1978: Tectonostratigraphic Succession and Development of the Finnmarkian Nappe Sequence, North Norway. *Norges geologiske undersøkelse 343*, pp. 53-71.

Zwaan, K.B., Bakke, I., Cramer, J.J. & Ryghaug, P. 1987: Rotsund berggrunnskart 1634 I, 1:50 000 foreløpig utgave. *Norges geologiske undersøkelse.*
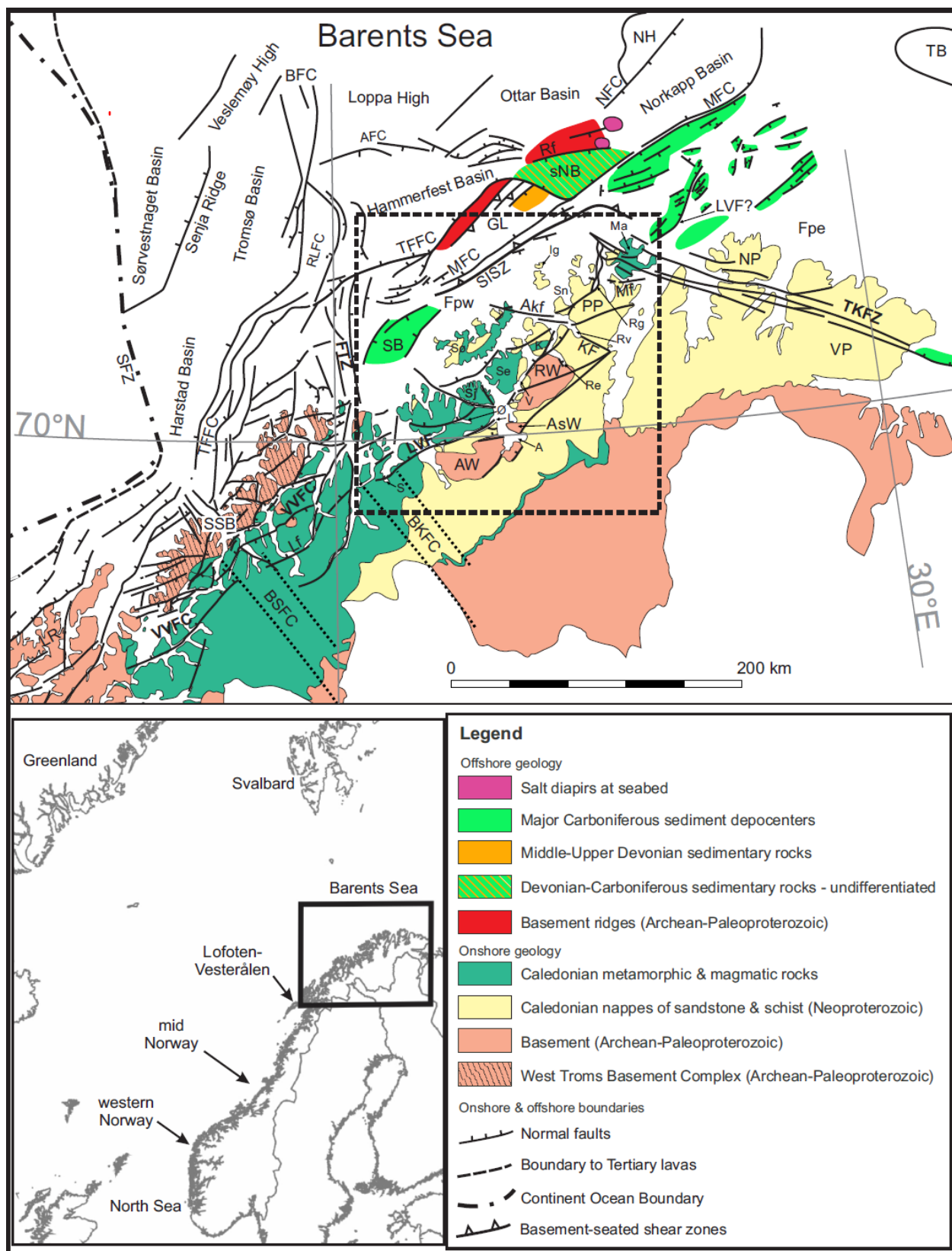
Figure 1. Regional tectonic map of the SW Barents Sea margin and North Norway (based on Bergh et al., 2007; Faleide et al., 2008; Hansen et al., 2012; Indrevær et al., 2013). Onshore geology is from Ramberg et al. (2008). The dashed frame locates Figure 2. Black frame in lower left inset locates the Barents Sea on the Norwegian continental shelf. Abbreviations: A = Altafjorden; AFC = Asterias Fault Complex; Akf = Akkarfjord fault; AsW = Altenes tectonic window; AW = Alta-Kvænangen tectonic window; BFC = Bjørnøyrenna Fault Complex; BSFC = Bothnian-Senja Fault Complex; BKFC = Bothnian-Kvænangen Fault

Complex; FTZ = Fugløya transfer zone; GL = Gjesvær Low; He = Helnes; KF = Kokelv Fault; Kv = Kvaløya; L = Langfjorden; Lf = Laksvatn fault; LR = Lofoten Ridge; LVF = Langfjord-Vargsund fault; Ma = Magerøya; Mf = Magerøysundet fault; MFC = Måsøy Fault Complex; NFC = Nysleppen Fault Complex; NP = Nordkinn Peninsula; PP = Porsanger Peninsula; Re = Repparfjorden; Rf = Rolvsøya fault; Rg=Ryggefjorden; RLFC = Ringvassøya-Loppa Fault Complex; Rv = Revsbotn; RW = Repparfjord-Komagfjord tectonic window; S = Sørkjosen; SB = Sørvær Basin; Se = Seiland; SFZ = Senja Fracture Zone; SISZ = Sørøya-Ingøya shear zone; Sj = Sjernøya; Sn = Snøfjorden; sNB = southwesternmost Nordkapp basin; SSB = Senja Shear Belt; Sø = Sørøya; TFFC = Troms-Finnmark Fault Complex; TKFZ = Trollfjorden-Komagelva Fault Zone; Tu = Tufjorden; V = Vargsund; VP = Varanger Peninsula; VVFC = Vestfjorden-Vanna fault complex.
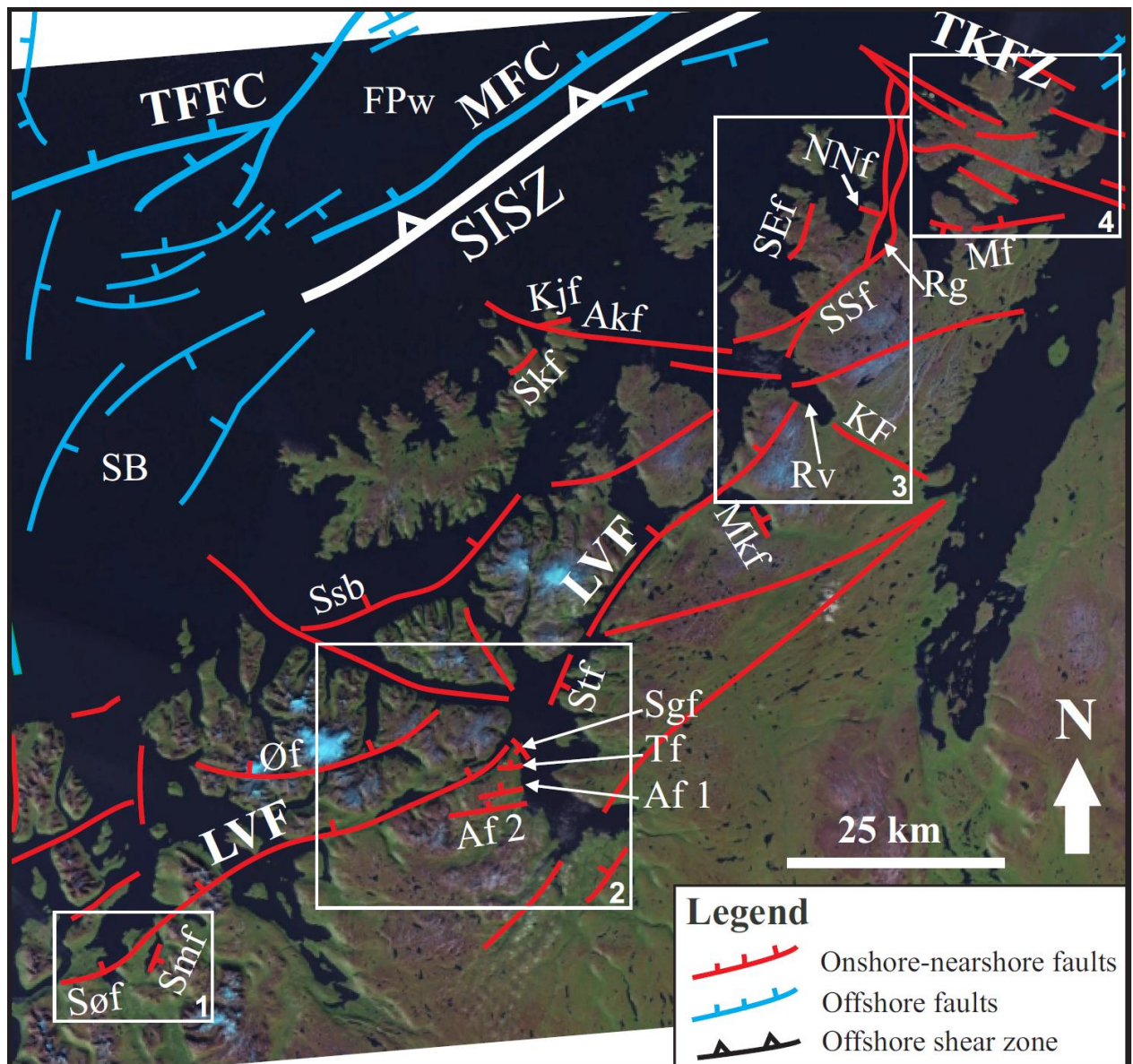
Figure 2. DEM satellite image of NW Finnmark showing major onshore and nearshore brittle faults belonging to the LVF and TKFZ. The map combines onshore faults from the present study and from Roberts (1971), Zwaan & Roberts (1978), Gayer et al. (1985), Townsend (1987a), Lippard & Roberts (1987), Rykkelid (1992), Marti (2013) and Torgersen et al. (2014). Offshore faults are from Indrevær et al. (2013) and Koehl et al. (2018). Satellite photographs of onshore areas are from www.norgei3d.no. See Figure for location. White boxes labelled 1-4 show the location of fault data acquired during fieldwork and displayed in stereo diagrams in Figure 3. Abbreviations: Af 1 = Altafjorden fault 1; Af 2 = Altafjorden fault 2; Akf = Akkarfjord fault; FPw = Finnmark Platform west; KF = Kokelv Fault; Kjf = Kjøtvika fault; Lf = Langfjord fault; LVF = Langfjord-Vargsund fault; Mf = Magerøysundet fault; MFC = Måsøy Fault Complex; Mkf = Markopp fault; NNf = Njoal-Neset fault; Rg = Ryggefjorden; Rv = Revsbotn; SB = Sørvær Basin; SEf = Selvika-Eiterfjorden fault; Sgf = Storhaugen fault; SISZ = Sørøya-Ingøya shear zone; Skf = Skarvdalen fault; Smf = Straumfjordbotn fault; Ssb = Sørøy sub-basin; SSf = Snøfjorden-Slatten fault; Stf = Storekorsnes fault; Søf = Sørkjosen fault; TFFC = Troms-Finnmark Fault Complex; TKFZ = Trollfjorden-Komagelva Fault Zone; Tf = Talvik fault; Øf = Øksfjorden fault.
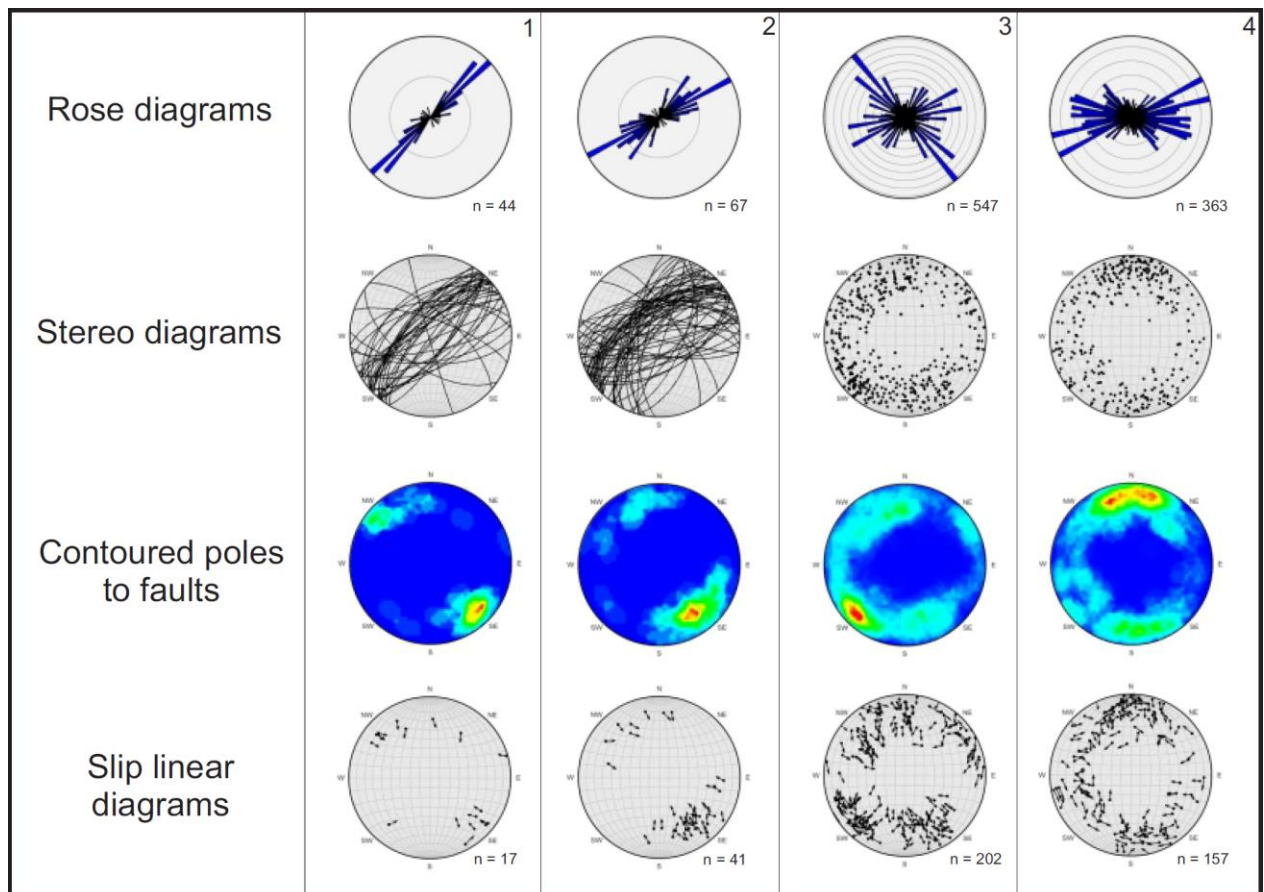
Figure 3. Brittle fault data from structural fieldwork including from top to bottom: rose diagrams of measured fault strikes (grey circles represent an increment of four measurements), lower hemisphere Schmid stereonets showing fracture trends and dips as great circles (column 1 & 2) and poles to fault surfaces (columns 3 & 4), Schmid stereonets showing fracture strike and dip as contoured poles (red indicates high fracture density and blue low fracture density), and slip-linear plots of slickenside lineations. Slip-linear is defined as the pole to the fault surface decorated by a line/arrow parallel with the direction of slip of the hanging-wall (movement plane; defined by the pole to the fault and the dip striae (Goldstein & Marshak, 1988). Note the change of dominant fault trend from southwestern areas in Sørkjosen (1) and Altafjorden (2) dominated by ENE-WSW and NNE-SSW trending brittle faults, compared with northeastern areas on the Porsanger Peninsula (3) and Magerøya (4), which display a dominance of WNW-ESE and ENE-WSW trending faults.
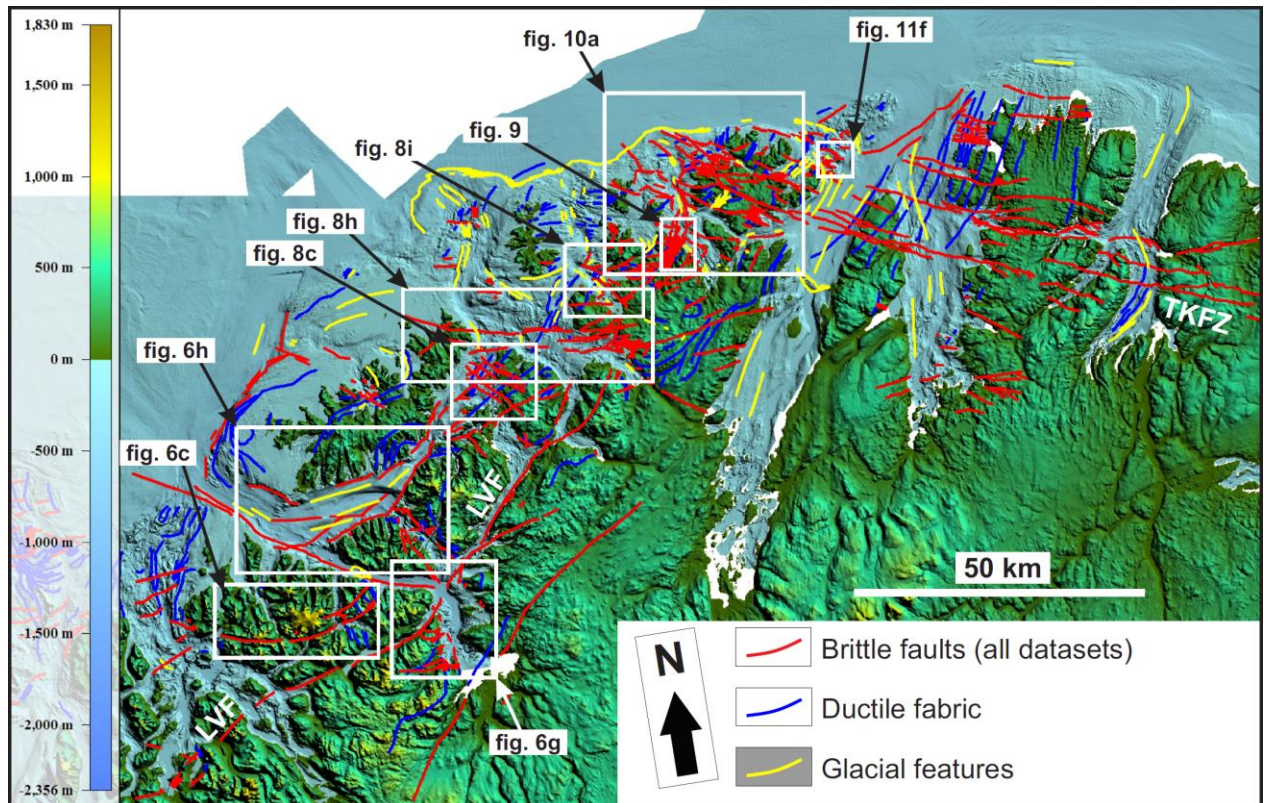
Figure 4. High-resolution topography and bathymetry data in NW Finnmark showing interpreted brittle faults (red lines) based on satellite images, structural field data, bathymetry (Mareano), topography and aeromagnetic data (Nasuti et al., 2015). Bedrock ductile fabrics (blue) dominantly trend NE-SW to NNE-SSW. The map also shows abundant glacial striations (yellow lines) and delineates three glacial sediment fans along the northern edge of the strandflat. The color scale bar on the left hand-side denotes depth above (yellow-green) and below (blue) sea level.

48
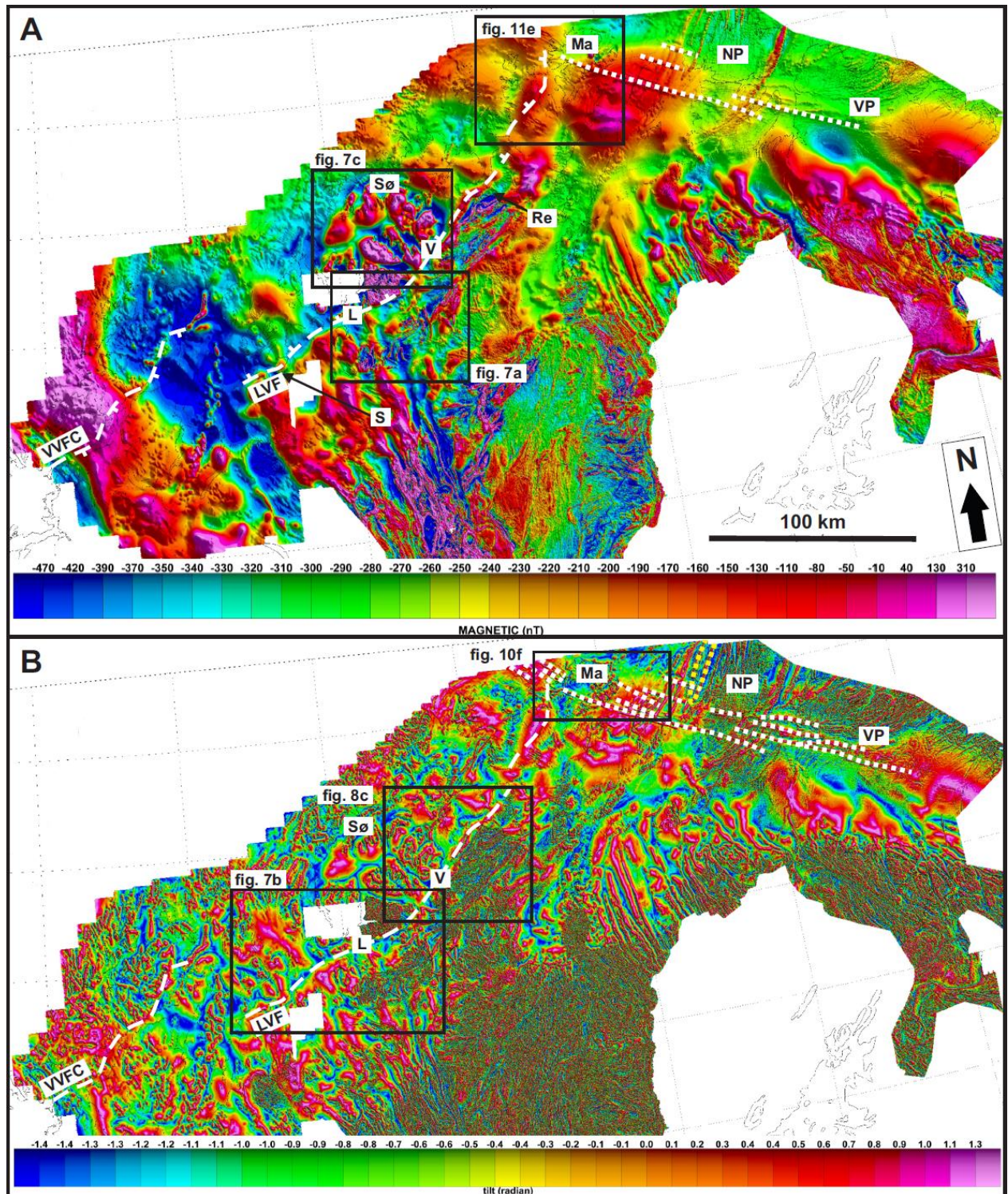
Figure 5. Aeromagnetic data from the Geological Survey of Norway (Nasuti et al., 2015). (a) Aeromagnetic anomaly map of Troms and Finnmark. Note the occurrence of large-scale, 10-80 km-wide, NW-SE to NNW-SSE trending, successive positive and negative anomalies depicting Precambrian granite-gneiss belts while NE-SW trending Caledonian (nappe) fabrics are more diffuse. Major brittle fault complexes such as the LVF and the VVFC are shown in dashed white lines. The data also highlight linear, elongated, WNW-ESE trending, positive anomalies (dotted white lines) on Magerøya (Ma) and on the Varanger Peninsula (VP); (b) Tilt-derivative aeromagnetic data of Troms and Finnmark. The dataset shows numerous WNW-ESE trending, high positive aeromagnetic anomalies interpreted as dolerite dykes extending from the Varanger Peninsula (VP) in the east to Magerøya (Ma) in the west (Nasuti et al., 2015). The dotted yellow curve in the north delineates a positive aeromagnetic anomaly that correlates with a major syncline structure in the

field, onshore the Nordkinn Peninsula (NP; cf. Roberts & Siedlecka, 2012 and Roberts & Williams, 2013). Major fault complexes (LVF and VVFC) are shown in dashed white.
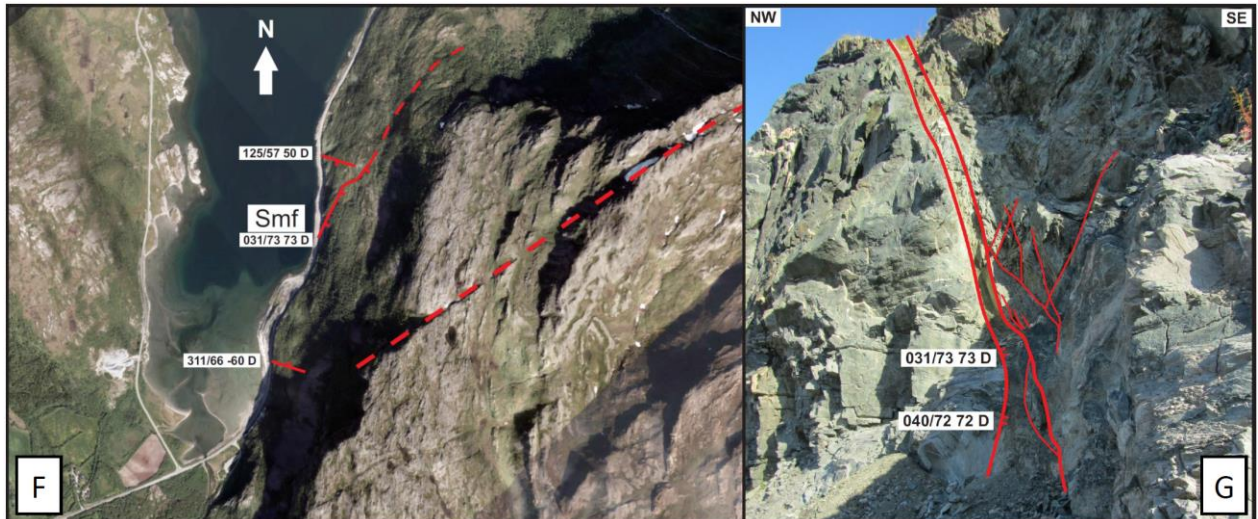
Brittle faults observed in the field
Major lineaments
Ductile fabric in the field
Offset mafic bed

Fault displacement estimated to 100-1000 m
Fault displacement of 1-10 m
Fault displacement of 0.01-1 m

100 m
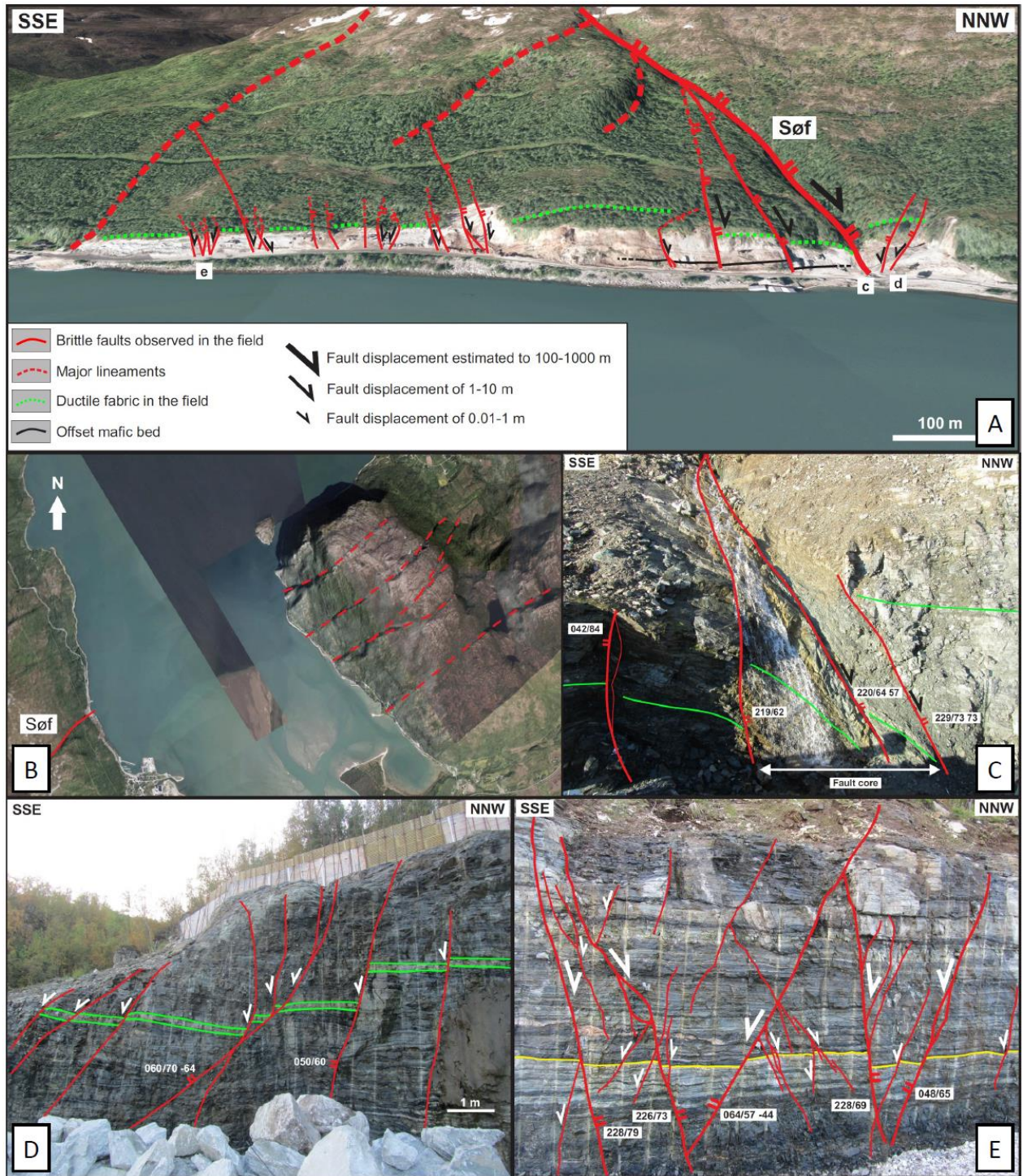
Figure 6. a) Outline of Sørkjosen fault (Søf), related subparallel minor faults (red lines) and E-W to WNW-ESE trending lineaments (dashed red lines) viewed in 3D satellite image along a ca. one km-long, NNW-SSE trending roadcut (see Figure & Figure 2 for location). The Sørkjosen fault seems to truncate and/or bend WNW-ESE trending lineaments. Note the southwards decrease in the amount of throw accommodated by brittle faults in the footwall of the Sørkjosen fault (cf. offset mafic bed). The dominant Caledonian bedrock fabric is sub-horizontal; b) Satellite image of the Sørkjosen fault (Søf; red line) and of NE-SW trending lineaments on the northeastern side of the fjord (dashed red lines) with associated fault strike and dip, and slickenside lineations (white boxes; D = down); c) Outcrop photograph of the Sørkjosen fault core with bedrock fabric (green lines) bending clockwise into the fault core. Location shown in (a); d) Outcrop photograph in the hanging-wall of the Sørkjosen fault showing antithetic, SSE-dipping, planar and listric minor brittle faults accommodating a few tens of cm of normal displacement (cf. offset felsic unit in green lines). Location is shown in (a); e) Outcrop photograph of a swarm of ENE-WSW to NE-SW trending, oppositely dipping, planar faults arranged in horst and graben structures and showing minor, cm-scale normal offsets of gneiss bands (yellow lines). Location shown in (a); f) Satellite image of the Straumfjordbotn fault (Smf; red line) and its possible extension to the northeast (dashed red lines). The photo also shows a large NE-SW trending lineament east of the fjord that may represent a brittle fault. See Figure 2 for location of the Straumfjordbotn fault; g) Outcrop photograph of the Straumfjordbotn fault with associated structural measurements.
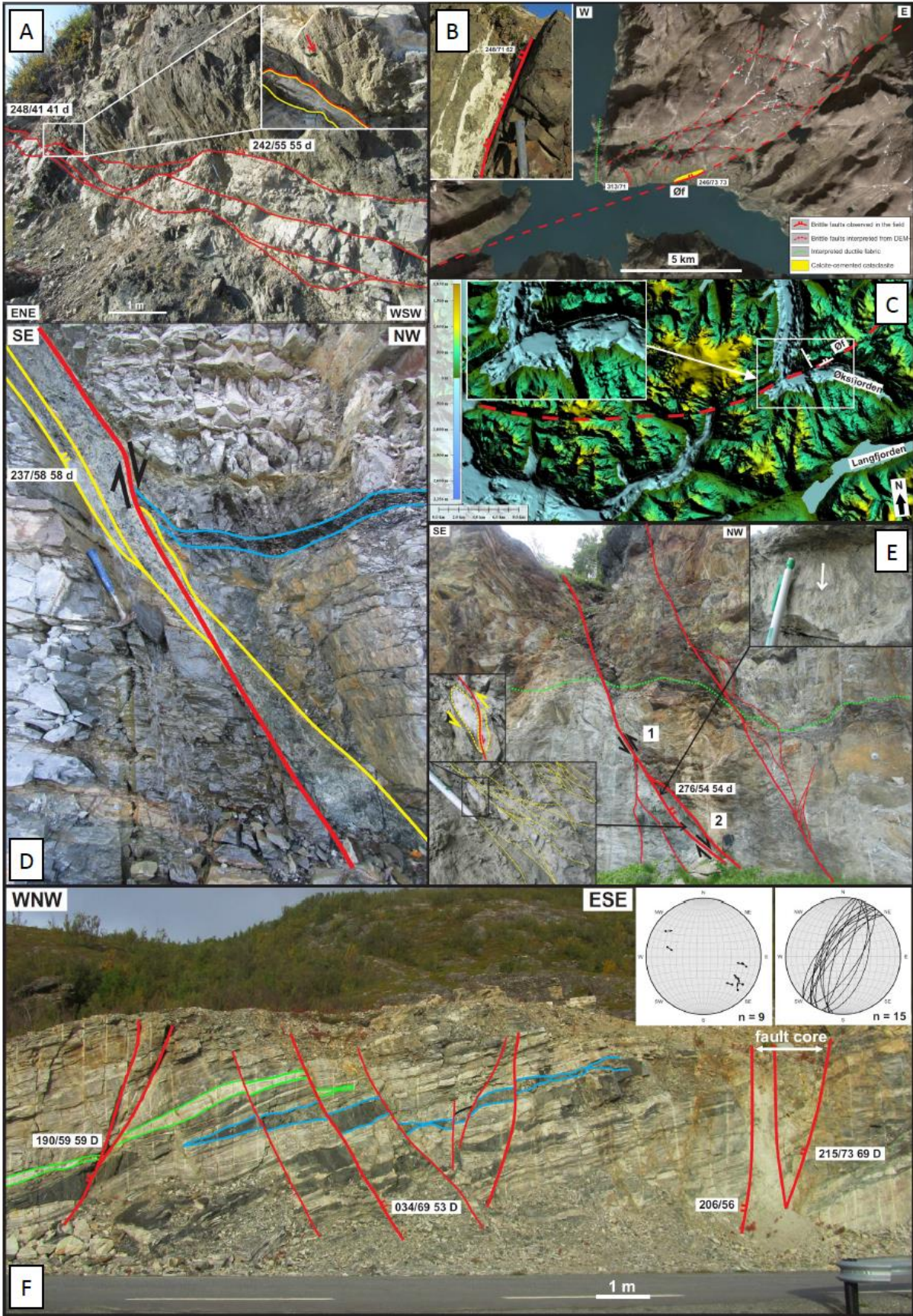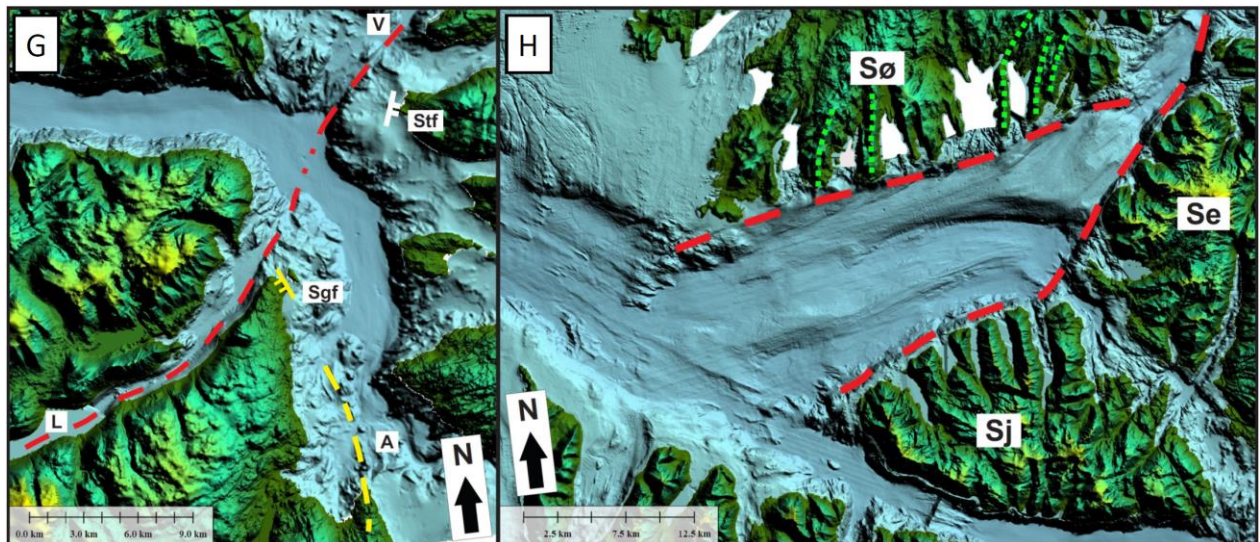
Figure 7. a) Outcrop photograph of NNW-dipping brittle faults along the northern shore of Langfjorden (cf. Figure 2 for location), showing irregular traces (red lines) and calcite-filled cataclastic fault-core (upper right frame). Slickengrooves (red arrow) consistently indicate normal dip-slip movement; b) Satellite image showing the Øksfjorden fault (Øf) and ENE-WSW and NNE-SSW trending lineaments (faults) in the Seiland Igneous Province. The inset frame shows detail of the Øksfjorden fault, which incorporates calcite-cemented cataclastic fault-rock. See location in Figure 2; c) Outcrop occurrence of the Øksfjorden fault (Øf; white line) and its possible westward extension along submarine escarpments that bend into an E-W to WNW-ESE trend westwards (dashed red line). Elevation color scheme shown here is common to all bathymetry figures. See Figure 4 for location. Areas colored in white are gaps in data coverage. Abbreviations are as in Figure & Figure 2; d) Outcrop photograph of the Altafjorden fault 1 and associated structural measurements. The main fault surfaces display slickensides that indicate down-to-the-NW, normal dip-slip movement. Note how the fault-core (yellow lines) is offset by a younger oblique fault surface (red line). Location shown in Figure 2; e) Outcrop photograph of the Talvik fault. The upper-right inset shows the main fault surface, displaying slickengrooves (white arrow) that indicate normal dip-slip movement. The lower-left inset shows the fault core with relic ductile shear-band fabric (dotted yellow) and quartz sigma-clasts (middle left inset) that indicate top-to-the-SE thrusting. The ductile fabric and sigma-clasts are crosscut by brittle fractures (cf. red in middle-left box), suggesting that normal faulting occurred after ductile thrusting. Location is shown in Figure 2; f) Horst-graben structures in foliated quartz-feldspatic Kalak Nappe Complex gneisses, shown by a network of NNE-SSW trending, oppositely dipping normal faults on the eastern shore of Altafjorden. Note normal offsets of boudinaged mafic (blue lines) and felsic (green lines) units. Structural measurements of slickenside lineations indicate normal dip-slip sense of shear; g) Bathymetry data at the intersection of Altafjorden (A), Langfjorden (L) and Vargsundet (V). Dashed red lines represent submarine escarpments linked to the Langfjorden and Vargsund fault segments of the LVF. Note thick glacial deposits in Altafjorden that partly cover the trace of the LVF in Altafjorden. The field location of the Storekorsnes fault is showed in white. Dashed yellow lines mark NNW-SSE trending submarine escarpments that trend parallel to the bedrock fabric along the western shore of Altafjorden (Roberts 1973) and that align with the exposed Storhaugen fault (Sgf; yellow line). Location in Figure 4; h) Large topographic depression between the islands of Sørøya (Sø), Stjernøya (Sj) and Seiland (Se), and the inferred Sørøy sub-basin, which is bounded by ENE-WSW and NNE-SSW trending, zigzag-shaped escarpments in the southeast. Location shown in Figure 4.
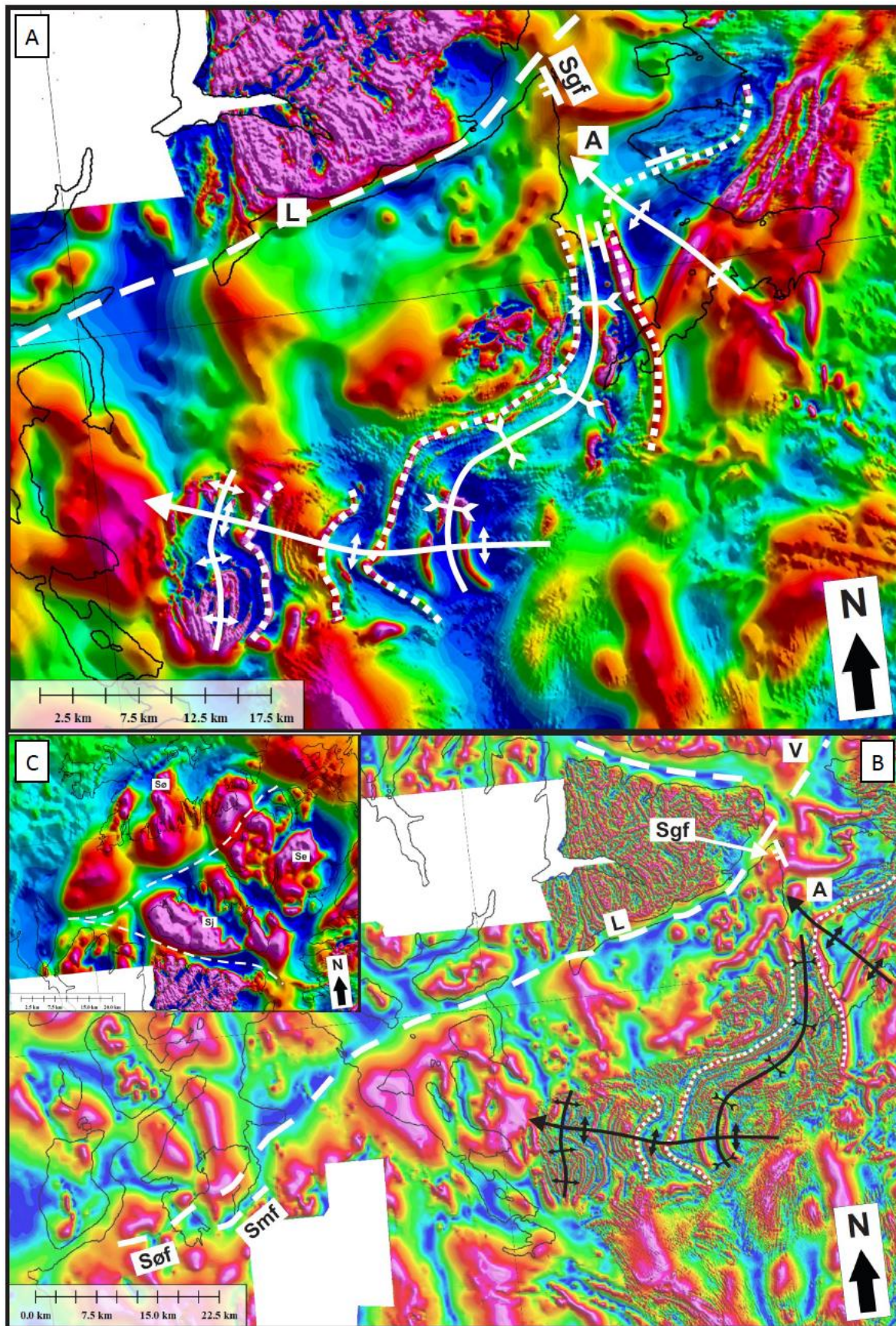
Figure 8. a) Aeromagnetic data south of Langfjorden (L) and in Altafjorden (A) showing positive aeromagnetic anomalies (dotted white lines) trending parallel to refolded steeply dipping, meta-volcanic

and sedimentary units of the Alta-Kvænangen and Altenes tectonic windows (Roberts, 1973; Bergh & Torske, 1988; Jensen, 1996), defining steep, NW-SE trending, NW-plunging folds (white lines). Note the contrast in orientation of anomaly patterns on either side of Altafjorden NNW-SSE trends to the west in the Alta-Kvænangen tectonic window, and ENE-WSW trends to the east in the Altenes tectonic window.This change in attitude of presumed fold limbs corresponds with a bend in the LVF farther north. The western limb of the antiform fold structure in Altafjorden trends parallel to the onshore occurrence of Storhaugen fault (Sgf), while the northern limb parallels the Langfjor-Vargsund fault in Langfjorden (L). White-shaded areas indicate a lack of data coverage. See Figure & Figure 2 for abbreviations, and Figure 5a for location and data color scheme; b) Tilt-derivative aeromagnetic data showing an ENE-WSW trending, negative anomaly (dashed white line) that follows the trace of the LVF in Langfjorden (L) and Sørkjosen (Søf). Aeromagnetic data also delineate possible refolded units (dotted white lines) in Proterozoic rocks of the Alta-Kvænangen tectonic window, forming steep, NW-plunging folds (black lines). See Figure & Figure 2 for abbreviations, and Figure 5b for location and data color scheme. White-shaded areas indicate a lack of data coverage; c) Aeromagnetic data north of Langfjorden showing highly magnetic rocks of the Seiland Igneous Province crosscut by a zigzaging, E-W to NE-SW trending, negative anomaly that coincides with the southeastern boundary-fault of the Sørøy sub-basin.
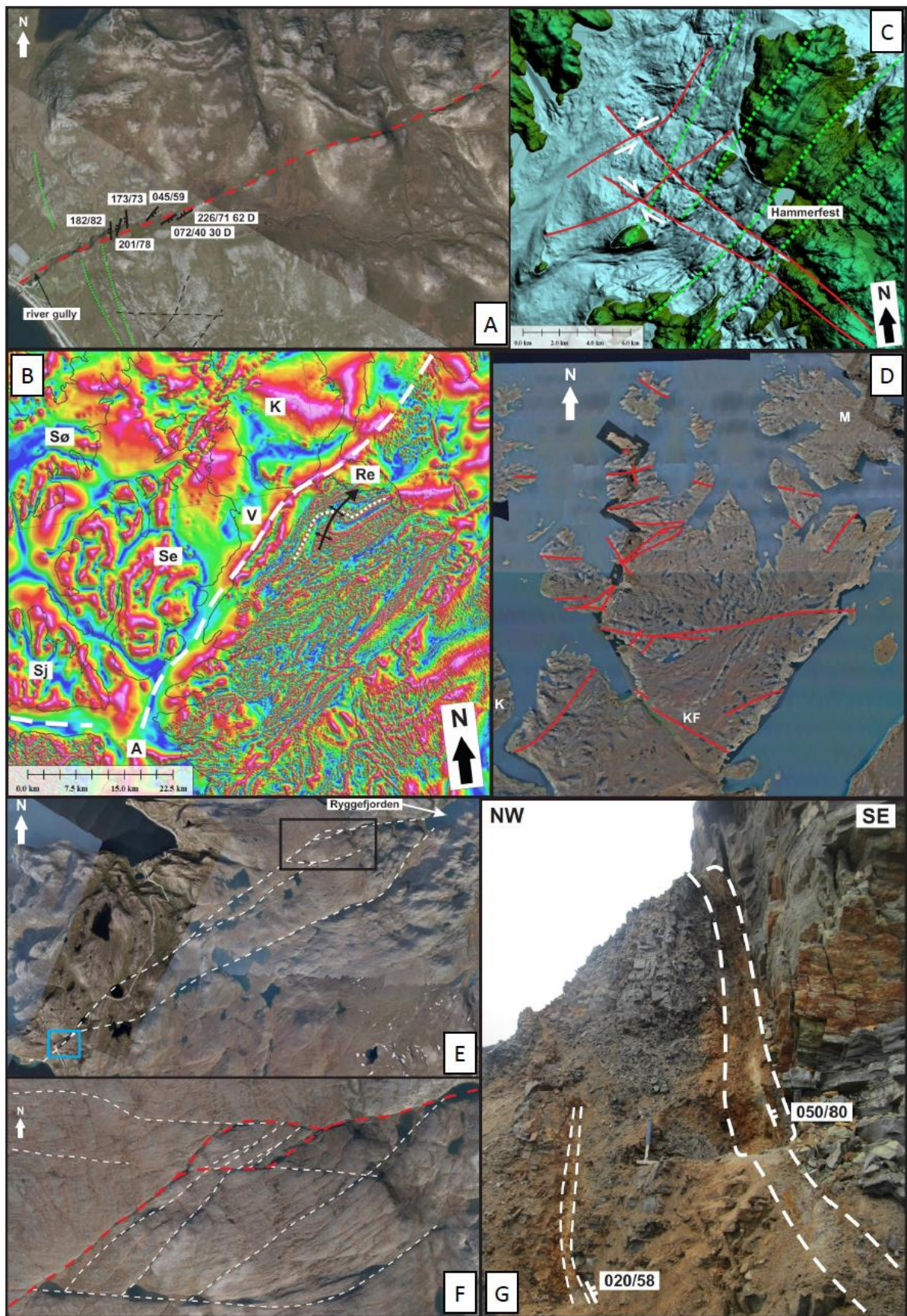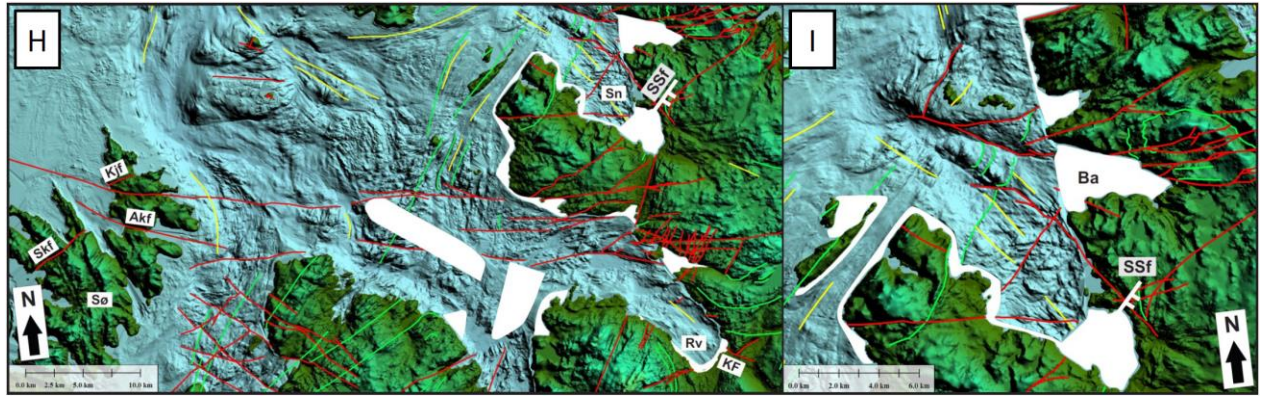
Figure 9. a) Satellite image northeast of Repparfjorden showing a large lineament (dashed red line) along a river gully representing a major segment of the LVF. Outcrops along the river gully show several minor NE-SW to N-S trending brittle splay faults (black lines). Ductile Caledonian fabric is shown in dotted green lines. See Figure for location of Repparfjorden; b) Tilt-derivative aeromagnetic data along Vargsundet (V) and Repparfjorden (Re) showing a NE-SW trending, positive anomaly (dashed white line) that correlates with the Vargsundet segment of the LVF. The anomaly widens and dies out north of Repparfjorden. Note the outline of a large NE-SW trending fold structure (dotted white line) mapped by Reitan (1963) in Proterozoic rocks of the Repparfjord-Komagfjord tectonic window, southeast of Vargsundet; c) Bathymetry data showing crosscutting brittle faults in red (relative motion as white arrows) west of Hammerfest on Kvaløya. Dotted green lines represent NNE-SSW trending corrugations that are correlated to the Caledonian bedrock fabric onshore. Location in Figure 4; d) Satellite images of the Porsanger Peninsula showing dominant WNW-ESE and ENE-WSW trending lineaments (red lines). K = Kvaløya; KF = Kokelv Fault; M = Magerøya; e) Central part of the Porsanger Peninsula (satellite image) displaying major lineaments (dashed white) that correspond to the LVF in the area between Snøfjorden and Ryggefjorden. The black frame shows the location of (f) and the blue frame indicates the location of (g); f) Satellite image showing duplex-like structure from interaction of WNW-ESE to E-W and NE-SW to ENE-WSW trending lineaments (dashed red and white lines) in the central part of the Porsanger Peninsula. The presumed LVF trace is outlined by dashed red lines. See black frame in (e) for location; g) Outcrop photograph of the SE-dipping Snøfjorden-Slatten fault core made up of cataclastic fault-rock and oxidized fault gouge (in between dashed white lines). See blue frame in (e) for location; h) Bathymetry data in Revsbotn (Rv) showing numerous E-W submarine escarpments that link up with E-W to ENE-WSW trending lineaments onshore the Porsanger Peninsula to the east, and with WNW-ESE trending lineaments and brittle faults (e.g. the Akkarfjord fault; Akf) onshore Sørøya (Sø) in the west. Bedrock foliation trends are shown by green lines and glacial plough marks by yellow lines. Outcrop occurrence of the Snøfjorden-Slatten fault (SSf; white line); i) Bathymetry data in Snøfjorden showing submarine escarpments interpreted as brittle faults (red lines), bedrock foliation (green lines) and glacial plougmarks (yellow lines). The outcrop occurrence of the Snøfjorden-Slatten fault (SSf) is shown as a white line. Note the clockwise curving of both onshore and nearshore ENE-WSW trending brittle faults into a major WNW-ESE trending lineament in Bakfjorden (Ba).
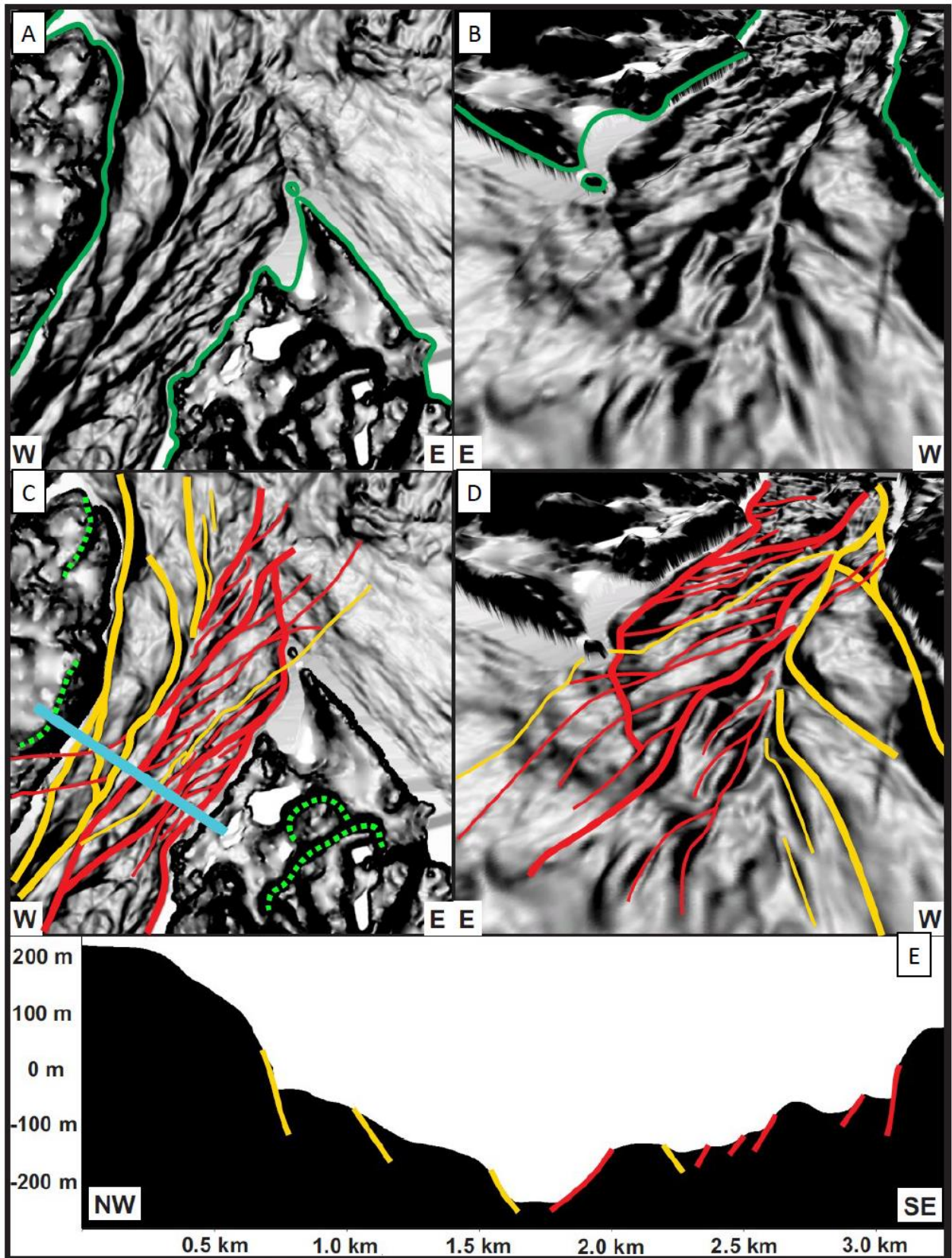
58

Figure 10. Detailed bathymetry data of Ryggefjorden, northeast of the Porsanger Peninsula (see Figure 4 for location) showing a network of interconnected, steep, NW and SE-dipping escarpments in the Ryggefjorden trough, non-interpreted (a & b) and interpreted (c & d). Figures (a) and (c) are map views and figures (b) and (d) show view towards the south of the Ryggefjorden trough. The coastline is marked as green line in (a) and (b). Bathymetry data in (a)-(d) are shown using a slope shader with steep slopes darker

59

and gentle slopes lighter shades. Note small gaps between the onshore and nearshore data in (b) and (d). Red curves symbolize NW- to W-dipping escarpments whereas orange curves represent E- to SE-dipping escarpments. The SE-boundary fault of the Ryggefjorden trough shows an arcuate geometry and curves from a NNE-SSW trend in the southwest to a N-S trend in the northeast. The bathymetry-topography profile displayed in (e) shows a gradual deepening of the trough through a succession of NW- (red) and SE-dipping (yellow) escarpments/faults, resulting in a graben-like geometry in cross-section. The profile is marked as a blue line in (c).
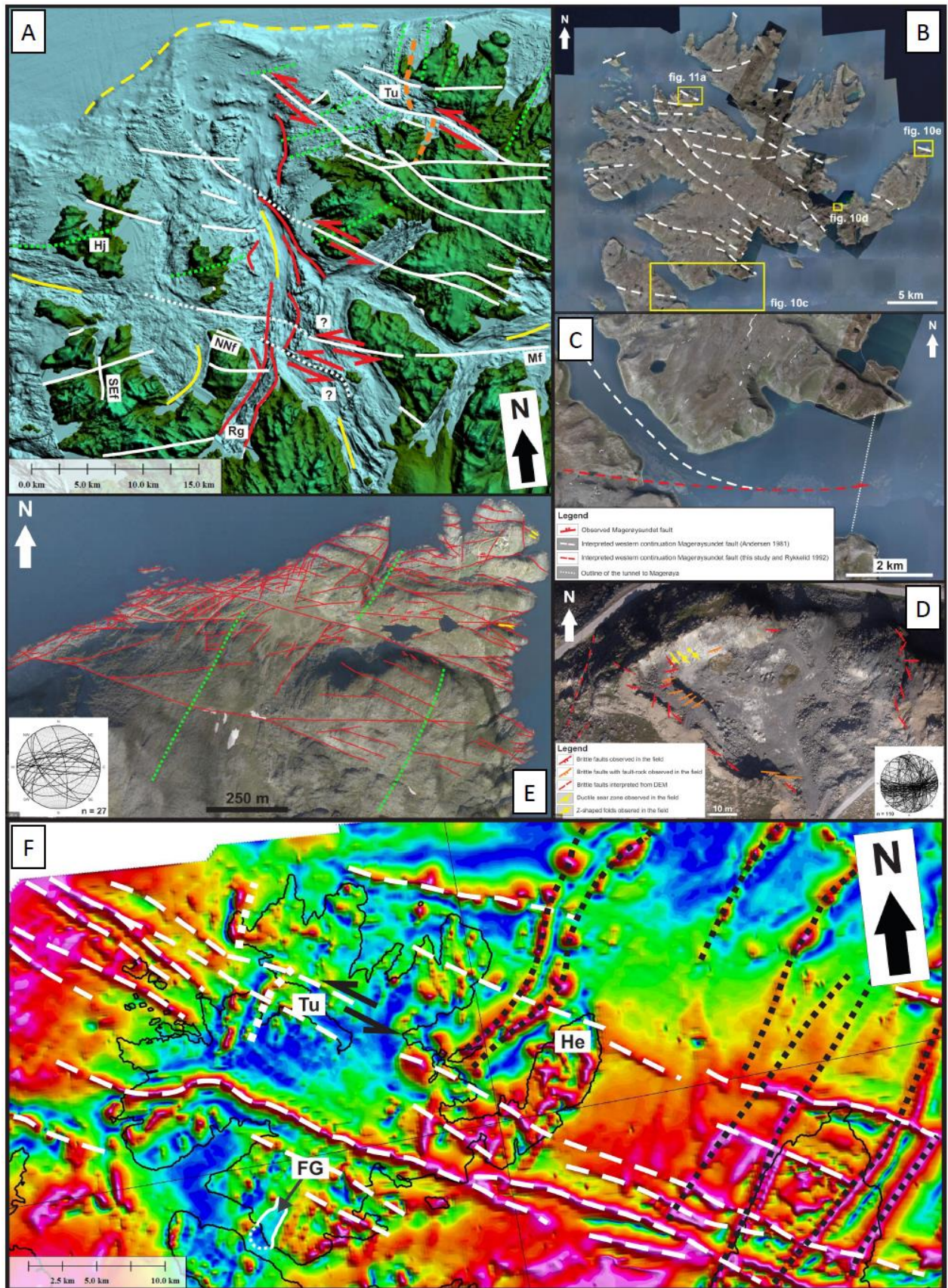
Figure 11. a) Shallow shelf and fjord bathymetry data west of Magerøya and north of the Porsanger Peninsula (location in Figure 4). Note the alignment of left-stepping, NNE-SSW trending, sigma-shaped submarine troughs including the Ryggefjorden trough in Ryggefjorden (Rg) and west of Magerøya. The

transitions from one trough to another coincide with WNW-ESE trending submarine escarpments and onshore lineaments (white lines). Inferred shear senses displayed as red arrows. The orange dashed lines in northern Magerøya mark the thrust contact between the Kalak Nappe Complex and Magerøy Nappe, which appears laterally offset by ca. 3-4 km across Tufjorden (Tu). The bedrock foliation is shown as dotted green lines and glacial ploughmarks as yellow lines. The dashed yellow curve displays the contours of a large glacial delta (Vorren et al., 1986); b) Satellite image of the island of Magerøya, which topography is dominated by WNW-ESE and ENE-WSW to E-W trending lineaments (dashed white lines). See Figure for location of Magerøya; c) Detail of southern Magerøya showing the western extent of the Magerøysundet fault in red (Rykkelid, 1992) and in white (Andersen et al., 1982). See (b) for location; d) Outcrop map of brittle faults in a quarry within the Honningsvåg Igneous Complex, showing a dominance of ENE-WSW and NNE-SSW trending faults (cf. stereoplot of fracture surfaces in the lower right corner). Location shown in (b); e) Interpreted satellite image in Helnes, eastern Magerøya, showing a strong dominance of WNW-ESE trending and E-W to ENE-WSW trending lineaments (cf. stereoplot of fracture surfaces in the lower left corner). NNE-SSW trending faults are subsidiary. The bedrock is made of gabbros from the Honningsvåg Igneous Complex and schists and meta-volcanics of the Magerøya Nappe. Dominant ductile fabrics represented as dotted green lines. Exposed, Caledonian mafic dykes are marked in yellow. Location displayed in (b); f) Aeromagnetic data of Magerøya displaying numerous, linear, WNW-ESE trending high positive anomalies (dashed white lines) correlated with dolerite dyke swarms intruded along brittle faults. These faults crosscut and locally, laterally offset NNE-SSW trending, positive anomalies (dotted black lines)interpreted as magnetite-rich metasedimentary units (Roberts & Siedlecka, 2012; Roberts & Williams, 2013). The thrust contact between the Magerøy Nappe and Kalak Nappe Complex (dotted white lines) coincides with a discontinuous, NNE-SSW trending, high positive aeromagnetic anomaly on Magerøya, which is offset (cf. black arrows) along a WNW-ESE trending submarine escarpment in Tufjorden (Tu). This scarp links up and merges farther west into a WNW-ESE trending, positive aeromagnetic anomaly interpreted as a dolerite dyke intruded along the same brittle fault. In the southern part of Magerøya, a negative anomaly (thin white and dotted line) correlates with the Finnvik Granite (FG; Andersen, 1981).
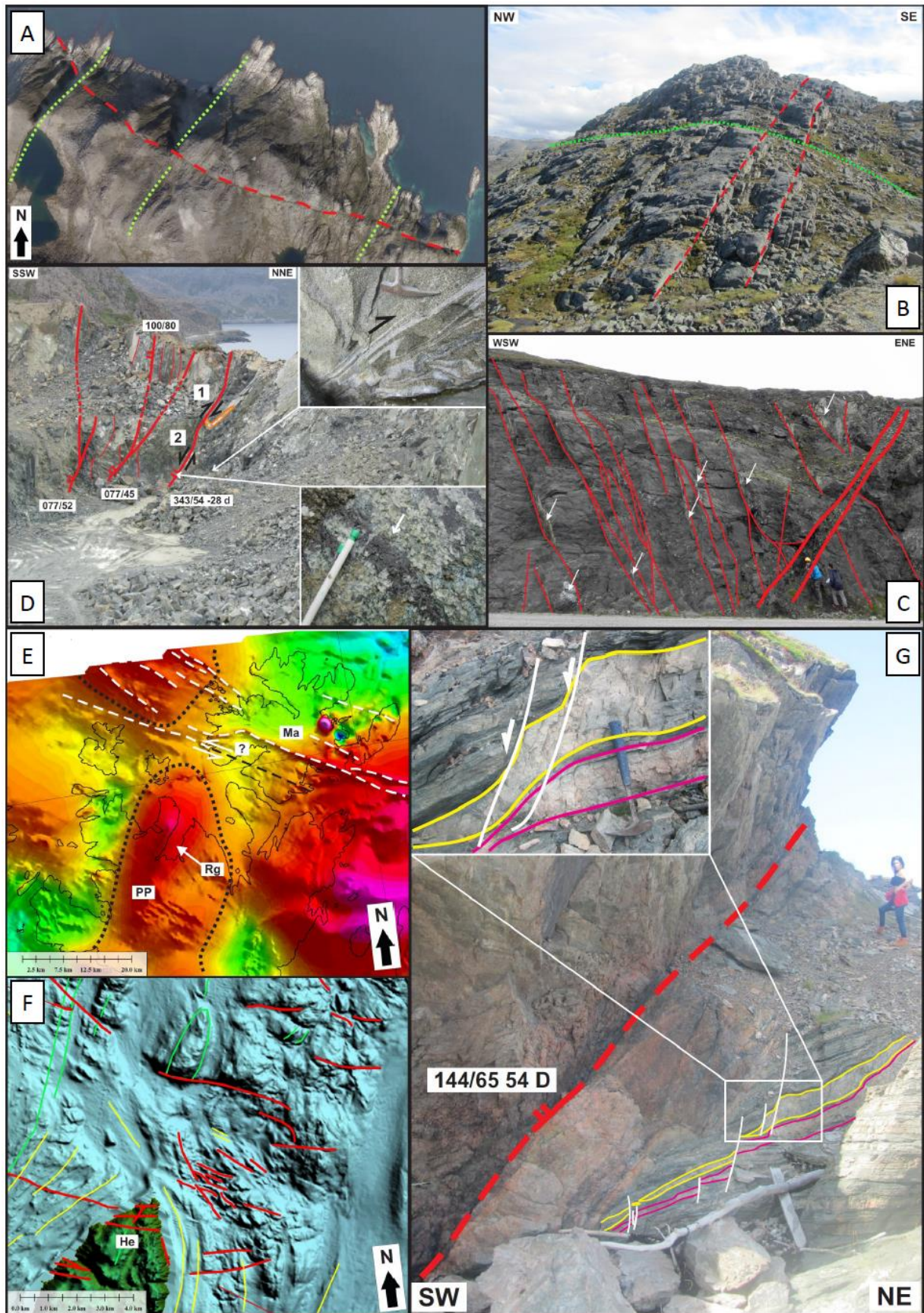
Figure 12. a) Satellite image of a prominent WNW-ESE trending lineament/brittle fault (dashed red line) that crosscuts bedrock foliation (dotted green lines). Location along the southern coast of Tufjorden on

Magerøya (Figure 11b); b) Pervasive, subvertical, WNW-ESE trending fractures (e.g. in dashed red lines) onshore western Magerøya that crosscut schists of the Kalak Nappe Complex. ESE-dipping Caledonian fabrics shown as a dotted green line; c) Half-graben structure in schists of central Magerøya, made of interacting, WNW-ESE trending brittle faults. The main fault core (thick red lines) comprises layered, calcite-rich, cataclastic fault-rocks. Calcite-rich fault-rock occur along minor WNW-ESE trending faults (white arrows); d) Network of listric faults (red lines) including 10-50 cm-thick lenses of cataclastic fault-rock along strike. Associated structural measurements in white boxes. A bolt-shaped felsic bed (orange line) indicates drag-folding along an adjacent SW-dipping ductile shear zone (upper inset), suggesting (1) top-to-the-NE ductile thrusting and (2) later down-to-the-SW, brittle, normal reactivation (cf. slickensided fault surface, i.e. white arrow, in lower right inset); e) Aeromagnetic data in Magerøya (Ma) and the northern part of the Porsanger Peninsula (PP). Note the presence of a broad, NE-SW trending, high positive anomaly (dotted black line) below Ryggefjorden (Rg) and the Porsanger Peninsula and of an analogous anomaly farther north. The separation of these two, positive anomalies coincides with a WNW-ESE trending escarpment (dashed white; cf. Figure 11a) that can be traced southeastward aligning with a large onshore brittle fault on Magerøya (Ma; dashed black line; cf. Figure 11a & b). The apparent left-lateral offset between the two positive anomalies (dotted black lines) may reflect km-scale, left-lateral offset along this WNW-ESE trending fault (white arrows); f) Bathymetry data north of Helnes (He; see Figure 4 for location) revealing the presence of a Z-shaped depression bounded by WNW-ESE and NNW-SSE trending brittle faults (red). Evelation of bathymetry and topography in (f) displayed in Figure 7c; g) Storhaugen fault core (red line) and adjacent footwall damage zone (inset box), where alternating felsic and mafic gneissic units (yellow and pink lines) are downthrown along minor, but steeper, syntethic brittle normal faults (white lines and arrows). Location is shown in Figure 2.
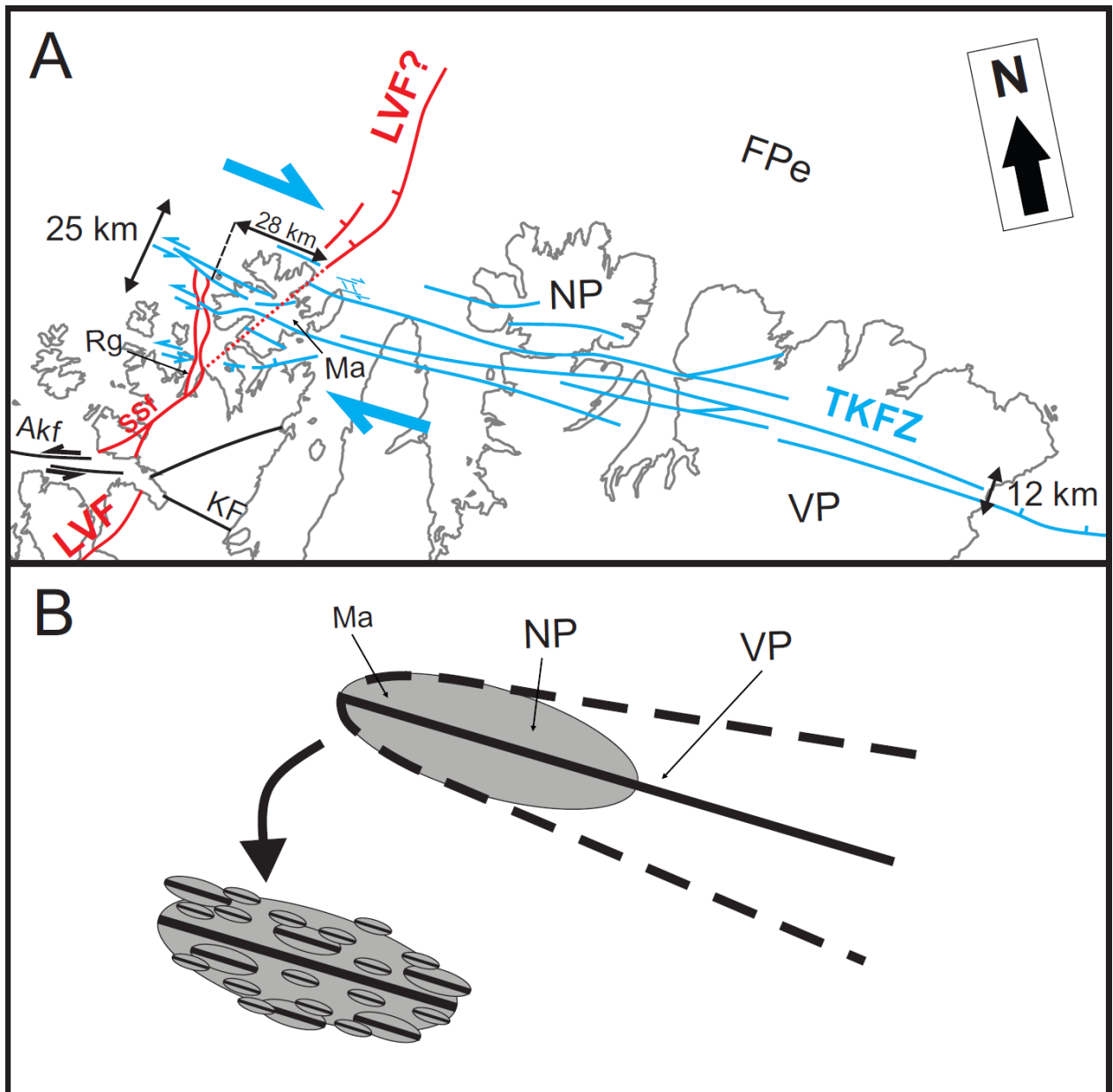
Figure 13. (a) Structural map of the interaction of the TKFZ (blue) and the LVF (red) in NW Finnmark during late Paleozoic extension. The Akkarfjord fault and other (conjugate) faults related to the TKFZ are displayed as black lines. The TKFZ offsets the LVF by ca. 28 km right-laterally between Ryggefjorden and (Rg) and the Finnmark Platform east (FPe; Koehl et al. 2018). Note that left- and right-lateral offsets of the LVF across fault segments of the TKFZ counter-balance one another so that the onshore-nearshore LVF and its offshore continuation remain aligned on a NE-SW trending axis (dotted red line). Note the significant width variation of the TKFZ from the Varanger Peninsula (ca. 12 km) to Magerøya (ca. 25 km). Abbreviations as in Figure ; (b) Conceptual fault-tip process zone model for the TKFZ based on Braathen et al. (2013). The fault-tip process zone is gray-shaded and shows a high number of minor, subparallel faults. On the Varanger Peninsula (VP) in eastern Finnmark, deformation localized along a few fault segments, while in NW Finnmark (Magerøya) deformation distributed along multiple fault segments. In onshore-nearshore areas of the Nordkinn Peninsula (NP), the TKFZ broadens and splays out into numerous fault segments that accommodate lower amount of displacement on Magerøya (from a few tens of meters to a few kilometers). This model implies that the TKFZ dies out west of Magerøya.
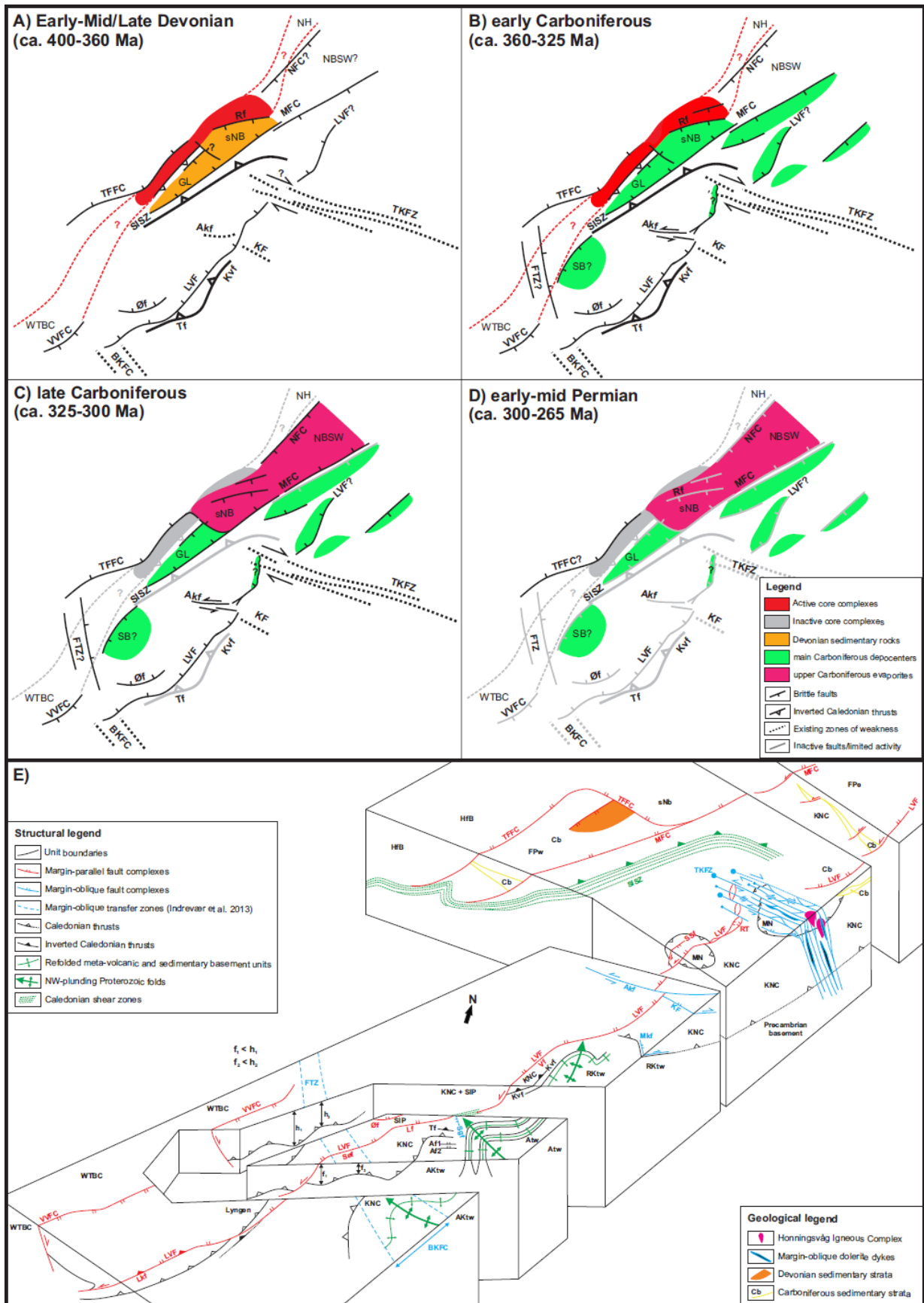
Figure 14. Map-view evolutionary model for brittle faults in NW Finnmark during post-Caledonian extension. Active brittle faults are shown in black and inactive faults in light grey. Dotted lines represent inherited Precambrian fault fabrics. a) Initiation of the collapse of the Caledonides in the Mid/Late Devonian along inverted, low-angle, NE-SW trending Caledonian ductile thrusts such as the Kvenklubben (Kvf) and Talvik fault (Tf). Inverted, low-angle Caledonian ductile thrusts quickly thinned the crust and became exhumed to shallow, brittle pressure/temperature conditions, i.e. reactivated as low-angle, brittle normal faults. Incremental extension led to the formation of high-angle brittle faults, e.g. the LVF and Øksfjorden fault, which possibly splayed upwards from Caledonian thrusts; b) early Carboniferous times are marked by the deposition of thick sedimentary deposits in offshore basins, on the Finnmark Platform and, potentially, in nearshore mini-basins (e.g. Ryggefjorden trough). The TKFZ was reactivated as strike-slip transfer fault that offset and segmented the LVF between Ryggefjorden and the Finnmark Platform. The Akkarfjord fault, a conjugate fault to the TKFZ, accommodated sinistral strike-slip displacement during post-Caledonian extension and also contributed to segment and offset the LVF; c) Inverted Caledonian thrusts (Tf & Kvf) became inactive and were decapitated due to continued extension along the LVF and related, high-angle brittle normal faults; d) Extension is believed to have come to a halt towards the end of the Carboniferous and NW Finnmark remained tectonically quiet through Permian to Cenozoic times; e) 3D diagram of NW Finnmark and the SW Barents Sea margin. Abbreviations: Af1 = Altafjorden fault 1; Af2 = Altafjorden fault 2; Akf = Akkarfjord fault; AKtw = Alta-Kvænangen tectonic window; Atw = Altenes tectonic window; BKFC = Bothnian-Kvænangen Fault Complex; Cb = Carboniferous; FPe = Finnmark Platform east; FPw = Finnmark Platform west; FTZ = Fugløya transfer zone; HfB = Hammerfest Basin; KF = Kokelv Fault; KNC = Kalak Nappe Complex; Kvf = Kvenklubben fault; Lf = Langfjorden fault; LVF = Langfjord-Vargsund fault; MFC = Måsøy Fault Complex; Mkf = Markopp fault; MN = Magerøy Nappe; RKtw = Repparfjord-Komagfjord tectonic window; RT = Ryggefjorden trough; SIP = Seiland Igneous Province; SISZ = Sørøya-Ingøya shear zone; sNb = southwesternmost Nordkapp basin; SSf = Snøfjorden-Slatten fault; Søf = Sørkjosen fault; Tf = Talvik fault; TFFC = Troms-Finnmark Fault Complex; TKFZ = Trollfjorden-Komagelva Fault Zone; VVFC = Vestfjorden-Vanna fault complex; WTBC = West Troms Basement Complex; Øf = Øksfjorden fault.